



**FRERES MENTOURI UNIVERSITY  
CONSTANTINE 1 -ALGERIA**

# **Journal of Sciences & Technology**

Semestrial Journal of Freres Mentouri University, Constantine, Algeria



---

**VOLUME 04 - ISSUE 02— DECEMBER 2019**

---

**EISSN: .....-.....**

**Freres Mentouri  
University Constantine**

**Ain El-Bey Road  
Constantine 25000  
Algeria**

Phone.Fax: 213 (0) 31. 81. 12.78

Email: [revues@umc.edu.dz](mailto:revues@umc.edu.dz)

Website :<http://revue.umc.edu.dz>

# Journal of Sciences & Technology

Volume 4 N° 2 December 2019

Semestrial Journal of Freres Mentouri Constantine 1  
University, Algeria

Journal Director

**Pr. El Hadi LATRECHE**  
Rector of the University

Editorial & Publishing Director  
Chief Editor of Sciences & Technology

**Pr. Nadir BELLEL**

Editorial Board

Pr. S. RHOUATI  
Pr. N. BEGHIDJA  
Pr. A. DJEMEL  
Pr. T. BOUFENDI  
Pr. A. DEBICHE  
Pr. A. BOUDJADA  
Pr. F. RAHMANI

An article proposed for publication should not be submitted  
at the same time to another journal.

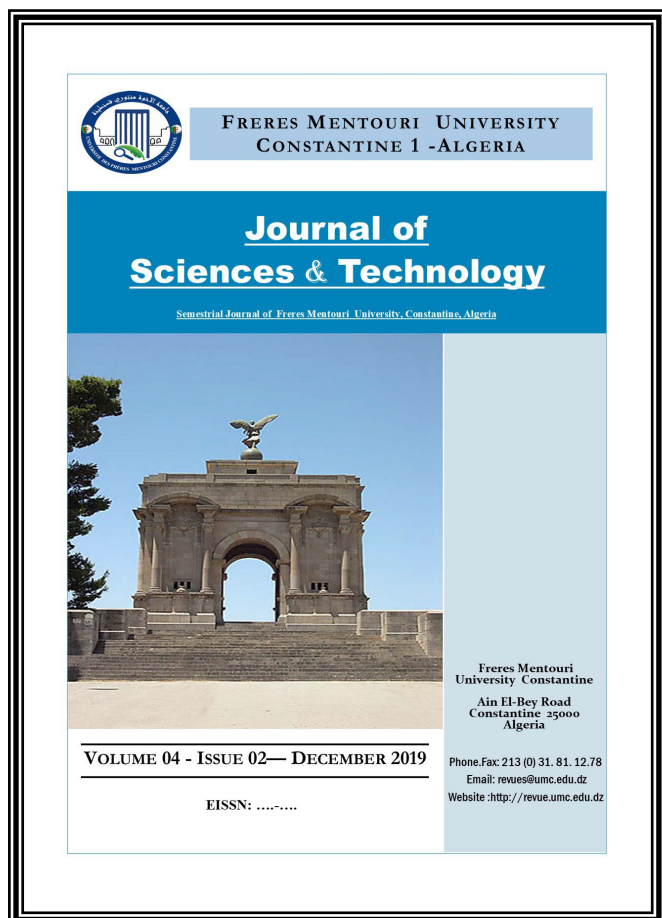
Manuscripts (original and two copies) should be sent to the  
following address:

Vice-Rectorate in charge of Post-Graduation and Scientific  
Research

Direction of Publications and Scientific Animation (15th floor)  
Constantine 1 University , Aïn-El-Bey Road, 25000 Constantine,  
ALGERIA.

Tél./Fax: 213 (0) 31.81.12.78

**e-mail: [revues@umc.edu.dz](mailto:revues@umc.edu.dz)**



---

---

**SCIENTIFIC COMMITTEE**

---

---

|                |   |
|----------------|---|
| D. AISSANI     | <i>Professor, Department of Mathematics, University of Bejaia (Algeria)</i>                                 |
| A. BOUCHERIF   | <i>Professor, Department of Mathematics, University of Tlemcen (Algeria)</i>                                |
| H. HUDZIK      | <i>Professor, Faculty of Mathematics and Computer Science, Adam Mickiewicz University (Poland)</i>          |
| F. REBBANI     | <i>Professor, Department of Mathematics, University of Annaba (Algeria)</i>                                 |
| M.-S. AIDA     | <i>Professor, Department of Physics, Constantine University 1 (Algeria)</i>                                 |
| J.P.CHARLES    | <i>Professor, Laboratory of Experimental Physics, University of Metz (France)</i>                           |
| B. BENYOUCEF   | <i>Professor, Department of Physics, University of Tlemcen (Algeria)</i>                                    |
| S.-E. BOUAOUD  | <i>Professor, Department of Chemistry, Constantine University 1 (Algeria)</i>                               |
| L. CHETOUANI   | <i>Professor, Department of Physics, Constantine University1 (Algeria)</i>                                  |
| D. HAMANA      | <i>Professor, Phases Transformations Laboratory, Constantine University1 (Algeria)</i>                      |
| L. OUAHAB      | <i>Professor, Laboratory of Solid and Inorganic Molecular Chemistry, University of Rennes 1 (France)</i>    |
| R. PENELLE     | <i>Profressor, Director of Research, Laboratory of Structural Metallurgy, University Paris-Sud (France)</i> |
| M. BELHAMEL    | <i>Professor, Director of the Renewable Energy Development Center Algiers (Algeria)</i>                     |
| T. SEHILI      | <i>Professor, Laboratory of Photochemistry and Environment, Constantine University 1 (Algeria)</i>          |
| L. ZOUIOUECHE  | <i>Professor, Laboratory of Asymmetric Synthesis and Biocatalysis, University of Annaba (Algeria)</i>       |
| J.Y. SAILLARD  | <i>Professor, Department of Chemistry, University of Rennes I (France)</i>                                  |
| M. AUCOUTURIER | <i>Professor, Center for Research and Restoration of the Museums of France, the Louvre, Paris (France)</i>  |
| M.A. DIDI      | <i>Professor, Department of Chemistry, University of Tlemcen (Algeria)</i>                                  |
| M. ZITOUNI     | <i>Professor, Department of Mathematics, University of Boumerdès (Algeria)</i>                              |
| N. ROUAG       | <i>Professor, Department of Physics, Constantine University 1 (Algeria)</i>                                 |
| Y. OUKNINE     | <i>Professor, Department of Mathematics, University of Cadi Ayyad, Marrakech, (Morocco)</i>                 |
| D. REYX        | <i>Professor, Laboratory of Macromolecular Chemistry, University of Le Mans (France)</i>                    |
| J. BARBIER     | <i>Professor, Laboratory of Chemistry, University of Poitiers (France)</i>                                  |
| T. SARI        | <i>Professor, Laboratory of Mathematics, University of Mulhouse (France)</i>                                |
| M. BLIDIA      | <i>Professor, Department of Mathematics, University of Blida (Algeria)</i>                                  |
| M. MOUSSAI     | <i>Professor, Department of Mathematics, University Center of M'Sila (Algeria)</i>                          |
| S.L. REVO      | <i>Professor, Taras Shevchenko National University of Kyiv, Ukraine</i>                                     |

## **INSTRUCTIONS TO AUTHORS**

### **I- Overview**

The journal Human Sciences publishes in three languages: Arabic, French and English. Two abstracts must be provided, one in the language of the article, the other in Arabic if the article is written in another language, or in French (or English) if the article is written in Arabic. Abstracts must not exceed 150 words. Unpublished articles are not returned to their authors.

### **II- Manuscripts**

The articles submitted for publication (three copies) must not exceed 20 typewritten pages (tables, figures, graphs, bibliography, ... included) with a large margin to the left (3 cm), printed on 21 x 29 paper, 7 cm (A4) with interline of good readability. Some flexibility is allowed to authors, but they should organize the text clearly in sections such as: Introduction, Experimental Details, Results, Discussion and Conclusion. The longer articles will be published by part in successive issues, each part being determined by the authors. Authors are kindly requested to accompany the summary of their articles with the most complete possible keywords.

In order to save time and respect deadlines for publication, it is recommended that authors take care of the complete capture of their article on a computer, and send it to the journal, after they have been informed. acceptance for publication, in the form of files on CD.ROM, which will be copied by the service.

However, since the final formatting of the article is done by P.A.O. (Computer Aided Publication), the authors are asked to avoid any formatting of their text. It will be necessary to avoid stylizing it.

### **III- Bibliography**

The bibliographic references quoted in the text must include only the reference number in square brackets (ex .: [5]). If the name of the author appears in the text, it must be followed by the reference number. When the reference contains more than two authors, only the first is cited, followed by "and al".

For articles, the complete reference includes the names of the authors followed by the initials of their first names, the title of the article, the title of the periodical (in conformity with the abbreviations allowed), the volume, the number of the periodical, the year of publication and the relevant pages.

For the works, the reference must include the names of the authors followed by the initials of their first names, the complete title of the work, the volume, the volume, the first and the last page relating to the results discussed, the number of the edition if there are several, the name of the publisher, the place and the year of edition.

For scientific meetings (congresses, proceedings, ...), the reference includes the names of the authors followed by the initials of their first names, the title of the communication, the identification of the meeting, the place, the period and the pages concerned.

### **IV- Iconography**

Tables, boards, charts, maps, photographs, etc. must be provided separately, inset. They must be presented on white sheets of A4 format, individually or in groups, and have underneath the words "table" or "figure" assigned a number.

The illustrations and figures must be clear, professionally made and adequate for reproduction: a 50% reduction, if any, must lead to a suitable size and thickness of characters for good readability. Moreover, for computer-generated figures, in order to maximize contrast, the use of a laser or inkjet printer is essential.

Legends assigned their numbers must be grouped in a separate page.

The final presentation of the article will be left to the discretion of the Editorial Board.

## SUMMARY

S  
U  
M  
M  
A  
R  
Y

7

THE WAR MEMORIAL OF CONSTANTINE FACING RISKS AND VULNERABILITY.

O BOUAMEUR AND N CHABI

15

CONSIDERATIONS ABOUT SEISMIC PERFORMANCES UPGRADING OF RC BUILDINGS USING CFRP WRAPPING.

K. DROUNA, N. DJEBBAR

23

APPLICATION OF THE ANALYTICAL HIERARCHY PROCESS (AHP) FOR LANDSLIDE SUSCEPTIBILITY MAPPING IN THE EAST REGION OF CONSTANTINE, NE ALGERIA.

N. MANCHAR, CH. BENABBAS, F. BOUAICHA AND K. BOUFAA

35

ESTIMATION FOR BOUNDED SOLUTIONS OF INTEGRAL INEQUALITIES SOME NEW NON-LINEAR RETARDER INTEGRO-DIFFERENTIAL INEQUALITIES.

M.E SMAKDJI AND H. KHELLAF

47

STUDY OF PLASMA-DEPOSITED LAYERS OF W-TIN ON CUTTING TOOLS.

A. DJERIBAA, E. FERKOUS, N. SAOULA AND I. AMARA

# THE WAR MEMORIAL OF CONSTANTINE FACING RISKS AND VULNERABILITY.

Submitted on 09/05/2018 – Accepted on 10/11/2019

## Abstract

The war memorial of Constantine is in a state of advanced degradation; despite its major importance, the monument and its surroundings are facing devastating factors that alter both its invaluable values and authenticity. So, what are the main factors that caused this degradation? Initially, the degradations noticed are due to a set of risks. The in situ survey conducted as well as the comparative study confirmed the presence of risks on the site through the identification of nine natural and anthropogenic hazards. Furthermore, the cross-examination of the data obtained from the subsequent studies showed that the damage of the risks influenced the monument in two forms: physical and functional. In conclusion, the effect of the damage increased the degree of vulnerability of the monument.

**Keywords:** Hazard; Degradation; Risk; Vulnerability; Heritage value; the war memorial of Constantine.

**O BOUAMEUR  
N CHABI**

Department of Architecture,  
University of Constantine 3  
Salah Boubenider, Algeria.

## I- INTRODUCTION

Today, disaster risk tends to increase. This situation is due to many factors such as accelerated urbanization, the demographic factor and climate change. For this reason, disaster risk reduction remains a major concern in the current scientific debates. Today, and like the other components of the urban setting, architectural heritage is increasingly exposed to several risks, posing a real threat to its heritage values, integrity and authenticity. Because of its fragility and age, architectural heritage properties seems to be much more vulnerable to the harmful effects of risks than contemporary built objects, designed according to security standards, and using the new technologies. However, in spite of the great importance given to architectural heritage properties as a real engine for the socio-economic development of the communities, some of them are completely neglected. They are facing the wear and tear of time, as well as the manmade destructive actions, which accelerated their deterioration and sometimes lead to their irremediable loss. Recent events showed the dramatic damage caused by risks on world heritage properties. For example, the historic center of the city of Bam, destroyed by the earthquake that hit the city in 2003. Moreover, the rich cultural heritage in the coastal provinces of Sri Lanka was also ravaged in 2004 by a tsunami; besides, the traditional church of New Orleans, was destroyed in 2005 after the hurricane of Katrina ... etc. This situation is perceived as paradoxical; heritage assets which are highly important for the humanity should be well protected by risk and heritage managers, through the implementation of preventive measures and appropriate strategies to reduce the hazard's effects on these assets. At the local level, this kind of situations was raised on a colonial architectural heritage, which is the war memorial of the city of Constantine. Dating back more than eighty-seven years, it is considered as one of the most symbolic landmarks of the city, due to its precious values and authenticity.

Nevertheless, it is in a state of advanced degradation, affecting both the physical aspect and its intangible dimension. Because of its abandonment by the authorities and the citizens, it suffers the harmful effects of many factors, causing considerable damage to its site. Therefore, a question arises: What are the factors responsible for the current degradation of the war memorial of Constantine? The aim of this study is to highlight the severity of the damage that affected the war memorial, and how the negligence of the authorities reinforced that. Then, to identify the factors which caused the degradations, while verifying its relationship with the risks. Finally, to identify the influence of the damage on the monument's degree of vulnerability.

The war memorial of Constantine is located near the university hospital center of Constantine, on the edge of the cornice, and on the heights of the old rock "Sidi M'cid" of nearly 700 m. It is recognized by its imposing urban site, which overlooks the old bridge of "Sidi M'cid", and offers an unobstructed panoramic view on the outskirts of the city (fig.1). Moreover, it benefits from an exceptional sunset that highlights the picturesque city of Constantine. With its singular characteristics, this site has been chosen to sublimate the architectural work.



Fig. 1. The panoramic view from the monument. (2013)

## II. METHODS & TOOLS

In order to achieve the above-mentioned key objective, the study was divided into three distinct parts, while all parts aim to a secondary objective. Each part will serve as a support for the unfolding of the next part. Therefore, the parts are interdependent and carefully combined. The three parts of this study are as follows:

### A. The determination of the heritage values of the monument

Each heritage object should be preserved and valued because for its very positive influence on many aspects of the way a community develops. This refers mainly to its valuable heritage values and to his capital as an excellent local educational resource for people of all ages. For this reason, before proceeding to the protection of the monument against the risks that it incurs, this part will estimate first the importance of this heritage for the city of Constantine, by detecting its heritage values and identifying how they can be a proven source of benefit to local economies. It concerns also the specification of the consequences of its loss or forgetfulness. *"The war memorial of Constantine holds a capital of interest and sympathy that far exceeds Constantine"*. [1]. The methodological tools to support this study are as follows: an analysis of the documentary content relating to the war memorial, including press articles, the archives of the city of Constantine, a field survey, the testimony of officials, associations and the citizens of the city.

### B. Comparative study: survey of deteriorations

In order to figure out the origin of the degradations raised on the monument and its surroundings, it is essential to identify all the deteriorations that affected the monument since its construction, as well as the moment and the place of their appearance. To carry out this work, a comparative study took place between the original physical aspect of the monument and its present state. The methodological tools used in this section are analysis of the documentary content, direct observation, architectural study of the monument, pathological survey, architectural survey, old photographs. To ensure accurate identification of the deteriorations, the perimeter of the study was divided into four main zones, containing the important parts of the monument. These parts are the exterior facades, the interior of the monument: the niches, the walls, the staircase, the decoration and the exterior layout: statue of victory, orientation table, side esplanades, access stairs, and immediate environment: road, green spaces.

### C. Survey of hazards

The Final part consists on the verification of the presence of all kinds of risks in the monument and its surroundings. This step is essential because it will precise the relationship between the appearance of the degradations and the occurrence of the risks. The main support used to carry out this study is the theoretical risk grid, which contains a set of hazards that can affect any heritage property. The presence of each type of hazard mentioned was checked at the monument and its surroundings using press articles, testimonials from citizens, associations and specialists, field visits, the vulnerability map of Constantine, and the expert study "Simecsol".

## III. RESULTS

### A. heritage values

The study of the monument's heritage values revealed the following results:

- **Historical value**

This value refers to the important historical event that the war memorial commemorate, which is the First World War (1914-1918). The monument was erected to the glory of the 844 soldiers of all faiths who died for France during this war. In fact, this historical event of massive devastation and loss of lives changed the history of the entire humanity. However, it stills alive due to this monument; it constitutes an immortal witness that transmits this important history from one generation to another. Moreover, this monument is exceptional, because it is the first war memorial of France to be built (fig.2).



Fig. 2. *Celebration of the memory of soldiers who died during the First World War. (Doumergue, 1930).*

- **Architectural value**

The monument remains a piece of art. As an arch of triumph, it is characterized by a colossal architectural style, particularly inspired by the arch of "Trajan" situated in the city of Timgad. It is also recognized by the rich architectonic elements of the Roman architecture such as column, bay, capital ... etc.). Besides, it is marked by a set of impressive decorative elements especially the statue of victory and the orientation table. In addition, the choice of noble materials is refined for its edification like carved stone, bronze ... etc. (Fig.3).



Fig. 3. *Architectural composition of the monument (Kherouatou, 2015)*

- **Economic value**

The monument is a valuable asset for the city, because it is a proven source of benefit to local economies, particularly through tourism. (Fig.4). Due to its high environmental quality, architectural style and its particular urban site, it contributes in the increasing of tourist attractiveness of Constantine; *"The war memorial is a real tourist stop and one of the jewels of tourism in Constantine for both foreign and domestic tourists"*. [2].



Fig. 4. *Frensh tourists visitng the monument (2017)*

- **Social value**

The urban environment of the monument promotes encounters between the citizens and social inclusion of the community. Thus, many associations organized several social events, and selected the monument and its surroundings as the appropriate venue for its course. Some of these social events are the ceremonial event of the release of balloons, Qwhet el Asser, Ramadhan evenings ... etc. as a result , the monument can offer a true area of relaxation and family reunification, through the solidifying of social ties between all social categories, and offering some opportunities to meet new people. (Fig.5).



Fig. 5. *The social event « the release of balloons ». (2013).*

- **Cultural value**

From another side, the natural majestic site where the monument is built endows it with an exceptional spiritual dimension, which constitutes a source of inspiration for many artists of the city including photographers. For others, the site of the monument is an open-air theater that can expose their artistic creativity. (Fig.6).



Fig. 6. *"The Bridge Symphony", hosted by the National Orchestra. (D.R ,2015)*

- **Political value**

The extent of the historical event that the monument commemorate goes far beyond the Constantine region, and even the national borders. The monument testifies a common history, shared between Algeria, France, and Germany because these three nations are concerned by the great world war (1914-1918). At Final, this war memorial can strengthen cooperation, exchange and international political relations between these nations. (Fig.7).



Fig. 7. *Ambassadors of the Three Nations Celebrate the Commemoration of the Armistice 1918. (Oudina. 2015).*

## B. The comparative study

The comparison between the original physical aspect of the monument and its present state ended with the identification of several modifications that the monument undergone. The raised changes are the result of indeterminate factors, as well as some actions made by citizens, associations and authorities. First, the impairments observed in each of the above-mentioned parties are as follows:

- **Exterior facades**

Graffiti on facade surfaces; the deterioration of the stone; many breaks on the stones particularly in the base; the dedication above the columns is no longer visible; the use of inappropriate paints on certain parts of the facades.

- **Interior space of the monument**

Existence of graffiti on the interior walls; the corrosion of the bronze plates, aging and breakage of some parts of the bronze plates. The disappearance of a big part of the central bronze plate; Dirt on the walls, on the floor of the interior

niches, and on the stairs; the removal of the lock of the staircase, the breaks and the degradations of the steps.

- **Decoration and landscaping**

The corrosion and the presence of graffiti on some parts of the statue of victory. Traces of delinquent acts: drug use and alcoholic beverages, suicide attempts...etc. The destabilization and breakage of the support that maintain the orientation table. Acts of vandalism on the map using sharp tools. The subsidence of the platforms in several parts of its esplanades. The breaks on the retaining wall and access stairs on the left. Sanitation problem caused by the closure of the inlets with cement.

- **Immediate environment**

Because of the low attendance in the monument, the visitors of the university hospital center transformed the access road into an illegal parking; thus, the massive loss of many trees in the upper part of the stairs leading to the "Sidi M'cid" bridge. Consequently, the beauty of the site is greatly altered. Moreover, the construction of an illegal habitat (makeshift housing) close to the monument.

On the subject of the actions undertaken by the citizens, associations and the authorities, they aimed at the rehabilitation of the monument in order to improve its current state and eliminate as possible the previous degradations. These actions were organized within the framework of volunteering, and they concerned: the washing and the painting of the graffiti found at the exterior facades and the interior walls of the monument; the operation of afforestation at the level of the green spaces surrounding the monument in order to replace the lost trees. On the other side, the authorities launched other actions, particularly in 2015, for the urgent rehabilitation of the monument, because in 2015, the city of Constantine hosted two major events, which are : Constantine, the capital of Arab culture in 2015, and the celebration of the armistice of 11 November 1918. The operations made to the monument and its surroundings are as follows: the substitution of the central bronze plate by a Marble plate; The covering of one of the internal niches built with authentic stone by faience; The painting of the statue of victory; the cleaning of the site, the lighting of the site, installing a police patrol for safety, laying garbage bins, installing barriers to prohibit illegal parking.

### C. The survey of risks

The study referring to the verification of hazards, based on the theoretical risk grid showed the presence of nine several hazards, of different origins. The following presentation of these hazards is made in chronological order: according to their moment of occurrence from the oldest to the most recent.

- **landslide (1930)**

This hazard is the oldest, since the monument was erected. "In 1930, at the time of its inauguration, the monument was already subjected to a geological problem related to the rock" [3]. Over time, this problem has become worse, creating very visible deformations in different parts of the site. According to Benabass [4], their appearance refers to two major reasons: first, the delicate position of the

monument on the natural limits of a "mega-block" of the rock, which is out of step with the second. This part of the rock is the most vulnerable, because it is subject to strong pressure. In addition, the presence of ancient limestones, as well as the circulation of warm waters loaded with Co2 (a weak acid) inside the rock, allowed the creation of empty internal cavities of a very weak structure. The natural fracture of its faults resulted in continuous subsidence (fig. 8), responsible for the destabilization of the structure of the monument. This situation was exacerbated in 2009, due to the shearing of the trees in the back part, on the pretext that they prevent the lighting of the site, but these trees strengthened the soil and contributed to the reduction of this phenomenon.

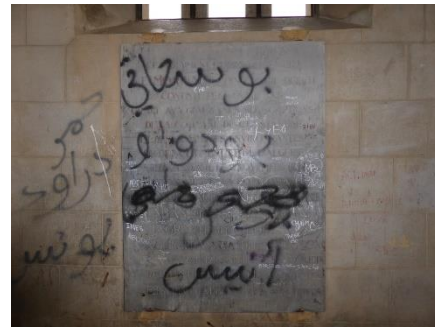


Fig. 8. Plan of the architectural survey on the location of the deformations at the level of the monument (2015).

- **Non-recognition of the monument as a "heritage"**

Until now, the monument is not registered in the national list of cultural heritage, it is still considered as a French legacy. Therefore, neither a patrimonialization process has been scheduled for the monument, nor a development program or budget was dedicated for its protection. The authorities neglected this war memorial for a long time, and even abandoned it to the destructive actions of man and nature, engendering other types of risks with a much more serious effect.

- **Insecurity and bad attendance (1990-2014)**

The abandon of the monument by the authorities and the citizens for a long time, transformed it into a meeting place for delinquents. For more than sixteen years, he suffered many social evils. The absence of guarding and the law attendance of the site favored the frequentation of the offenders and the insecurity. "Groups of young people are hiding in certain corners to consume drugs and alcoholic beverages, with impunity, and all the knife brawls that can occur." [5] Consequently, the idea of going to the monument under penalty of aggression was perceived as a dangerous initiative: "it was too risky to pass even in the vicinity" [6]. This risk has affected negatively the reputation of this highly symbolic site of Constantine, and reduced its attractiveness to tourism.

- **Vandalism (1990-2014)**

Many parts of the monument have suffered serious acts of vandalism: the interior walls of stone, the bronze plaques, and the exterior facades have been deformed by insolent graffiti (Fig. 9). In addition, the recently installed marble slab

and the bronze plates were vandalized using sharp tools. Furthermore, the lock that closed the stairwell was broken off to reach the ridge. Even the orientation table in the posterior esplanade has been seriously damaged: its support suffers from instability due to an attempt to pull it out, and the map has been disfigured with white weapons (fig.10). The impact of such actions is considerable; they jeopardize its authentic original appearance, and accelerate its natural deterioration.

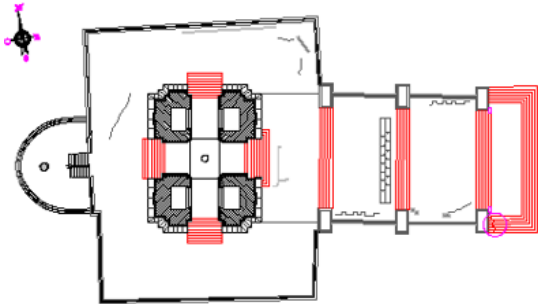


Fig. 9. Vandalism on one of the interior plates by graffiti (2013).



Fig. 10. Vandalism on the orientation table (2017).

• **Climate factors**

The war memorial is exposed to several adverse effects due to climatic factors. First, heavy precipitation, especially during the winter, blocks the only mechanical access leading to the monument with a large area of stagnant water. This phenomenon made the access to the monument impossible, particularly for tourists. In addition, this precipitation aggravated the problem of landslides by activating the movement of land. Moreover, the climatic effect has accelerated the corrosion of the bronze of the interior plates, as well as the statue of victory (fig.11). Due to its chemical composition containing more than 54% copper, it oxidizes with atmospheric air under the effect of moisture and carbon dioxide, creating a layer of a color called "patina" Or "grey screen". The consequences of this chemical reaction on the state of the metal are important: "A bronze statue of 70 years has lost on average 10 to 20% of its metal" [7]. This is the case of the monument, which dates back more than 85 years.



Fig. 11. The corrosion of the statue of victory (2013).

• **Environmental pollution (1990-2014)**

According to the survey, there are two types of pollution in the monument's site, which are visual and olfactory. Starting with the olfactory pollution; because of the absence of regular maintenance and cleaning for the different parts of the monument, especially the interior spaces, it has turned into "public urinal". In addition to the staircase and the interior walls, "the four niches under the arch and the walls covered with obituary registers of bronze, have become urinals» [8]. The interior spaces of the monument are filled with unbearable dirt and ammonia odors (fig.12). Concerning the outside environment, the visual pollution refers to the garbage bins, which are never collected regularly by the rippers. The associations or the citizens mostly handle this mission. Furthermore, the presence of a precarious habitat approximately to the monument, built of makeshift materials created a remarkable mess at the site. All these forms of pollution undermined the particular urban view of the monument, and affected negatively its reputation.



Fig. 12. Dirt in the inner niche (2013).

• **Fire (2013/2016)**

In October 2013, a fire destroyed a big part of the undergrowth situated in the lower part of the staircase joining the monument to the "Sidi m'cid" bridge. A plenty of centuries-old trees of all kinds were burned by fire and disappeared. The same accident occurred one more time in July 2016. Although these fires have been controlled without causing direct damage to the monument, the risk of fire is nevertheless present with a high possibility of occurrence, putting in danger the monument itself and / or its surroundings. Whether it is of human or natural origin, fire remains among the most difficult risks to control due to its rapid spread, and the irreversible damage that it can cause.

- **Theft (2014)**

On January 23, 2014, the Commemorative plaques of bronze were severely massacred by some persons who seized the opportunity of the Algeria-Tunisia match during the African Cup to execute their crime. Using a chainsaw, two of the eight commemorative bronze plaques were torn off. A Street light powered the electric saw used in this act. Therefore, this highly historic site has been disfigured, becoming unrecognizable. The plates are unrecoverable after passing them into a foundry of copper traffic. The former mayor of Constantine stated: "We are consulting with the heritage commission of the municipality in order to call on experts and historians to provide us with the exact names of all soldiers who appeared on the missing plate. Even so, it is a hard job, but we are going to do it." [9] This irreversible loss is very serious, because it has affected the most important part of the monument. The bronze plaques represent the main reason for the edification of this monument. Certainly, a restoration will allow the recovery of the missed plate, but only in its physical aspect. The authenticity and the originality are lost forever. In fact, this kind of risks is due to the abandonment, bad attendance, and particularly the absence of security at the site. The night watchman of the monument is retired, but the municipality has not assigned a replacement to protect this war memorial. (Fig.13).



Fig. 13. *Stolen Central Bronze Plate (2013).*

- **Inadequate processing operations (2015)**

This risk is the most recent. It appeared mostly during the preparations for the celebration of the 1918 armistice at the level of the monument, which was planned on November 11, 2015. After a long period of abandonment, the commune, in collaboration with the French Embassy in Algeria, undertook a plenty of operations aimed at its rehabilitation. The main operation consisted of a restoration: the lost bronze plates were replaced by others in marble, bearing the same names of the soldiers. In fact, according to Eugène Viollet-le-Duc, the restoration of a building "is not to maintain it, to repair it, or to do it, but to restore it to a complete state that may never have existed." [10]. thus, the restoration consists of the refurbishment of the object, and returning it as close as possible to the original state. However, it was not the case in the restoration of the monument; the marble used does not match with the original bronze (fig.14). This failed operation lead to a disfigurement of the site. The identity of the monument was altered after causing this discordance with the original state. A similar situation in a city renowned for its craftsmanship of brassware and the massive availability

of copper arouses a lot of debate. This kind of operations was repeated for the interior walls of the monument after the installation of a faience cladding, above the authentic stone. In addition, the painting of the statue of victory to hide the effect of corrosion, which completely changed the original color. Such actions seem futile and harmless, but in reality, they seriously jeopardize the monument's heritage values, in particular its integrity and authenticity. These two fundamental elements constitute its importance and at the same time entail its safeguarding.



Fig. 14. *Marble plaque replacing the stolen central bronze plate (2017).*

As well, to ensure the safety of the monument and the visitors, a police patrol was permanently installed (Fig.15). Certainly, delinquency has disappeared and the citizens are safe, but its remarkable location gives the visitor a feeling of fear and dangerousness, which makes the monument much less attractive. The ideal solution would be to revitalize it, by giving it a use value, that refers to the participative social activities and animation. This kind of functions allows the installation of a set of infrastructures that encourage the regrouping of people such as cafeterias, restaurants ... etc. In this way, the site will be more lively, attractive, and secure.



Fig. 15. *Installation of a police patrol (2017).*

## VI. DISSCUSIONS

In conclusion, the study carried out on the identification of the monument's heritage values revealed the following points:

### A. *The variety*

The war memorial of Constantine contains an invaluable variety of values, which concerns different aspects. In fact, they can be grouped into two distinct categories.

- **Values of existence** : they refer to the historical and the architectural value.
- **Values of use** : represented by the social, economic, cultural, and political value.

**B. The war memorial: an engine for the development**

The values of the monument are a valuable asset for the city, because of its important role in the city's cultural and socio-economic development, thus they can make a very positive contribution in improving the quality of life of the citizens. Furthermore, the attractiveness of the historic environment of the monument assists in attracting all types of external investment not only the tourism. Besides the current study showed how the monument could be a potent driver for the community action.

As for the comparative study, the degradations raised in the form of alterations affect the war memorial in two different forms, according to the type of their impact, namely:

**A. Physical impact**

- The alteration of its physical integrity.
- Defacement of the original architectural identity of the monument, as well as its materials such as stone and bronze. This leads to the loss of its authenticity.
- Degradation of its environmental quality.

**B. Functional impact**

- Downgrade the war memorial by putting at risk its irreplaceable heritage values.
- These deteriorations reduce its attractiveness to tourism, even its abandonment, which leads to the insecurity and bad attendance.
- The deterioration of an important part of history without its evanescence can lead in the long term to its forgetfulness.

Regarding the survey of risks, the verification of their presence was positive, and the risks identified can be classified according to two criteria: the origin of the hazard, which is natural and anthropogenic, as well as its process of slow or rapid development:

**C. Primary hazards**

With a catastrophic effect, characterized by a low frequency and speed occurrence, but their impact is rapidly perceived.

**D. Secondary hazards**

Characterized by a slow and gradual occurrence process. Their impact is not immediately perceived, it evolves over time.

| Natural origin                                       | Anthropogenic origin  |
|--|---|
| Geological risk: landslides; Climatic factors; Fire. | Legal risk: the non-recognition of the monument as a heritage; Insecurity and bad attendance; Vandalism; Theft, inadequate processing operations. |

Table 1. Classification of risks according to the origin of hazards

| Primary hazards  | Secondary hazards  |
|--|--|
| Fire ; Inadequate processing operations; Vandalism; Theft. | Geological risk: landslides; Legal risk: the non-recognition of the monument as a heritage; Insecurity and bad attendance; The climatic factors. |

Table 2. Risk classification according to the hazard development process.

On the other hand, the matching of the data obtained from the comparative study (the nature of the degradations, the place and the time of their appearance), and the survey of risks, (Place and time of occurrence) is identical. Degradations occur simultaneously with the risks. This situation validates the statement of the hypothesis and confirms that the degradations are generated by the risks.

Finally, the impact of the damage caused after the occurrence of the previous risks has considerably increased the vulnerability of the monument. Beyond the factors of time and the authority's negligence, the degree of vulnerability depends also on the occurrence of risks and the resilience of the monument.

**V. CONCLUSION**

By way of conclusion, the objective of this study is achieved. The hypothesis is tested and found to be correct, and the study brought a new knowledge about this monument. It showed the inestimable importance of this architectural work for all humankind, revealing its wealth in terms of values. Furthermore, it highlighted the harmful impact of the raised degradations on the integrity and the authenticity of this monument, and its relation with the degree of vulnerability. It has also identified the factors that are at the origin of their appearance, and which are natural and anthropogenic risks, in the course or slow process. Moreover, the results of this research can be used in a practical implication. This study is the preliminary and the fundamental phase in the implementation of a strategy to manage the disaster risks to which this monument is exposed. The identification of risks and their assessment is the first step in the process of disaster risk management. The war memorial of Constantine is one of many other cases that suffer daily from the devastating impact of the risks. Although there have been several international actions to reduce the impact of risks on built

heritage properties, it is still insufficient in the absence of a framework for coordination and exchange of experiences among nations. Therefore, it is highly important that risk managers take charge of built heritage, and dedicate the necessary human and financial resources to ensure its protection from all kinds of hazards, and reduce their harmful impact on its values. Consequently, heritage properties will have a longer life and the future generations will have the opportunity to discover their history.

### ACKNOWLEDGMENT

We are grateful to Pr. BENABBASS Chawki and Pr. SAHRAOUI BELABED Badia for insightful discussions, and we would like to thank CHAFI Sara and TAIB Hania for their assistance in data acquisition.

### REFERENCES

- [1] S. Gilard, Constantine d’hier et d’aujourd’hui [Online], Constantine.2017 [cited in: February 05. 2017], Available : [http://www.constantine-hier-aujourd'hui.fr/LaVille/monument\\_aux\\_morts](http://www.constantine-hier-aujourd'hui.fr/LaVille/monument_aux_morts).
- [2] I.T, a quand la réhabilitation du site ? Le monument aux morts fortement dégradé”, Le temps d’Algérie [Online], March 04. 2009, [cited in: January 22. 2017], Available : <http://www.djazairess.com/fr/letemps/11089> .
- [3] B. Sahraoui Belabed , professeur at the faculty of architecture and urban planning of Constantine.
- [4] C. Benabbass, professeur at the faculty of earth sciences and geography of Constantine.
- [5] A.Selmane, “Jeux dangereux au Monument aux morts Constantine”, El Watan [Online], January 15. 2015, [cited in: January 16. 2017], Available : <http://www.djazairess.com/fr/elwatan/47812> .
- [6] A.Selmane, “ Monument aux morts de Constantine : un site qui s’offre une seconde jeunesse”, El Watan [Online], August 15. 2015, [cited in: January 16. 2017], Available : <http://www.djazairess.com/fr/elwatan/501572>.
- [7] C. Payer “Les bronzes urbains : Patine ou corrosion”, le patrimoine vert, n°21, pp. 48–48, 1983.
- [8] G.Seguy, “ Le monument aux morts de Constantine ”, La mémoire vive, Historical Documentation Center on Algeria, n°47, Aix en provence. 2011.
- [9] B.Driss , “ profanation du monument aux morts a Constantine irréparable”, La liberté [Online], february 28. 2013, [cited in: March 03. 2017], Available : [http://www.constantine-hier-aujourd'hui.fr/LaVille/monument\\_aux\\_morts.htm](http://www.constantine-hier-aujourd'hui.fr/LaVille/monument_aux_morts.htm).
- [10] E.E. Viollet-le-Duc, Stichwort “Restauration”, In : Dictionnaire raisonné de l'architecture française du XIe au XVe siècle, Paris 1854-1868.

## CONSIDERATIONS ABOUT SEISMIC PERFORMANCES UPGRADING OF RC BUILDINGS USING CFRP WRAPPING.

Submitted on 11/04/2018 – Accepted on 16/12/2019

### Abstract

Knowing that the rehabilitation practice in Algeria is not codified yet, the principal aim of this paper is to evaluate seismic performance of retrofitted reinforced concrete buildings by CFRP wrapping using a Pushover analysis to estimate the structural capacity in both strength and ductility. A nonlinear analysis is conducted on a series of low-rise buildings with poor concrete strength of their vertical components where the CFRP wrapping is adopted as a rehabilitation solution. An explanation of the simulation work before and after the retrofitting operation is given through the modeling approach of the nonlinear sectional behavior based on a combination of confining effects, helping in Moment-Curvature analysis and user defined plastic hinges modeling. Finally, seismic performance enhancement is evaluated in local and global behavior considering several structural criteria.

**Keywords:** CFRP wrapping, pushover analysis, seismic retrofitting, Plastic hinge.

K DROUNA<sup>1</sup>  
N DJEBBAR<sup>2</sup>

<sup>1</sup> Civil Engineering Department, University Freres Mentouri Constantine, Algeria.

<sup>2</sup> Civil Engineering Department, LMDC, University Freres Mentouri Constantine, Algeria.

### INTRODUCTION

The primary objective of this paper is to evaluate seismic performance of vulnerable low rise reinforced concrete buildings having poor concrete compressive strength for their well reinforced columns by using nonlinear static procedure. For that, a series of typical regular building has been considered. This work is conducted in order to situate how much such buildings are safe against earthquake attack. After evaluating the seismic capacity of buildings, the resulting damage is assessed. The obtained results showed that all the columns of the considered buildings will lose their structural stability since their resistance capacity was found insufficient comparatively with what is required by the Algerian seismic regulation (RPA99 version 2003). Because of this, a retrofit solution is needed in order to enhance both resistance and ductility capacities. The use of jackets around existing deficient columns induces lateral confining stresses in the concrete as it expands laterally in the compression zone as a function of axial compression strains or in tension zone as a function of dilatation of lap splices under incipient splice failure. Since CFRP wrapping of vulnerable elements partially or completely present a preferable solution for seismic performances upgrading regarding its simplicity, rapidity of execution and immediate performances enhancement, this retrofitting technique is used. The needed clarifications related to the numerical modelling of the doubly confined concrete of the rehabilitated buildings are introduced. A particularity is addressed to the influence of the axial load intensity which can be satisfied despite the low compressive strength leading by the way to an under-estimation of the severity of the problem if the verification is focussed on the resistance capacity only. The importance of the axial load strength

cannot be ignored while considering the local and global ductility since it has a more defining role in failure mechanism and energy dissipation under seismic action.

### 1. BACKGROUND FOR NONLINEAR ANALYSIS

In recent years, a breakthrough of simplified Nonlinear Static Procedures has been observed. These nonlinear static methodologies were initially proposed and verified for seismic assessment and retrofitting of buildings. Owing to their simplicity compared to the inelastic dynamic analysis, they were implemented into the modern guidelines and codes (ATC-40, FEMA 273, FEMA 356 and CEN, 2005). Well known as a simplified method for buildings seismic behaviour modelling, inelastic static analysis commonly referred to as the pushover analysis is widely adopted by researcher's community [1,2] where nonlinear behaviour of buildings is represented by plastic hinges assigned to critical sections.

The pushover analysis can be conducted using finite element software that take into account both geometrical and material nonlinearity, but the result's precision is directly influenced by the input data especially in post-elastic behaviour modeling. Sectional analysis must represent the most possible realistic state of the elements since shear and flexural behaviour of critical sections can change the global response of the building hence its performance. Shear effects are generally neglected and the nonlinear behaviour of buildings is represented only by moment hinges. Also assigned plastic hinges conditioning the nonlinear global response of the building needs more caution and precision. Differences of pushover analysis results due to default and user defined plastic hinges have been studied which results implement the use of user defined plastic hinges [3]. The important number of plastic

hinges to generate varies depending on material properties, reinforcement and axial load level, based on Moment-Curvature analysis of each element. For simply reinforced concrete section, it can be directly issued from one of the finite element software depending on geometrical, mechanical properties and axial load intensity.

However strengthened sections (RC jacketing, FRP wrapping, steel casing,...) needs more focus because of the lack of experimental results or programs to get Moment-Curvature curve in a reinforced concrete element with another confining layer [4]. In this area, a modeling approach for the considered CFRP wrapped sections has been performed in two steps to get Moment-Curvature curves for these composite sections.

## 2. NONLINEAR ANALYSIS OF THE FRAMES

Plastic behavior of the elements was characterized using two nonlinear hinges at the ending member sections based on the lumped plasticity concept. A simplified bilinear moment-curvature curve was used for each plastic hinge. The nonlinear static (pushover) analysis was performed in order to estimate the seismic response of the structures. A finite element analysis program, SAP 2000 [5], commonly used by structural engineering professionals, was utilized to run the nonlinear static analysis.

### 2.1 Nonlinearity section analysis

The moment-curvature properties of the plastic hinges were determined using fiber analysis while considering section properties, reinforcement details and a constant axial load. Axial loads on the columns resulted from dead loads plus 20% of live loads as recommended by the Algerian code of practice for seismic resistant design of buildings [6]. However, beams are purely flexural elements. For the original frames the commonly used confined concrete model proposed by Mander *et al.* [7], was implemented while an elastic perfectly plastic model with parabolic strain hardening was considered for steel. For the steel confined concrete core values of  $f_{cc}$ ,  $\epsilon_{cc}$  and  $\epsilon_{cu}$  according to Mander's model for simply confined RC sections. The ultimate strain of the confined concrete core

$$\epsilon_{cu} = 0.004 + \frac{1.4\rho_{sh}f_{yh}\epsilon_{su}}{f'_{cc}} \text{ is limited to } \epsilon_{cu} = 6\%, f_{yh} = 400\text{Mpa.}$$

For CFRP wrapped sections, the superposition of the analytical effects of external and internal confinement judges reasonably the experimentally obtained response of doubly confined concrete [8]. The Moment-Curvature state of CFRP wrapped sections was obtained through the integration of the nonlinear (M-Ø) response of the individual fibers in which the section has been subdivided. The doubly confined section was analyzed in two steps:

**First**, considering the doubly confined effect of both internal transverse reinforcement and external CFRP wrapping for the hole section, material properties  $f_{cc}$  and

$\epsilon_{cc}$  obtained according to below formula [9] for monotonic loading:

$$\frac{f_{cc}}{f_c} = 1 + 0.7 \frac{\alpha_f \rho_f E_f \epsilon_{uf}}{f_c} + \frac{\rho_w f_{yw}}{f_c} + 0.85 \frac{\rho_{tot} f_y}{f_c} \quad (1)$$

$$\epsilon_{cc} = 0.0035 + x \left( \frac{10}{h(\text{mm})} \right)^2 + 0.57 \alpha_f \cdot \alpha_{eff,j} \min \left[ 0.5, \frac{\rho_f f_{uf}}{f_{cc}} \right] \quad (2)$$

**Second**: the effect of transverse reinforcement for the well reinforced initial section applies to the inside concrete core, the outside concrete cover is assumed to be crushed instantly with CFRP layers; because if the CFRP gives a light confinement and the steel ties a heavy one, the column may survive rupture of the CFRP and reach later an ultimate curvature controlled by the inside concrete core confined by ties [10, 11].

The Moment- Curvature curve for both simply and doubly confined sections has been idealized using the first yield and the ultimate state points corresponding to the performance levels as a fraction of the hinge plastic capacity [3, 12]:

- 10% for the immediate occupancy level corresponding to minor damage,
- 60% for the life safety level
- 90% for the collapse prevention level where non-reparable damage is envisaged [13].

Thus, defining user defined plastic hinges to introduce for the nonlinear analysis.

### 2.2 Plastic hinge length

Plastic hinges occur in RC columns when they are overloaded, particularly under an earthquake excitation. Performance-based design of RC columns also requires the knowledge of plastic hinge length for displacement calculation [14]. Plastic hinge failure can be mitigated by confining columns with a jacket. The length of the plastic hinge zone should be known because flexural jacketing needs to cover the confining region which is function of the plastic hinge length. For ordinary RC columns, the plastic hinge length depends on many factors:

- 1) axial load intensity;
- 2) moment gradient;
- 3) level of shear stress in the plastic hinge region;
- 4) mechanical properties of reinforcement;
- 5) concrete strength;
- 6) level of confinement in the potential hinge region [14].

Many formulas based on analytical or experimental investigations under monotonic or cyclic loading have been proposed. In this context, Park and Priestley [7] suggested the following expression for cantilever columns subjected to an axial load and a lateral force at the top:

$$L_p = 0.08L + 6d_b \quad (3)$$

Paulay and Priestley [15] ameliorated the above equation to account for different grades of flexural reinforcement:

$$L_p = 0.08L + 0.022d_b f_y \quad (4)$$

$f_y$ : yield strength of longitudinal reinforcement.

$d_b$ : is the diameter of longitudinal reinforcement.

Many researchers provided other formula [16, 17] but equation (4) is still the most used regarding its simplicity and good accuracy to experimental results. In this study for the calculation of plastic hinges length for initial structures equation (4) has been adopted. Plastic hinge length for CFRP wrapped members has not been widely mathematically expressed; Gu et al [18] provided the following expression:

$$L_p = L_{p0} + L_{pCFRP} \quad (5)$$

$$L_p = 0.08L + 0.022f_y d_b + \begin{cases} 3.28\lambda_f & \text{when } 0 \leq \lambda_f \leq 0.1 \\ ((0.51 - 2.30\lambda_f + 2.28\lambda_f^2)L & \text{when } 0.1 < \lambda_f < 0.5 \end{cases}$$

(6)

The performance of their model using the previous equation compared to the test results collected from the literature presents acceptable approximation to test results [14]. For that, it is adopted for the calculation of the plastic hinge length for CFRP wrapped columns in this study.

### 3. VERIFICATION OF THE MODELLING ASSUMPTIONS

Before implementing user defined hinges in the push over analysis for the selected structures of the case study, a checking phase is envisaged. Since the effect of the sectional analyses is a primordial step within nonlinear analysis. The obtained modeled plastic hinges are implemented in the pushover using SAP2000 [5] for tested retrofitted or non-retrofitted frames.

These frames consisted of one floor and one span presenting poor concrete strength and low reinforcement ratio, subjected to a pseudo static test before and after CFRP wrapping [4]. The obtained numerical results were compared to test results show acceptable accuracy when simulating the nonlinear static response of RC frames retrofitted for both considered cases. It is to note that frame 2 was retrofitted with partially CFRP wrapping of the column (700mm) in both extremities.

A reduction factor  $r$  was assigned to elements stiffness to consider the antecedent of deformation caused by pushing frame 2 to a displacement of 1% of the total height before applying the CFRP wrapping.

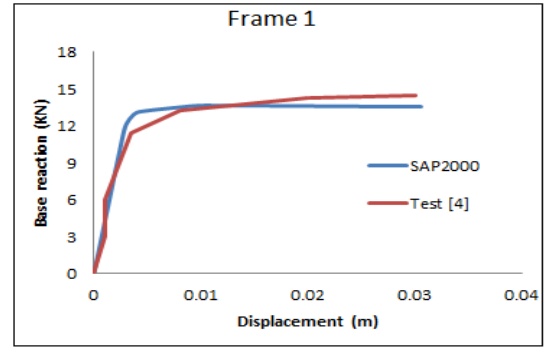


Figure1. Initial frame: simulations/test results

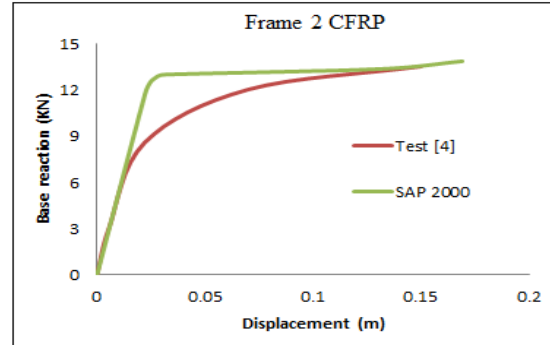


Figure2. Strengthened frame: simulation /test results

- The obtained results show that NL analysis RC frames can give good approximation to test results if more caution and precision are given to different stages of the simulation process especially for sectional analysis, plastic hinges definition and the consideration of cracked stiffness.
- The user defined plastic hinges of CFRP wrapped RC elements obtained by an equivalent Moment-Curvature curve based on two steps sectional analysis gives the possibility to the pushover analysis to approximate reasonably test results.

The second part of the study consists on a numerical investigation conducted on the efficiency of carbon fibre reinforced polymers (CFRP) in improving the seismic performance of RC frames. The evaluation of seismic performance is established through structural criteria to a series of vulnerable low rise buildings before and after the strengthening with full CFRP wrapping.

### 4. CASE STUDY

A series of typical vulnerable low rise buildings constructed after 1999 with poor concrete compressive strength for their vertical components ( $f_{c0} = 15MPa$ ), against well reinforcement according to RPA 2003[6] with steel reinforcement FeE 400 type; presents a particular casual case in construction site of buildings in Algeria. Inelastic static pushover analysis is used for the post-elastic response simulation.

It should be noted that the obtained results while conducting an early investigation [19], aiming to compare inelastic pushover analysis to inelastic dynamic analysis show that the triangular load shape is adequate to predict

the global response of low rise frames and almost an identical response is observed between the dynamic analysis best-fit envelopes and the static response obtained from the triangular and multimodal distributions.

The initial structures are modeled and analyzed by using Sap2000 nonlinear analysis program. A first estimation of seismic performances is conducted through static pushover analysis since the first structural mode of vibration in

dominating. A re-evaluation of the performances using the same technical analysis of the retrofitted considered structures by CFRP strengthening of all columns, using three layers of CFRP SIKA wrap 230C/45 product unidirectional wrap with:  $E = 34\text{Gpa}$ , tensile strength  $450\text{ Mpa}$ , thickness (per ply)  $1\text{mm}$  and ultimate strain  $14\%$  is also presented and discussed.

| Structures | Properties |           |          |                  |                |                |                     |                 |                 |                    |                     |
|------------|------------|-----------|----------|------------------|----------------|----------------|---------------------|-----------------|-----------------|--------------------|---------------------|
|            | Height (m) | Width (m) | Beam (m) | Column (m)       | $f_{c0}$ (MPa) | $f_{cc}$ (MPa) | $f_{cc,CFRP}$ (MPa) | $\epsilon_{c0}$ | $\epsilon_{cU}$ | $\epsilon_{cCFRP}$ | $\epsilon_s$        |
| 3stories   | 09.18      | 12        | 0.3x0.35 | 0.3 x0.3<br>8Ø14 | 15             | 19.64          | 39.95               | 2 ‰             | 3.5‰            | 14‰                | $0.5 \epsilon_{sU}$ |
| 4stories   | 12.24      | 12        | 0.3x0.35 | 0.3 x0.3<br>8Ø14 | 15             | 19.64          | 39.95               | 2 ‰             | 3.5‰            | 14‰                | $0.5 \epsilon_{sU}$ |
| 5stories   | 15.3       | 12        | 0.3x0.35 | 0.3 x0.3<br>8Ø14 | 15             | 19.64          | 39.95               | 2 ‰             | 3.5‰            | 14‰                | $0.5 \epsilon_{sU}$ |

**Table1.** Geometrical, mechanical properties of materials for studied structures

Cracked stiffness was assigned to structural elements according to Paulay- Priestley [16], columns and beams are modeled as nonlinear frame elements with lumped plasticity regions in both extremities and P-M-M hinges were assigned to columns and flexure hinges to beams. The beam-column joints were assumed to be rigid [20].

**4.1 Sectional analyses:**

Results of sectional analyses before and after CFRP strengthening are presented in figure 3.

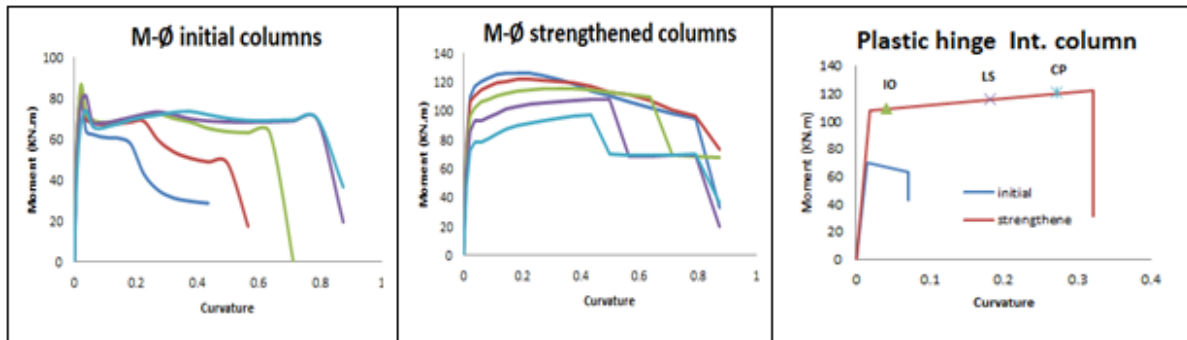


Figure 3. Moment-curvature curves and user defined plastic hinge presentation for internal column.

A moment curvature analyse is carried out considering section properties and constant axial loads. The obtained moment values for different building column sections are gathered in table 2. We can notice that the resistance criterion is not satisfied since the column’s resistance capacity is less than its resistance demand leading to a structural collapse. It is evident that the considered building columns must be retrofitted.

The use of CFRP allowed the enhancement of the sectional state for the initial columns not responding to seismic requirements, from fragile ( $\nu > 0.3$ ) ,characterized by a brittle failure, to a highly ductile state by increasing the compressive resistance capacity, thus lightening the reduced axial load  $\nu$  and increasing the ultimate concrete strain capacity  $\epsilon_{cU}$ .

| Structure | Reduced axial load<br>$P/A_g * f_c$ |                  |             | Moment (KNm)        |             |                 |                |             |                 | Curvature ductility<br>$\mu_\phi = \frac{\phi_u}{\phi_y}$ |             |                 |
|-----------|-------------------------------------|------------------|-------------|---------------------|-------------|-----------------|----------------|-------------|-----------------|---|-------------|-----------------|
|           | v<br>Initial<br>(1)                 | v<br>Wrap<br>(2) | Gain        | $M_F$               |             |                 | $M_U$          |             |                 | Initial<br>(1)  | Wrap<br>(2) | Gain<br>(2)/(1) |
|           |                                     |                  |             | Initial<br>1<br>(1) | Wrap<br>(2) | Gain<br>(2)/(1) | Initial<br>(1) | Wrap<br>(2) | Gain<br>(2)/(1) |   |             |                 |
| 3 Stories | 0.43                                | 0.16             | <b>2.69</b> | 83.10               | 87.73       | <b>1.06</b>     | 69.75          | 110.49      | <b>1.59</b>     | 2.5   | 15.40       | <b>6.16</b>     |
| 4 Stories | 0.57                                | 0.21             | <b>2.71</b> | 75.90               | 103.09      | <b>1.36</b>     | 66.75          | 112.84      | <b>1.62</b>     | 2.26  | 18.04       | <b>7.98</b>     |
| 5 Stories | 0.70                                | 0.26             | <b>2.69</b> | 71.78               | 107.96      | <b>1.50</b>     | 63.86          | 113.32      | <b>1.74</b>     | 2.5   | 17.21       | <b>6.88</b>     |

Table 2: Sectional analyses results.

The increase of columns carrying capacity enhances significantly the local ductility  $\mu_\phi$ , as presented in table 2, which has a positive influence on the overall behavior of the structures.

#### 4.2 Interaction curves:

The examination of the P-M curve interaction for internal column (fig.4), illustrates the enhancement of axial load and moment capacity for the strengthened elements. This is due to the use of unidirectional CFRP tissue that increased the capacity of radial deformation and the flexure strength of the section without influencing the initial stiffness [21].

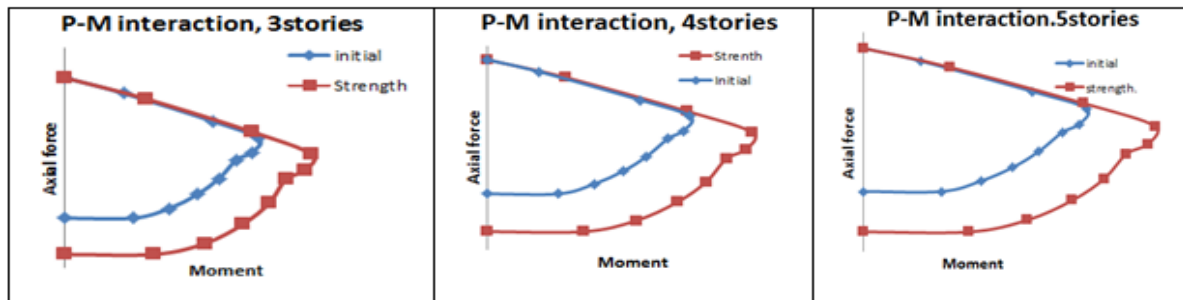


Figure 4. P-M interaction curves before and after intervention

#### 4.3 Structural behavior- Pushover analysis results

##### a- Capacity curves:

Three different damage levels [6] are incorporated within the idealized user defined plastic hinge:

- Minimum damage limits (MN):  $\epsilon_c = 0.0035$        $\epsilon_s = 0.01$
- Safety limits (SL):  $\epsilon_c \leq 0.0135$        $\epsilon_s = 0.04$
- Failure limits (FL):  $\epsilon_{cu} \leq 0.0180$        $\epsilon_s = 0.06$

Relating base shear to roof displacement is presented in figure 5. The CFRP wrapping confers a valuable improvement on the global behaviour through deformation and strength capacities; thus, satisfying seismic performances criteria. The initial stiffness is conserved so the original conception and ductility class remains the same while a great benefit in displacement capacity is registered.

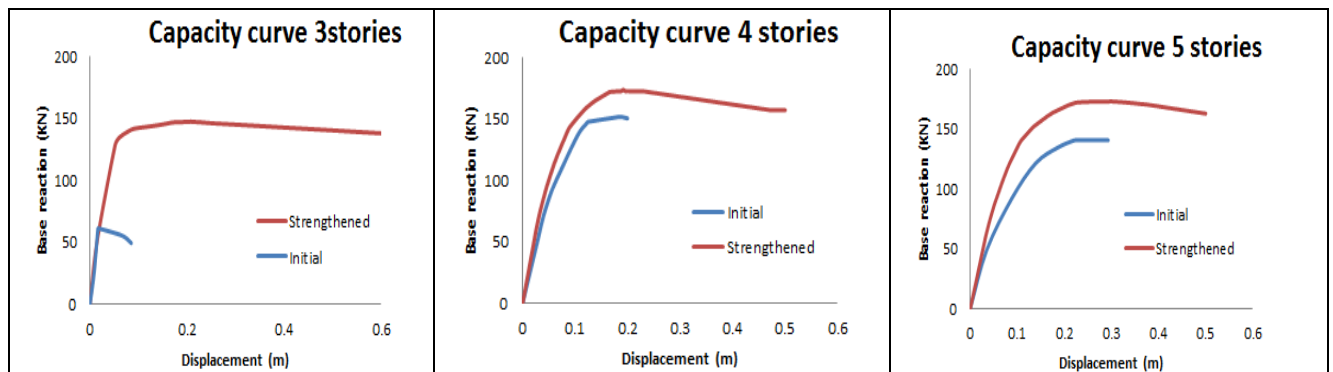


Figure 5. Pushover curves for initial and strengthened structures.

**b- Roof displacement:**

| Structure | Δ.max  |       |             | Δ. 1 <sup>st</sup> LS hinge |       |             | Δ. 1 <sup>st</sup> CP hinge |       |             |
|-----------|--------|-------|-------------|-----------------------------|-------|-------------|-----------------------------|-------|-------------|
|           | before | after | Gain        | before                      | after | Gain        | before                      | after | Gain        |
| 3 Stories | 0.005  | 0.20  | /           | 0.0022                      | 0.13  | /           | 0.00225                     | 0.16  | /           |
| 4 Stories | 0.08   | 0.217 | <b>2.71</b> | 0.04                        | 0.15  | <b>3.75</b> | 0.05                        | 0.175 | <b>3.5</b>  |
| 5 Stories | 0.10   | 0.242 | <b>2.24</b> | 0.05                        | 0.189 | <b>3.78</b> | 0.065                       | 0.219 | <b>3.37</b> |

**Table3.** Registered displacement in different stages of energy dissipation

For all cases, the displacement of 1% building height related to life safety performance level [6] supposed to be satisfied by the initial conception was not achieved. Failure mechanisms appeared before that consideration is attained. The CFRP strengthening permits to satisfy largely the previous condition while delaying the appearance of the collapse prevention level. (for the 5 stories building the first CP hinge appears after major displacement corresponding to 1.5% drift of building height).

**C - Resistance capacity:**

Base shear demand is calculated according to RPA 99, version 2003 (eq. 10). The base shear capacity is issued

directly from the pushover analysis. The obtained results are gathered within table 4.

$$V = \frac{A \cdot D \cdot Q}{R} * W \tag{10}$$

A: zone acceleration coefficient, D: dynamic amplification factor, Q: factor related to materials quality and execution, R: behavior factor and W: total weight of the building. The initial structures present a base shear capacity lower than what is required by the code. The adopted strengthening solution has enhanced the global resistance capacity.

| Structure | Initial structures |           |                 | Strengthened structures |           |                 |
|-----------|--------------------|-----------|-----------------|-------------------------|-----------|-----------------|
|           | Vdemand            | Vcapacity | Remarque        | Vdemand                 | Vcapacity | Remarque        |
| 3 Stories | 110.97             | 60.876    | <b>C &lt; D</b> | 110.97                  | 146.96    | <b>C &gt; D</b> |
| 4 Stories | 150.03             | 140.80    | <b>C &lt; D</b> | 150.03                  | 172.29    | <b>C &gt; D</b> |
| 5 Stories | 179.17             | 146.35    | <b>C &lt; D</b> | 179.17                  | 188.86    | <b>C &gt; D</b> |

**Table 4.** Base shear demand /capacity for studied structures

**d- Failure mechanisms:**

**1. Initial structures**

The registered failure mechanism for initial structures is qualified by the philosophy of seismic design as the most dangerous. It is characterized by concentration of plastic hinges in the columns of the first story with migration of hinges to the top of columns. These later attain the CP performance level (in yellow) for all studied cases before

beams start to dissipate energy. This is a clear illustration of strong beam- weak column state. This severity is much more pronounced when the 3 story structure is considered where the collapse is straightforward (plastic hinges in red). Its great rigidity (squat structure) does not enable it to be dissipative structure energy.

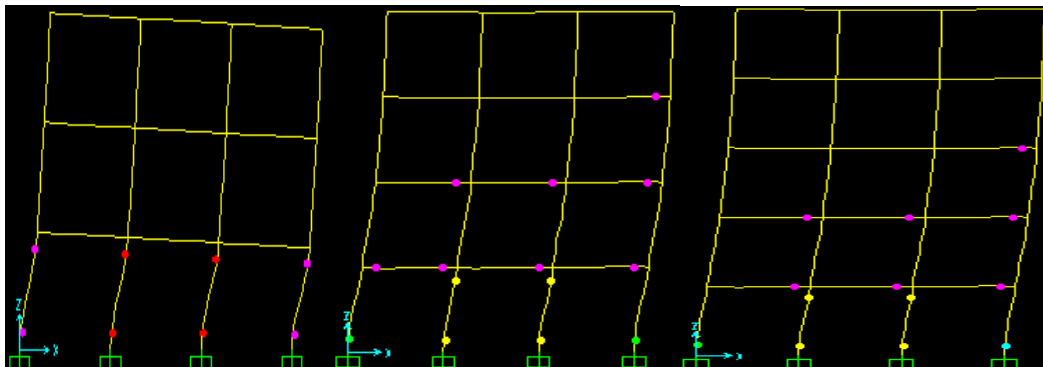


**Figure6.** Sequence of plastic hinge apparition before intervention.

2. Strengthened structures

For CFRP strengthened structures, general improvement in the global behavior where a participation of more members in the energy dissipation process is noticeable. The life safety performance level related to the Algerian seismic code (characterized by a 1% drift displacement) is achieved without any plastic hinge in columns. Pushing to collapse, the participation of upper floors beams in the dissipating process is remarkable (immediate occupancy level in blue and life safety in light blue). The failure mechanism is reached by appearance of CP hinges in both extremities of beams while some hinges at the top columns, exceed slightly the yielding limit (hinges in pink).

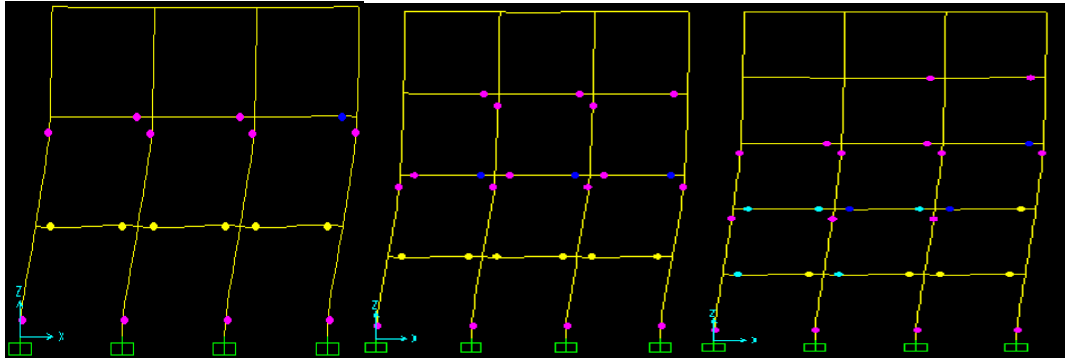


Figure7. Sequence of plastic hinge apparition for strengthened structures

4.4- Reinforcement exploitation:

| Performance level | Steel strain. before |          | Observation            | Steel strain. after |        | Observation                                  |
|-------------------|----------------------|----------|------------------------|---------------------|--------|--|
|                   | LS                   | CP       |                        | LS                  | CP     |  |
| 3 stories         | 2.13E-03             | 8.26E-03 | $\epsilon_{sy} = 10\%$ | 0.0355              | 0.0424 | $\epsilon_{sy} < \epsilon_s < \epsilon_{su}$ |
| 4 stories         | 1.67E-03             | 6.71E-03 | $\epsilon_{sy} = 10\%$ | 0.0317              | 0.0443 | $\epsilon_{sy} < \epsilon_s < \epsilon_{su}$ |
| 5 stories         | 1.25E-03             | 4.99E-03 | $\epsilon_{sy} = 10\%$ | 0.028               | 0.0434 | $\epsilon_{sy} < \epsilon_s < \epsilon_{su}$ |

Table5. Steel strain exploitation.

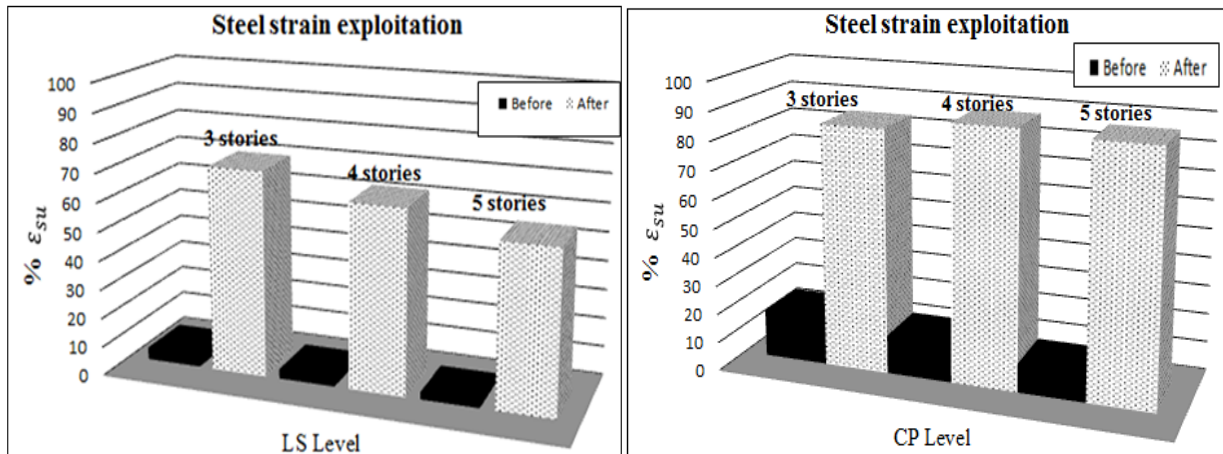


Figure8. Steel strain exploitation.

The poor concrete compressive strength for initial structures limits the exploitation of reinforcement strain capacity. The steel yielding value was not attained because of the fragile behavior of the elements. That's why the selection of CFRP jackets is desirable in such situation where the objective is to increase the elements flexural strength while maintaining the initial stiffness and

permitting a full exploitation of the strain capacity of longitudinal reinforcement [22].

5- CONCLUSION:

This study confirms the possibility of nonlinear analysis to simulate reasonably structural behavior under seismic loading if more caution is afforded to sectional analyses in post-elastic stage and the attribution of particular user

defined plastic hinges for each structural component. A well reinforced column against poor concrete compressive strength doesn't reduce the severity of the problem of brittle failure and the dangerous failure mechanism under seismic excitation.

In fact, it limited the exploitation of the deformation capacity of longitudinal reinforcement. This can be solved using external CFRP wrapping which conserves initial stiffness by limiting concrete cracking and enhancing its strength, leading to a better exploitation of steel strain. The proposed modeling approach of CFRP wrapped RC sections gives acceptable estimation of the sectional capacity thus; acceptable plastic hinges can be defined based on it. In seismic rehabilitation, if the objective is maintaining or marginally enhancing the flexure strength without changing the initial stiffness, CFRP wrapping is the more accommodate solution particularly for low-rise buildings braced by beam-column system.

### REFERENCES:

1. Nonlinear static analysis of retrofitted RC building, A. Ismail. 1687-4048 © 2013 Production and hosting by Elsevier B. V.. <http://dx.doi.org/2013.07.002>
2. On the pushover analysis as a method for evaluating the seismic response of RC buildings. P. P. Diotallevi & L. Landi Depart. of Civil Eng. DISTART, Bologna University, Italy Earthquake Resistant Eng. Structures V203, WIT Transactions on The Built Environment, Vol 81, © 2005 WIT Press [www.witpress.com](http://www.witpress.com), ISSN 1743-3509
3. Re-evaluation of building damage during recent earthquakes in Turkey. Inel M, et al Eng. Structures 2007.
4. Considerations about non linear static analysis of a RC frame retrofitted with FRP. M. Savoia et al. Mecánica Computacional Vol XXIX. 10173-10182 Buenos Aires, Argentina, 15-18 Nov. 2010 <http://www.amcaonline>
5. SAP 2000, Integrated software for Structural analysis & design, Computers & Structures, Inc, Berkeley, USA.
6. RPA 99. Version 2003, Algerian Seismic code.
7. Strength and ductility of concrete bridge columns under seismic loading. Priestley, M. J. N., and Park, R. (1987). ACI Struct. J., 84(1), 61–67.
8. On the effect of external active confinement on spirally RC columns, H. Moghaddam, et al. The 14<sup>th</sup> World Conf. on Earth. Eng. Oct 12-17, 2008 Beijing, China. 14<sup>th</sup> WCEE.
9. CFRP confined square columns in cyclic axial compression, stress-strain model, Wang Z, Wang D, Smith ST, Lu D. ASCE. J. Compos. Constr. 2012; 16(2). 161-70.
10. Models for FRP-wrapped rectangular RC columns with continuous or lap-spliced bars under cyclic lateral loading. Biskinis D, Fardis MN, Engineering Structures 57 (2013) 199-212; 0141-0296 -© 20 Elsevier Ltd.
11. Fib model code 2010 – Final draft. Bulletin 65/66. Federation Internationale du Béton. Lausanne; 2012
12. FEMA – 356 Prestandard and commentary for seismic rehabilitation of buildings. 2000 Washington DC.
13. Seismic performances of existing buildings strengthened by RC jacketing. Application of the pushover analysis. Karima Drouna, Djebbar Nabil. 2<sup>nd</sup> ECEES 24-29 August 2014, Istanbul Turkey. <http://www.eaee.org/proceedings-of-2ecees-eaee-sessions>
14. Plastic Hinge Length of FRP-Confined Square RC Columns. Cheng Jiang, Yu-Fei Wu, and Gang Wu; DOI: 10.1061/(ASCE)CC.1943-5614.0000463. 2014 ASCE.
15. Seismic design of RC and masonry buildings, Paulay T and Priestley M 1992, J. Wiley and sons, New York 1992.
16. “Performance modeling strategies for modern RC bridge columns.” Berry, M. P. 2006. PhD thesis, Univ. of Washington.
17. “Flexure-controlled ultimate deformations of members with continuous or lap-spliced bars.” Biskinis, D., and Fardis, M. N. Struct. Concr. 2010, 11(2), 93–108.
18. “Plastic hinge analysis of FRP confined circular concrete columns.” Gu, D. S., Wu, Y. F., Wu, G., and Wu, Z. S. Constr. Build. Mater, 2012, 27(1), 223–233.
19. ‘Static pushover versus dynamic collapse analysis of RC buildings.’ A.M. Mwafy, A.S. Elnashai, Engineering Structures 23 2001 407-424
20. Scott, M.H.; Fenves, G.L.; McKenna, F.; Filippou, F.C. Software patterns for nonlinear beam-column models. J. Struct. Eng. 2008, 134, 562–571.
21. Detailing procedures for seismic rehabilitation of RC members with fiber reinforced polymers, Tastani S.P, Pantazopoulou S.J, Eng. Structures. 0141-0296 -© 20 Elsevier Ltd. Doi: 10.1016/j.engstruct.2007.03.028.

## APPLICATION OF THE ANALYTICAL HIERARCHY PROCESS (AHP) FOR LANDSLIDE SUSCEPTIBILITY MAPPING IN THE EAST REGION OF CONSTANTINE, NE ALGERIA.

Submitted on 25/04/2018 – Accepted on 07/11/2018

### Abstract

Landslides constitutes one of the main geological dangers to human being. Proper analysis and suitable modeling of these dangers may reduce accident risks. In this study, we used remote sensing techniques and GIS tools to establish landslide susceptibility map of the East of Constantine. To evaluate the landslide risks in the study area, analytical hierarchy process (AHP) method and Weighted Linear Combination (WLC) were used. In this method, we performed quantification of the factors on a priority basis by pair-wise comparison of the factors. The local data includes slope, slope aspect, elevation, distance from drainage, lithology, distance from faults, precipitation, and Normalized Difference Vegetation Index (NDVI) and springs density. The landslide susceptibility index (LSI) was calculated using the WLC technique based on the assigned weight and rating by AHP method. The results were verified using actual landslide locations (43 location points) where the accuracy rate 61% of predict values and 58 % of success values. The validation results with that indicated suitable agreement between the susceptibility map and the existing data on landslide locations.

**Keywords:** Landslides, Susceptibility, AHP, GIS, Mapping, Constantine.

**N MANCHAR**<sup>1</sup>  
**CH BENABBAS**<sup>2</sup>  
**F BOUAICHA**<sup>3</sup>  
**K BOUFAA**<sup>4</sup>

<sup>1</sup> Department of geology sciences, University of Freres Mentouri Constantine, Algeria.

<sup>2</sup> Geology and environment laboratory (L.G.E), University of Constantine 3, Algeria.

<sup>3</sup> Department of applied biology, university of Frères Mentouri Constantine 1, Constantine, Algeria.

<sup>4</sup> Laboratory of Geological Engineering (L.G.G), University of Jijel, Algeria.

### INTRODUCTION

Landslides are destructive natural hazards that frequently leads to serious problems. In northern Algeria, the Constantine's region in particular, East of the city is severely affected by recurrent landslides causing damage to property and infrastructure ([1]; [2]; [3]; [4]; [5]; [6]; [7]; [8]). To the East of the city, a 10 Km segment of East-West highway experienced many landslides during construction. This segment is hosting two tunnels (Djebel Ouahche's tunnel and Kellal's tunnel) near which several landslides and instabilities occurred especially in Dj Ouahche. The most recent landslides occurred in 2008, 2011, and 2013 caused serious damage to the highway's infrastructures; such as the tunnel of Djebel Ouahche, and embankment of the highway.

Landslide susceptibility zonation (LSZ) is defined as dividing land areas into homogeneous domain based on their potential landslide occurrence ([9]; [10]; [11]). LSZ was developed by a variety of methods and techniques which are carried out into two approaches: (i) a qualitative approach that is based on expert knowledge of the target area and portrays susceptibility zoning in descriptive terms; and (ii) a quantitative approach based on statistical algorithm ([12]; [13]; [14]; [15]; [16]; [17]; [18]).

Recently, quantitative approaches are commonly used. It is based on mathematical expressions of the relationship between causal factors and the landslides. The two principles methods for quantitative analysis are the deterministic and

statistical method, which includes multivariate and bivariate statistical models, Fuzzy logic, logistic regression and artificial neural network analysis ([19]; [13]; [20]; [21]; [22]; [23]). Deterministic methods are based on engineering principles of slope instability defined in terms of the factor of safety. However these methods are useful for mapping only small areas.

The qualitative approach is based on expertise reports for which a landslide inventory map is not necessary. Maps resulting from quantitative techniques are influenced by the subjectivity of the experts involved.

The Analytical Hierarchy Process (AHP) is a semi-quantitative method. It is based on decomposition, the comparison between different pairs of elements, and synthesis of priorities for regional susceptibility studies. This method was introduced by [36] Saaty (1980) and depends on the expert knowledge ([24]; [25]). In this study, AHP along with GIS are powerful instruments to inspect criteria in modelling process.

The purpose of this research is to present landslide susceptibility map for the east of Constantine city (Northeast of Algeria), using AHP method in the framework of GIS.

### 2. GEOLOGICAL AND GEOMORPHOLOGICAL SETTINGS

The study area is located in the Northeast of Algeria. It concerns the zoning perimeter with 1/50 000 scale

(geological map of Algeria; map N°74 EL ARIA), covering an area of about 639.56 km<sup>2</sup>. This region is affected by several landslides, due to its geological and geomorphological particularities. Also, the anthropogenic factors are responsible for many landslides triggering in the area such as roads, highways and tunnels.

The geomorphology of Constantine region is particular in Tellian Atlas Mountains of northeast Algeria with deep gorges (Rhumel, Rocher de Constantine) and mountains (Dj Kellal “950 m”, Kef El Akahl “1200 m”, Dj Ouahche “1100 m”). The altitude ranges from 500 m to 1200 m. The area characterized by a dense hydrographic network with main draining valleys such as Oued Boumerzoug, Oued Hamimin, Oued Bousteila in the west and Oued El Kram, Oued El Aria and Oued en Naga in the east which have permanent flow. However, the temporary flow presented by Oued El Anga, Oued El Mellah and Oued Boudeb, often these streams are flowing to the Northeast direction.

The study area is characterized by a semi-arid climate with high temperature (28 -41°C) and low precipitation (from 600 to 900 mm) in the summer, and high humidity, precipitation and low temperature in the winter. Two typical rainy and dry seasons are in contrast. About 63% of the annual rainfall quantity concentrated between Decembers to February period. The rainstorm represents the triggering factor for most of landslides.

Geologically, the study area is characterized by superposition of thrust sheet units made up from the base to the top (Fig. 1) by:

Neritic unit (Cretaceous carbonate), Ultra-Tellian unit (Cretaceous-Eocene marls and marly limestone), Tellian s.s. (sensu-structo) with Marly dominance (Cretaceous-Eocene), Numidian unit with sandstone Burdigalian, clay and flysch (Eocene), and Mio-Plio-Quaternary formations which are represented by sandy clays, marls and conglomerate (Mio-Pliocene) and alluvial terraces and lacustrine calcareous formations with Quaternary age ([26]; [27]; [28]; [29]; [30]). This edifice was deposited during paroxysmal compressional phases Eocene and Miocene ([26]; [31]; [32]; [30]).

### 3. METHODOLOGY AND ANALYSIS

The instability complexity at this site is results of the combination of several factors that may or may not act synchronously. Nine possible landslide causative factors such as slope, slope aspect, elevation, distance from drainage, lithology, distance from faults, precipitation, NDVI and springs density were used. These factors were analyzed and taken into account to procedure landslide susceptibility of the study area. The layers were generated from the various data sources.

#### 3.1. Data presentation and analysis

The data used in the present study are satellite image (Landsat-7 ETM satellite images (Resolution 30 m), aerial photo, geological map and topographical map (Table 1).

The contour map at 10 m interval was prepared and digitized from Constantine’s topographical map (1980) at the scale 1/50000 and subsequently employed for generating the DEM

using GIS software. Elevation, slope, and slope aspect were extracted from DEM with 10 m grid cell size (Fig. 2a, b, c). Slope gradient with seven classes, slope aspect, was classified into the eight known main direction. Seven main lithological classes and transformed into raster value domain on GIS software (Fig. 2g). The class weight value for each strength was identified and described by GIS. Drainage buffering map was made on the distances interval 200 m from the topographic map at the 1/25000 scale and classified with ten intervals (Fig. 2e). The precipitation is considered as the most common trigger of landslides ([33]; [34]). Five hydro-climatic stations such as Constantine, Hamma Bouziane, Ain El Bey, Fourchi and Bir Drimil of the **Agence Nationale des Ressources Hydrauliques (ANRH, Algiers)**, and the **Office National de Météorologie (ONM, Algiers)** was selected. The precipitation values was used to create the precipitation map during 32 years (1980-2012) (Fig. 2, i). Fault buffering was made on a distance interval of 400 m from the geological map at the 1/50000 scale and classified with ten intervals. Spring water layer was extracted from the topographical map at the 1/50000 scale (Fig. 2, d). The NDVI map was created from Landsat-7 TM satellite images (Resolution 30 m) (Fig. 2, f). The prepared NDVI by a non-linear transformation of the visible or red and near-infrared bands of satellite images [35]. It can be calculated using the formula:

$$NDVI = (NIR - R) / (NIR + R) \quad (1)$$

Where NIR and R are the observed reflectance in the near infrared and red portions of the electromagnetic spectrum, respectively. The values were ranged from -1 to +1 (pixel values 0-255) (Fig. 2).

#### 3.2. Methodology

In the present research, the AHP technique was applied and the Weighted Linear Combination (WLC) was performed by integrating factors weight and class weight/ rank value to compute landslide susceptibility index (LSI) for each pixel:

$$LSI = \sum_{i=1}^n (W_i * R_i) \quad (2)$$

Where LSI is the required landslide susceptibility index of the given pixel, Ri and Wi are class weight.

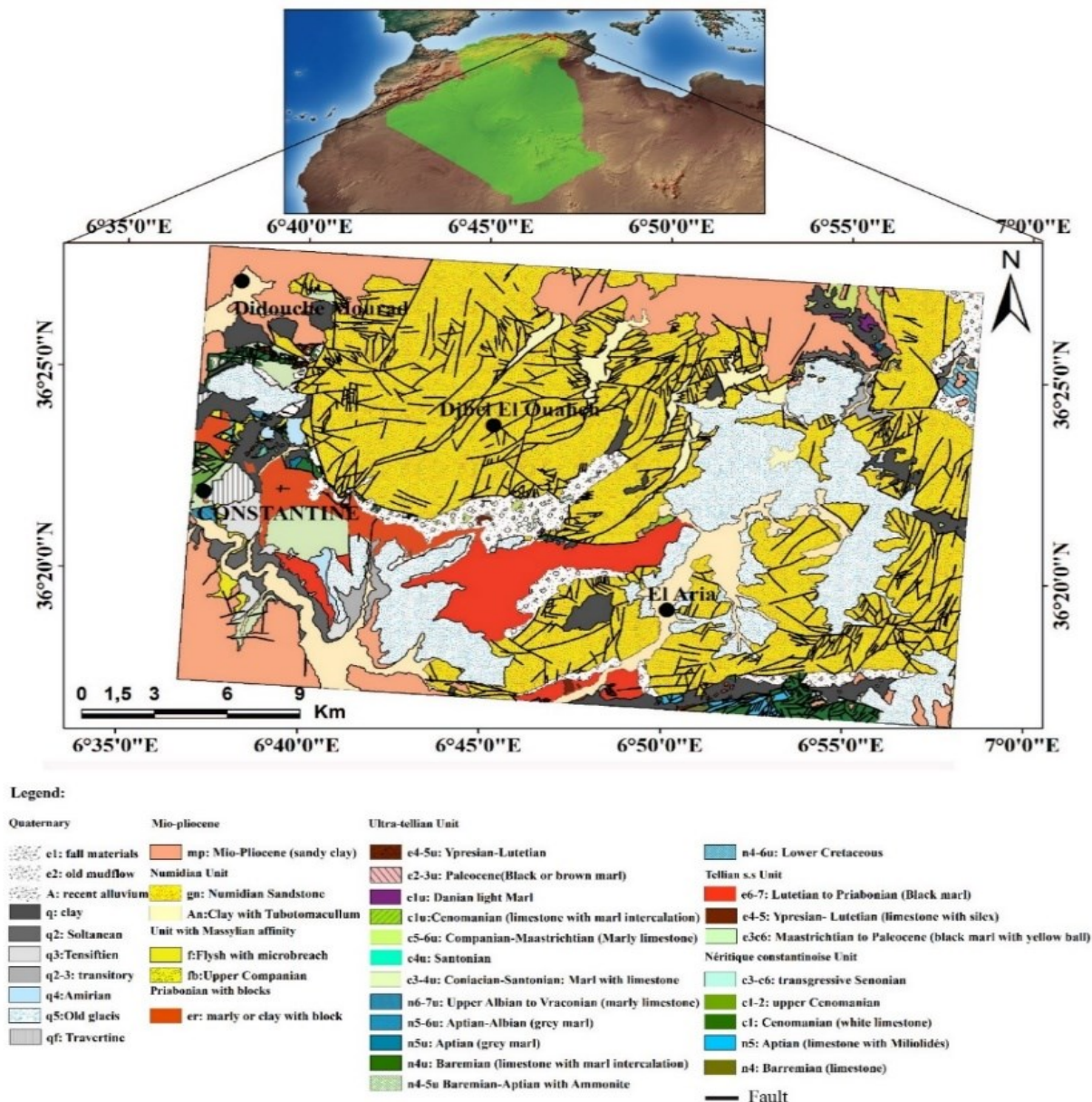


Fig. 1: Geological map of Study area, after Coiffait and Vila, 1977 (modified).

Table. 1 Spatial data layers used in the study.

| Category          | Layer                  | Data type    | Scale    | Data Source  |
|-------------------|------------------------|--------------|----------|--|
| Topographic map   | MNT                    | GRID & point | 1/50000  | I. N. C. T. (Institut National de la Cartographie et de Télédetection) |
|                   | hypsoetry              |              |          |  |
|                   | Slope angle            |              |          |  |
|                   | Slope aspect           |              |          |  |
|                   | Water springs          |              |          |  |
| Topographic map   | Distance from drainage | Polygone     | 1/25000  | A. N. G. C. M. (Agence Nationale de la Géologie et du Contrôle Minier) |
| Geological map    | Lithology              | Polygone     | 1/50000  |  |
|                   | Distance from fault    |              |          |  |
| Precipitation map | Precipitation          | GRID         | 1/50000  | ANRH (Agence National des Ressources Minérales)                        |
| NDVI map          | NDVI                   | GRID         | 30m x30m | Landsat-7 ETM+ Satellite image (scene P193R35, year 2001)              |

Table 2: Scale of preference between two parameters in AHP (Saaty, 2000)

| Scale       | Degree of preferences | Explanation   |
|-------------|-----------------------|---|
| 1           | Equally               | Two activities contribute equally to the objective,   |
| 3           | Moderately            | Experience and judgement slightly to moderately favor one activity over another                         |
| 5           | Strongly              | Experience and judgement strongly or essentially favor one activity over another                        |
| 7           | Very Strongly         | An activity is strongly favored over another and its dominance is showed in practice                    |
| 9           | Extremly              | The evidence of favoring one activity over another is of the highest degree possible of an affirmation. |
| 2,4,6,8     | Intermediate Values   | Used to represent compromises between the preferences in weights 1, 3, 5, 7 and 9.                      |
| Reciprocals | Opposites             | Used for inverse comparison.  |

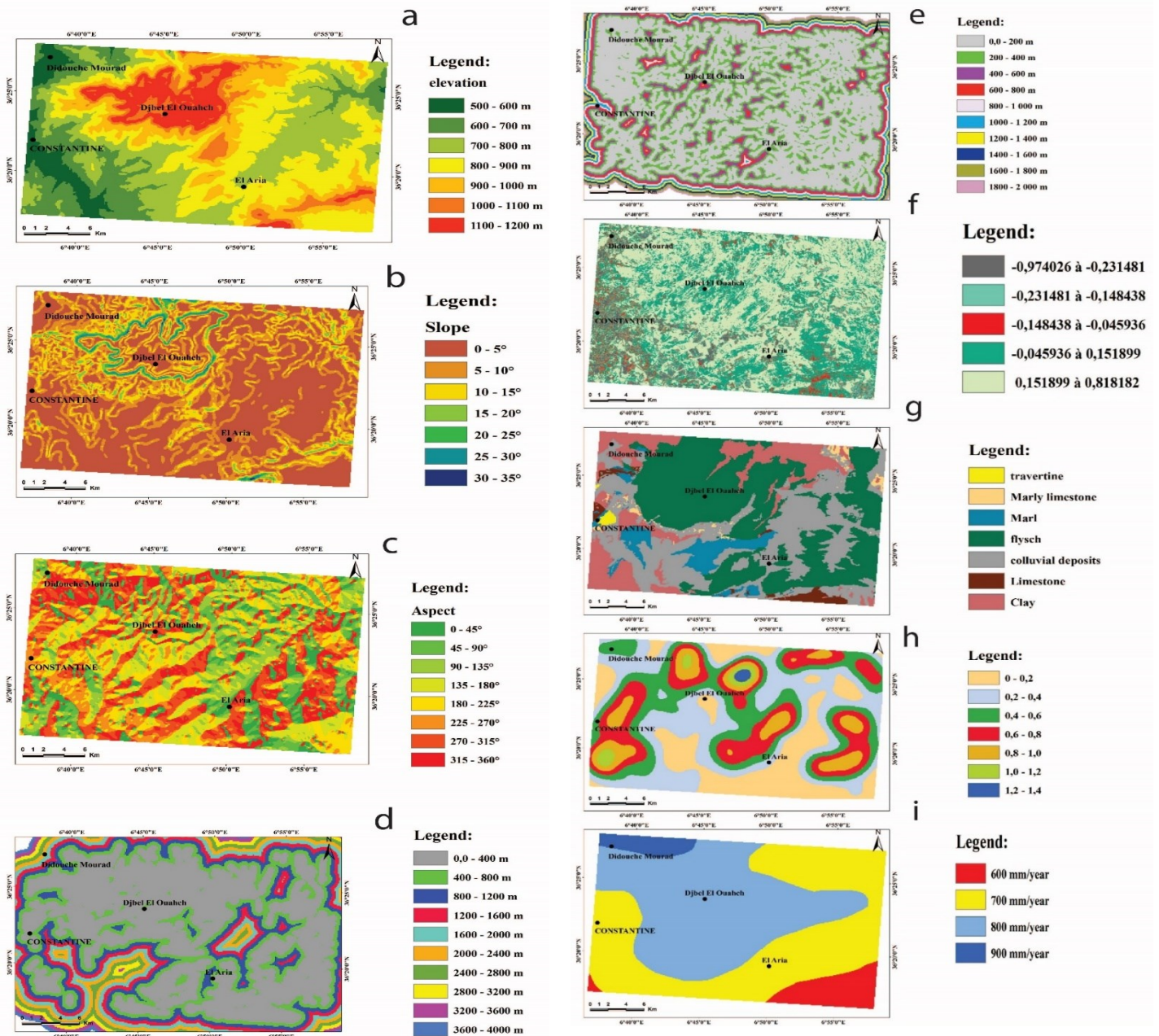


Fig. 2 Landslide related factors in the study area: (a) elevation (b) Slope angle (c) Slope aspect (d) distance from faults (e) distance from drainage (f) NDVI (g) Lithology (h) density of springs (i) precipitation

**Analytical Hierarchy Process**

The analytical hierarchy process (AHP) is a semi-quantitative and multicriteria decision-making method, enables to organize, analyze, and can find an answer to a complex decision problem [36]. This approach is based on three principles: decomposition, comparative judgment, and synthesis of priorities [37]. It involves a matrix-based pair-wise comparison of the decomposed elements inside a given level of hierarchical structure with respect to the following higher level (Table 2). By building a pair-wise comparison matrix with scores which are providing in a fundamental numerical scale, range between 1 and 9, to get factor weights. In the construction of a pair-wise comparison matrix, each factor is rated against every other factor using that scale. Then, in order to calculate the final weight for each conditioning factor, the per-wise comparison matrix for each element was generated in the software with a consistency ratio (CR) expressed as:  $CR = (CI/RI)$

Where: RI the consistency index average depending on the order of the matrix given by Saaty (1980). CI is the consistency index expressed as:  $CI = (\lambda_{max} - n) / (n - 1)$ . Where  $\lambda_{max}$  is the largest or principal eigenvalue of the matrix and n is the order of the matrix.

**Geoprocessing**

The aim of the building of per-wise comparison matrix is to get factor weights and class weights, and calculated consistency ratio (CR), is computed to check the construction of matrix which depends on the number of parameters.

The CR value requirement should be less than 0.1 to accept the computed weights. Then the matrix can be considered as having an acceptable consistency [38]. A CR greater than 0.1 were automatically rejected and requires revision of judgment in the matrix.

The required weights were used to calculate the landslide susceptibility. It's made by Weighted Linear Sum procedure [39]. The CR found in this study is 0.00005, the ratio indicates an acceptable value for a reasonable level of consistency into the pair-wise assessment, and validate the factor weights. Therefore, the lithology factor have the highest weights with value of 0.15. However, elevation, distance to fault, and distance to drainage factors have the same lowest values of weights 0.08 (Table. 3).

**Table. 3: The pair-wise comparison matrix, factor weights, class weights (rating) and consistency ratio.**

| Factor                             |                 |       |       |       |   |     |       |   |   |               |
|------------------------------------|-----------------|-------|-------|-------|---|-----|-------|---|---|---------------|
| <i>Lithology</i>                   |                 |       |       |       |   |     |       |   |   |               |
|                                    |                 |       |       |       |   |     |       |   |   | <i>Weight</i> |
| 9                                  | Clay            | 1     |       |       |   |     |       |   |   | 0.269753      |
| 8                                  | Colluvium       | 0.889 | 1     |       |   |     |       |   |   | 0.220726      |
| 6                                  | Marl            | 0.667 | 0.75  | 1     |   |     |       |   |   | 0.179833      |
| 1                                  | Limestone       | 0.111 | 0.125 | 0.167 | 1 |     |       |   |   | 0.02997       |
| 2                                  | Marly-Limestone | 0.222 | 0.25  | 0.333 | 2 | 1   |       |   |   | 0.059943      |
| 3                                  | Travertine      | 0.333 | 0.375 | 0.5   | 3 | 1.5 | 1     |   |   | 0.089916      |
| 5                                  | Flysch          | 0.556 | 0.625 | 0.833 | 5 | 2.5 | 1.667 | 1 |   | 0.149859      |
| <i>Consistency Ratio: 0.00882</i>  |                 |       |       |       |   |     |       |   |   |               |
| <i>Slope aspect</i>                |                 |       |       |       |   |     |       |   |   |               |
|                                    |                 |       |       |       |   |     |       |   |   | <i>Weight</i> |
| 7                                  | 0-45°           | 1     |       |       |   |     |       |   |   | 0.159091      |
| 5                                  | 45-90°          | 0.714 | 1     |       |   |     |       |   |   | 0.113633      |
| 1                                  | 90-135°         | 0.143 | 0.2   | 1     |   |     |       |   |   | 0.022725      |
| 1                                  | 135-180°        | 0.143 | 0.2   | 1     | 1 |     |       |   |   | 0.022725      |
| 5                                  | 180-225°        | 0.714 | 1     | 5     | 5 | 1   |       |   |   | 0.113633      |
| 7                                  | 225-270°        | 1     | 1.4   | 7     | 7 | 1.4 | 1     |   |   | 0.159091      |
| 9                                  | 270-315°        | 1.286 | 1.8   | 9     | 9 | 1.8 | 1.286 | 1 |   | 0.20455       |
| 9                                  | 315-360°        | 1.286 | 1.8   | 9     | 9 | 1.8 | 1.286 | 1 | 1 | 0.20455       |
| <i>Consistency Ratio: 0.000059</i> |                 |       |       |       |   |     |       |   |   |               |
| <i>Slope angle</i>                 |                 |       |       |       |   |     |       |   |   |               |

|                                    |                   |       |       |     |       |       |       |   |   | <i>Weight</i> |          |         |
|------------------------------------|-------------------|-------|-------|-----|-------|-------|-------|---|---|---------------|----------|---------|
| 1                                  | 0-5°              | 1     |       |     |       |       |       |   |   |               | 0.026273 |         |
| 3                                  | 5-10°             | 3     | 1     |     |       |       |       |   |   |               | 0.075067 |         |
| 5                                  | 10-15°            | 5     | 1.667 | 1   |       |       |       |   |   | 0.131378      |          |         |
| 6                                  | 15-20°            | 6     | 0.333 | 1.2 | 1     |       |       |   |   | 0.136648      |          |         |
| 7                                  | 20-25°            | 7     | 2.333 | 1.4 | 1.167 | 1     |       |   |   | 0.183933      |          |         |
| 8                                  | 25-30°            | 8     | 2.667 | 1.6 | 1.333 | 1.143 | 1     |   |   | 0.210209      |          |         |
| 9                                  | >30°              | 9     | 3     | 1.8 | 1.5   | 1.286 | 1.125 | 1 |   | 0.236491      |          |         |
| <i>Consistency Ratio: 0.019221</i> |                   |       |       |     |       |       |       |   |   |               |          |         |
| <i>Distance from faults</i>        |                   |       |       |     |       |       |       |   |   |               |          |         |
|                                    |                   |       |       |     |       |       |       |   |   | <i>Weight</i> |          |         |
| 9                                  | 0-400             | 1     |       |     |       |       |       |   |   |               | 0.300006 |         |
| 7                                  | 400-800           | 0.778 | 1     |     |       |       |       |   |   |               | 0.233336 |         |
| 5                                  | 800-1200          | 0.889 | 0.714 | 1   |       |       |       |   |   | 0.166666      |          |         |
| 3                                  | 1200-1600         | 0.333 | 0.429 | 0.6 | 1     |       |       |   |   | 0.1           |          |         |
| 1                                  | 1600-2000         | 0.111 | 0.143 | 0.2 | 0.333 | 1     |       |   |   | 0.33332       |          |         |
| 1                                  | 2000-2400         | 0.111 | 0.143 | 0.2 | 0.333 | 1     | 1     |   |   | 0.33332       |          |         |
| 1                                  | 2400-2800         | 0.111 | 0.143 | 0.2 | 0.333 | 1     | 1     | 1 |   | 0.33332       |          |         |
| 1                                  | 2800-3200         | 0.111 | 0.143 | 0.2 | 0.333 | 1     | 1     | 1 | 1 | 0.33332       |          |         |
| 1                                  | 3200-3600         | 0.111 | 0.143 | 0.2 | 0.333 | 1     | 1     | 1 | 1 | 1             | 0.33332  |         |
| 1                                  | 3600-4000         | 0.111 | 0.143 | 0.2 | 0.333 | 1     | 1     | 1 | 1 | 1             | 1        | 0.33332 |
| <i>Consistency Ratio: 0.000032</i> |                   |       |       |     |       |       |       |   |   |               |          |         |
| <i>Distance from drainage</i>      |                   |       |       |     |       |       |       |   |   |               |          |         |
|                                    |                   |       |       |     |       |       |       |   |   | <i>Weight</i> |          |         |
| 9                                  | 0-200             | 1     |       |     |       |       |       |   |   |               | 0.300006 |         |
| 7                                  | 200-400           | 0.778 | 1     |     |       |       |       |   |   |               | 0.233336 |         |
| 5                                  | 400-600           | 0.889 | 0.714 | 1   |       |       |       |   |   | 0.166666      |          |         |
| 3                                  | 600-800           | 0.333 | 0.429 | 0.6 | 1     |       |       |   |   | 0.1           |          |         |
| 1                                  | 800-1000          | 0.111 | 0.143 | 0.2 | 0.333 | 1     |       |   |   | 0.33332       |          |         |
| 1                                  | 1000-1200         | 0.111 | 0.143 | 0.2 | 0.333 | 1     | 1     |   |   | 0.33332       |          |         |
| 1                                  | 1200-1400         | 0.111 | 0.143 | 0.2 | 0.333 | 1     | 1     | 1 |   | 0.33332       |          |         |
| 1                                  | 1400-1600         | 0.111 | 0.143 | 0.2 | 0.333 | 1     | 1     | 1 | 1 | 0.33332       |          |         |
| 1                                  | 1600-1800         | 0.111 | 0.143 | 0.2 | 0.333 | 1     | 1     | 1 | 1 | 1             | 0.33332  |         |
| 1                                  | 1800-2000         | 0.111 | 0.143 | 0.2 | 0.333 | 1     | 1     | 1 | 1 | 1             | 1        | 0.33332 |
| <i>Consistency Ratio: 0.000032</i> |                   |       |       |     |       |       |       |   |   |               |          |         |
| <i>NDVI</i>                        |                   |       |       |     |       |       |       |   |   |               |          |         |
|                                    |                   |       |       |     |       |       |       |   |   | <i>Weight</i> |          |         |
| 9                                  | 0.974026-0.231481 | 1     |       |     |       |       |       |   |   |               | 0.36001  |         |
| 7                                  | 0.231481-0.148438 | 0.778 | 1     |     |       |       |       |   |   |               | 0.280002 |         |
| 5                                  | 0.148438-0.045936 | 0.556 | 0.714 | 1   |       |       |       |   |   | 0.199995      |          |         |
| 3                                  | 0.045936-0.151899 | 0.333 | 0.429 | 0.6 | 1     |       |       |   |   | 0.119997      |          |         |

|                                    |                               |       |       |       |       |       |       |      |       |               |          |
|------------------------------------|-------------------------------|-------|-------|-------|-------|-------|-------|------|-------|---------------|----------|
| 1                                  | <i>0.151899-0.818182</i>      | 0.111 | 0.143 | 0.2   | 0.333 | 1     |       |      |       | 0.039996      |          |
| <i>Consistency Ratio: 0.000056</i> |                               |       |       |       |       |       |       |      |       |               |          |
| <i>Elevation</i>                   |                               |       |       |       |       |       |       |      |       |               |          |
|                                    |                               |       |       |       |       |       |       |      |       | <i>Weight</i> |          |
| 2                                  | <i>500-600</i>                | 1     |       |       |       |       |       |      |       | 0.041665      |          |
| 6                                  | <i>600-700</i>                | 3     | 1     |       |       |       |       |      |       | 0.124999      |          |
| 6                                  | <i>700-800</i>                | 3     | 1     | 1     |       |       |       |      |       | 0.124999      |          |
| 8                                  | <i>800-900</i>                | 4     | 1.333 | 1.333 | 1     |       |       |      |       | 0.166664      |          |
| 8                                  | <i>900-1000</i>               | 4     | 1.333 | 1.333 | 1     | 1     |       |      |       | 0.166664      |          |
| 9                                  | <i>1000-1100</i>              | 4.5   | 1.5   | 1.5   | 1.125 | 1.125 | 1     |      |       | 0.187504      |          |
| 9                                  | <i>1100-1200</i>              | 4.5   | 1.5   | 1.5   | 1.125 | 1.125 | 1     | 1    |       | 0.187504      |          |
| <i>Consistency Ratio: 0.000023</i> |                               |       |       |       |       |       |       |      |       |               |          |
| <i>Density of spring water</i>     |                               |       |       |       |       |       |       |      |       |               |          |
|                                    |                               |       |       |       |       |       |       |      |       | <i>Weight</i> |          |
| 2                                  | <i>0-0.2</i>                  | 1     |       |       |       |       |       |      |       | 0.05534       |          |
| 2                                  | <i>0.2-0.4</i>                | 1     | 1     |       |       |       |       |      |       | 0.05534       |          |
| 4                                  | <i>0.4-0.6</i>                | 2     | 2     | 1     |       |       |       |      |       | 0.110681      |          |
| 5                                  | <i>0.6-0.8</i>                | 2.5   | 2.5   | 1.25  | 1     |       |       |      |       | 0.138352      |          |
| 6                                  | <i>0.8-1</i>                  | 3     | 3     | 1.25  | 1.2   | 1     |       |      |       | 0.166023      |          |
| 8                                  | <i>1-1.2</i>                  | 4     | 4     | 2     | 1.6   | 1.333 | 1     |      |       | 0.221364      |          |
| 9                                  | <i>1.2-1.4</i>                | 4.5   | 4.5   | 2.5   | 1.8   | 1.5   | 1.125 | 1    |       | 0.2529        |          |
| <i>Consistency Ratio:0.001923</i>  |                               |       |       |       |       |       |       |      |       |               |          |
| <i>Précipitation</i>               |                               |       |       |       |       |       |       |      |       |               |          |
|                                    |                               |       |       |       |       |       |       |      |       | <i>Weight</i> |          |
| 3                                  | <i>600</i>                    | 1     |       |       |       |       |       |      |       | 0.125         |          |
| 5                                  | <i>700</i>                    | 1.667 | 1     |       |       |       |       |      |       | 0.208         |          |
| 7                                  | <i>800</i>                    | 2.333 | 1.4   | 1     |       |       |       |      |       | 0.292         |          |
| 9                                  | <i>900</i>                    | 2.333 | 1.8   | 1.286 | 1     |       |       |      |       | 0.375         |          |
| <i>Consistency Ratio:0.000035</i>  |                               |       |       |       |       |       |       |      |       |               |          |
| <i>Global matrix</i>               |                               |       |       |       |       |       |       |      |       |               |          |
|                                    |                               |       |       |       |       |       |       |      |       | <i>Weight</i> |          |
| 9                                  | <i>lithology</i>              | 1     |       |       |       |       |       |      |       | 0.147544      |          |
| 8                                  | <i>Slope angle</i>            | 0.889 | 1     |       |       |       |       |      |       | 0.131147      |          |
| 7                                  | <i>Slope aspect</i>           | 0.778 | 0.875 | 1     |       |       |       |      |       | 0.114754      |          |
| 5                                  | <i>Elevation</i>              | 0.556 | 0.625 | 0.714 | 1     |       |       |      |       | 0.081966      |          |
| 5                                  | <i>distance from drainage</i> | 0.556 | 0.625 | 0.714 | 1     | 1     |       |      |       | 0.081966      |          |
| 5                                  | <i>distance from faults</i>   | 0.556 | 0.625 | 0.714 | 1     | 1     | 1     |      |       | 0.081966      |          |
| 8                                  | <i>Densité_ d'eau</i>         | 0.889 | 1     | 1.143 | 1.6   | 1.6   | 1.6   | 1    |       | 0.131147      |          |
| 6                                  | <i>NDVI</i>                   | 0.667 | 0.75  | 0.857 | 1.2   | 1.2   | 1.2   | 0.75 | 1     | 0.098361      |          |
| 8                                  | <i>Precipitation</i>          | 0.889 | 1     | 1.143 | 1.6   | 1.6   | 1.6   | 1    | 1.333 | 1             | 0.131147 |
| <i>Consistency Ratio: 0,000015</i> |                               |       |       |       |       |       |       |      |       |               |          |

**4. RESULTS AND DISCUSSION:**

By overlaying the layers in GIS environment and using relative weights by AHP method, the final score LSI (Landslide Susceptibility Index) is computed by using Equation (2). The final results from calculated values of LSI, it was found its minimum value of 2.985, and a maximum value of 7.38, and standard deviation of 0.62. The LSI represents the relative susceptibility of a landslide occurrence. Therefore the higher the index, the more

susceptible the area is to landslides. These LSI values were then divided into five (5) classes based on the natural breaks range, which represents different zones in the landslide susceptibility map. These are Very High (VHS), High (HS), Moderate (MS), Low (LS), and Very Low (VLS) susceptibility zones (Fig. 3). The study concluded that East of Constantine, around Djebel Ouahche zones were very vulnerable to a landslide; around the NE and South of Aria were registered with low to very low susceptibility; and the rest of the area of moderate landslide potentiality (Fig.3).

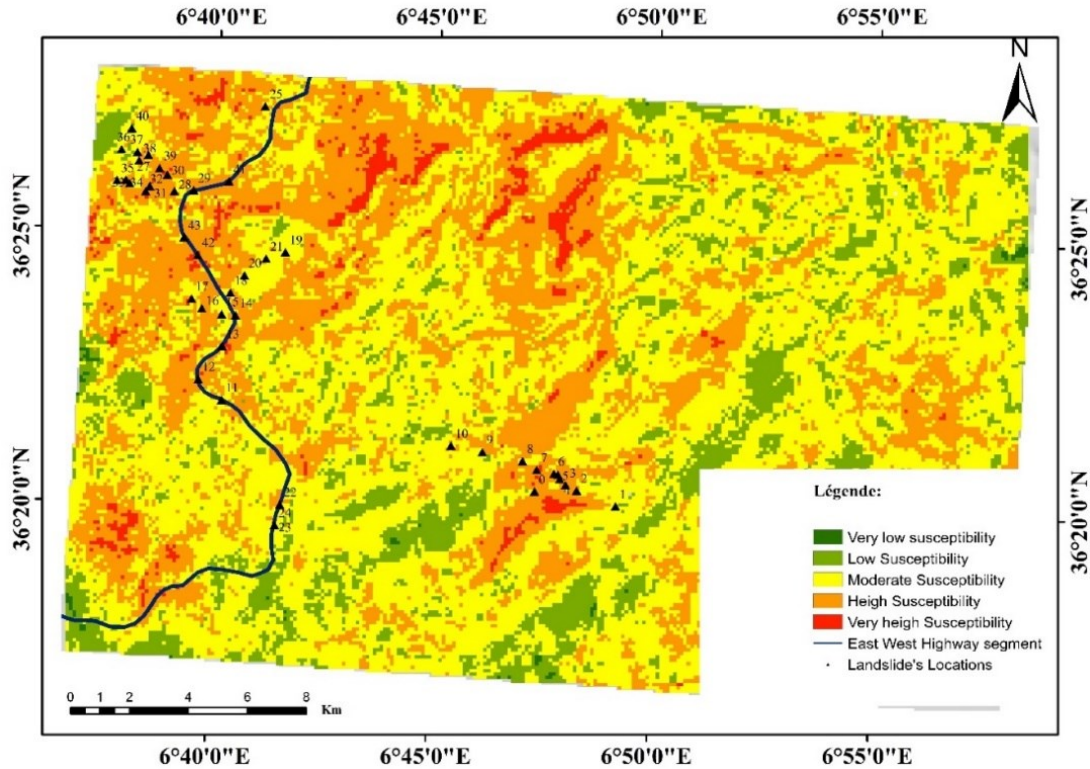


**Fig. 3** The landslide susceptibility map based on AHP with 43 known landslide location on the basis of natural break classification.

The study revealed that around 33% of the total area were classified as being in the VHS (2.1%) or HS (30.84%) landslide susceptibility zones, but they had represented by about 60% (Fig.4) of the landslides reference points (Table 4). Other classes MS, LS and VLS are represented, respectively, by 54.15%, 12.61%, and 0.3% of the total surface and only one landslide incidence (out of 43) in the LS zone. To check the validity of the results seen in Table 4 more quantitatively, the frequency ratio (FR) values for each class are also given. These values were calculated from the ratio of the percentage landslide occurrences and the percentage area coverage (for each class to the whole study area). The values begin from 0 continuing where relatively high ones (e. g. close to 0) indicate a higher chance of having landslides while low values (e.g., Close to 0) indicate a lower chance of having landslide over the area. FR equals (1) means the considered area is having an equal chance for landslide occurrence to that of the average value for the entire area. The FR values of 5.71 for the VHS zone and 1.55 for the HS zone involves the remarkable higher chance of

having landslide activities in these areas when compared to those of MS (0.66) and LS (0.31).

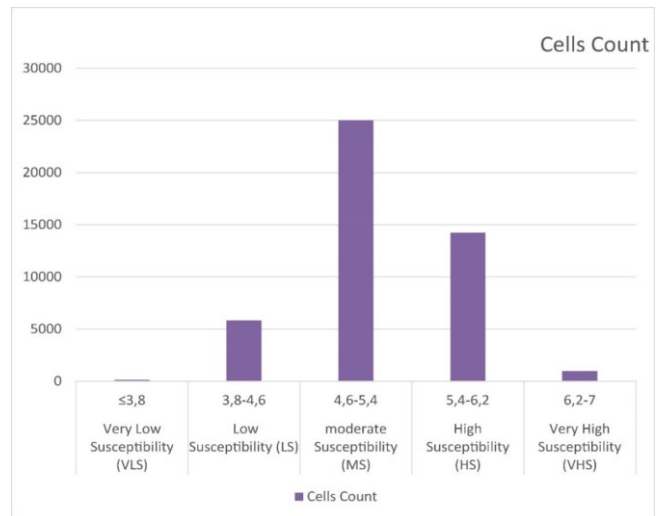


**Fig. 4** Pixel wise landslide susceptibility distribution.

**Table. 4: Allocation of the reference landslide points within the defined landslide susceptibility classes and the associated frequency ratio (FR) of each class.**

| Susceptibility Class           | Susceptibility Index | Area percentage | Landslide Point location number | Fréquency Ratio (FR) | Cells Count |
|--------------------------------|----------------------|-----------------|---------------------------------|----------------------|-------------|
| Very Low Susceptibility (VLS)  | ≤3,8                 | 0,30%           | _ (0%)                          | 0                    | 139         |
| Low Susceptibility (LS)        | 3,8-4,6              | 12,61%          | 1 (2,32%)                       | 0,3172               | 5829        |
| moderate Susceptibility (MS)   | 4,6-5,4              | 54,15%          | 13 (30,23%)                     | 0,6648               | 25030       |
| High Susceptibility (HS)       | 5,4-6,2              | 30,84%          | 23 (53,5%)                      | 1,5564               | 14254       |
| Very High Susceptibility (VHS) | 6,2-7                | 2,10%           | 6 (14%)                         | 5,7143               | 970         |

### 5. PERFORMANCE EVALUATION OF SUSCEPTIBILITY MAPS

To test the compatibility of the model and determination of its prediction ability, the area under the curve (AUC) method was used [40]. Generally, this approach compares the map of known landslides inventory with the susceptibility map. The range of the area under to ROC curve varies between 0 and 1 for a good fit, while values close to 1 being perfect and blow 0.5 defining a stochastic approximation [41]. The AUC is known as the best indicator to successfully differentiate possible landslide areas from regions with no predictable landslides [42]. In AUC curve assessment, Sensitivity (true-positive rate is the portion of false-positives out of the total actual positives) and 1-Specificity (false-positive rate is the portion of false-positives out of the total actual negatives) was performed for the model validation.

The AUC value is 0.61 and 0.59 (Fig 5), indicate the good ability of a function to correctly distinguish between failed and unfailed groups in the sample used for building the model, which means that the total success rate is 0.59.

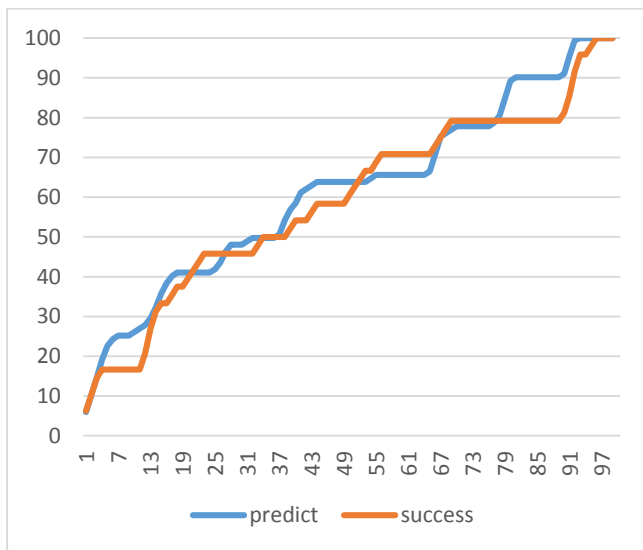


**Fig. 5** Receiver operating characteristics (ROC) curves representing quality of AHP model used.

### 6. CONCLUSION:

Landslide like other geological hazards is difficult to predict. However, it could be managed by the proceeding of the mapping of susceptibility to this phenomenon.

In this study, the analytical hierarchy process was used, and a susceptibility map is made for the east of Constantine which is located in the NE Algeria. To do that, nine (9) landslide causative factors were considered. Using AHP technique, an evaluation of these factors was applied, and factor weights and class weights were attributed to each of the associated factors. The most influencing factors to landslide activity according to their associated weights are precipitation (0.14), lithology (0.15) and slope angle (0.13).

The obtained susceptibility map give that the high and very high susceptible zones cover about 33% of the area while only 13% were classified as being the low and very low susceptible areas. About 54% of the area is moderate susceptible zone, the anthropogenic factor or trigger factors (heavy rainfall and earthquake) are enough of to reclassify the corresponding area in high susceptibility class. The map was verified using existing landslide location data based on the area under curve method from which the prediction accuracy of 61% was accomplished.

### REFERENCES

[1] Bougdal R., Belhai D., Antoine P. (2007) Géologie détaillée de la ville de Constantine et ses alentours: une donnée de base pour l'étude des glissements de terrain. *Bull Serv Géol de l'Algérie*, 18(2):161-187.

[2] Pincent B., Bougdal R., Panet M., Bentabet A. (2008). Le pont Sidi Rached à Constantine, Algérie : une culée dans un grand glissement de terrain. *Bull Serv Ge'ol de l'Algérie*, 19(3):197-215.

[3] Machane, D., Bouhadad, Y., Cheikhounis, G., Chatelain, J., Oubaiche, E., Abbes, K., Guillier, B. and Bensalem, R. (2008). Examples of geomorphologic and geological hazards in Algeria. *Natural Hazards*, 45(2), pp.295-308.

[4] Guemache, M., Chatelain, J., Machane, D., Benahmed, S. and Djadia, L. (2011). Failure of landslide stabilization measures: The Sidi Rached viaduct case (Constantine, Algeria). *Journal of African Earth Sciences*, 59(4-5), pp.349-358.

[5] Manchar, N., Benabbas, C., Kacimi, M., Mimoun, A. and Bouaicha, F., (2012). Risque de glissements et aménagement: l'exemple d'un remblai autoroutier à Taffrent (NE de Constantine, Algérie nord orientale). 1<sup>er</sup> Congrès international de génie civil et d'hydraulique, Univ. 8 Mai 1945, Guelma, Algérie.

[6] Bougdal, R., Larriere, A., Pincent, B., Panet, M. and Bentabet, A. (2013). Les glissements de terrain du quartier Bélouizdad, Constantine, Algérie. *Bulletin of Engineering Geology and the Environment*, 72(2), pp.189-202.

- [7] Bourenane, H., Bouhadad, Y., Guettouche, M. and Braham, M. (2014). GIS-based landslide susceptibility zonation using bivariate statistical and expert approaches in the city of Constantine (Northeast Algeria). *Bulletin of Engineering Geology and the Environment*, 74(2), pp.337-355.
- [8] Bourenane, H., Guettouche, M., Bouhadad, Y. and Braham, M. (2016). Landslide hazard mapping in the Constantine city, Northeast Algeria using frequency ratio, weighting factor, logistic regression, weights of evidence, and analytical hierarchy process methods. *Arabian Journal of Geosciences*, 9(2).
- [9] Varnes, D.J. 1984. Landslide Hazard Zonation: a Review of principles and practice. Natural Hazards. N°. 3. 1<sup>st</sup> ed. UNESCO, Paris, France, 63p.
- [10] Dai, F., Lee, C. and Ngai, Y. (2002). Landslide risk assessment and management: an overview. *Engineering Geology*, 64(1), pp.65-87.
- [11] Guzzetti, F., Reichenbach, P., Cardinali, M., Galli, M. and Ardizzone, F. (2005). Probabilistic landslide hazard assessment at the basin scale. *Geomorphology*, 72(1-4), pp.272-299.
- [12] Sharma, V. K., 2006. *Landslide hazard zonation: an overview of emerging techniques*. Journal of Engineering Geology, XXXIII, 73-80.
- [13] Guzzetti, F., Carrara, A., Cardinali, M., & Reichenbach, P. 1999. *Landslide hazard evaluation: a review of current techniques and their application in a multi scale study, Central Italy*. Journal of Geomorphology, 31, 181-216. Elsevier, London.
- [14] Carrara, A., Cardinali, M., Guzzetti, F., & Reichenbach, P. 1995. *GIS-Based techniques for mapping landslide hazard in Geographical Information System in Assessing Natural Hazards*. Dordrecht: Academic
- [15] Saha, A. K., Gupta, R. P., et Arora, M. K., 2002. *GIS based landslide hazard zonation in the Bhagirathi (Ganga) Valley, Himalayas*. International Journal of Remote Sensing, 23, 357-369pp.
- [16] Lee S. (2005). Application of logistic regression model and its validation for landslide susceptibility mapping using GIS and remote sensing data. *Int J Remote Sens* 7:1477-1491.
- [17] Van Westen, C. J., Castellanos Abella, E., et Sekhar, L. K., 2008. *Spatial data for landslide susceptibility, hazards and vulnerability assessment: an overview*. Engineering Geology, 102, 112-131.
- [18] Soeters, R., & Westen, C. J. 1996. *Slope instability recognition, analysis and zonation*. In A. K. Turner and R. L. Schuster (Eds), Landslides: Investigation and Mitigation. Transportation Research Board Special Report 249, 129-177.
- [19] Rowbotham D., Dudycha D. (1998). GIS modelling of slope stability in Phewa Tal watershed, Nepal. *Geophys J Roy Astron Soc* 26:151-170.
- [20] Lee S, Pradhan B. (2006). Probabilistic landslide hazard and risk mapping on Penang Island, Malaysia. *J Earth Syst Sci* 115:661-672.
- [21] Muthu, K., Petrou, M., Tarantino, C., and Blonda, P. (2008). Landslide Possibility Mapping Using Fuzzy Approaches. *IEEE Transactions on Geoscience and Remote Sensing*, 46(4): 1253-1265.
- [22] Pradhan, B. (2010). Remote Sensing and GIS-based landslide hazard analysis and cross validation using multivariate logistic regression model on three test areas in Malaysia. *Advances in Space Research*, 45, 1244-1256.
- [23] Pradhan, B. and Lee, S. (2010). Delineation of landslide hazard areas using frequency ratio, logistic regression and artificial neural network model at Penang Island Malaysia. *Environ Earth Sci* (2010) 60:1037-1054. DOI: 10.1007/s12665-009-0245-8.
- [24] Ma, F., Wang, J. Yuan, R, Zhao, H, Guo, J. (2013). Application of analytical hierarchy process and least square method for landslide susceptibility assessment along Zhong-Wu natural gas pipelines. *China Landslides Doi*, Doi: 10.1007/s10346-013-0402-8.
- [25] Kavzoglu, T., Sahin, E., and Colkensen I. (2013). Landslide susceptibility mapping using GIS based multi-criteria decision analysis, support vector machines and logistic regression. *Landslides*, doi:Doi: 10.1007/s10346-013-0391-7.
- [26] Guiraud, R. (1973). Evolution post-triasique de l'avant pays de la chaîne alpine en Algérie. D'après l'étude du bassin du Hodna et des régions voisines. Thèse de Doctorat Es Science, stratigraphie, Nice, 270pp.
- [27] Coiffait, P.-E., and VILA J M., 1977: Carte géologique de l'Algérie aux 1/50.000 feuilles d'El Aria avec notice explicative.
- [28] Coiffait, P.-E., 1992. Un bassin post-nappe dans son cadre structural: l'exemple du bassin de Constantine (Algérie nord-orientale). *Th. Doct. Etat Sci. Nat.*, Nancy, 1: 405.
- [29] Vila, J.-M., 1980. La chaîne alpine d'Algérie orientale et des confins algéro-tunisiens. Thèse Sc. Univ. Paris VI, 3 vol, 663 p., 199 fig., 40 pl., 7 pl.h.t.
- [30] Lahonder, J., C, 1987. Les séries ultratelliennes d'Algérie Nord-Orientale et les formations environnantes dans leur cadre structural, Paul Sabatier, Toulouse, France, 242 pp.
- [31] Raoult, J.F., (1974). Géologie du centre de la chaîne numidique (nord du constantinois, Algérie). , Paris, France, 156 pp.
- [32] Durand-Delga M(1969) Essai sur la structure du NE de la Berberie. *Bull Serv Carte geol Algérie* 39:89-181.
- [33] Crozier, M. J. (1986). *Landslides: causes, consequences and environment*, Croom Helm, London.
- [34] Coromina, J. (2000). Landslides and climate. Keynote lecture, in: *Proceeding of the 8<sup>th</sup> International Symposium on Landslides*, Balkema, Cardiff, 4, 1-33.

- [35] Tucker, C.J., Dregne, H.E. and Newcomb, W.W., 1991. Expansion and contraction of the Sahara Desert. *Science*, 253, pp.299-301.
- [36] Saaty, T.L. 1980. *The Analytical Hierarchy Process*. McGraw Hill, NY, 350p.
- [37] Malczewski, J. 1999. *GIS and Multi-Criteria Decision Analysis*. 1<sup>st</sup> ed. Jhon Wiley and Sons, NY, 392p.
- [38] Saaty, T. L. 1977. A scaling method for priorities in hierarchical structures. *Journal of mathematical psychology*, 15(3), 234-281.
- [39] Voogd, H. (1983). *Multicriteria Evaluation for Urban and regional Planning*. 1<sup>st</sup> ed. Pion Ltd., London, 367p.
- [40] Zweig MH, Campbell G (1993) Receiver-operating characteristics (ROC) plots. *Clin Chem* 39: 561–577.
- [41] Hanley JA, McNeil BJ (1983). A method of comparing the areas under receiver operating characteristic curves derived from the same cases. *Radiology* 148:839–843.
- [42] Lee S. (2005). Application of logistic regression model and its validation for landslide susceptibility mapping using GIS and remote sensing data. *Int J Remote Sens* 7:1477-1491.

# ESTIMATION FOR BOUNDED SOLUTIONS OF INTEGRAL INEQUALITIES SOME NEW NON-LINEAR RETARDER INTEGRO-DIFFERENTIAL INEQUALITIES.

Submitted on 20/12/2018 – Accepted on 10/07/2019

## Abstract

In this paper, we establish some new non-linear retarded integro-differential inequalities in tow and n independent variables.

**Keywords:** boundary Value Problems ; Retarded integro-differential Equations ; Partial integro-differential equations ; integral inequalities.

**M.E SMAKDJI  
H. KHELLAF**

Department of Mathematics,  
Frères Mentouri  
University, Constantine, Algeria.

## INTRODUCTION

The study of integral inequalities involving functions of one or more independent variables Is an important tool in the study of existence, uniqueness, bounds, stability, invariant manifolds and other qualitative properties of solutions of differential equations and integral equations (see : [1-6, 8,12]).

The study of integro-differential inequalities for functions of two or n variables is very significant and plays a role in the study of the existence and uniqueness of the solutions of Wendroff type integro-differential inequalities and equations as well as the boundedness of the solutions of the initial value problem of non-linear retarded hyperbolic partial integro-differential equations for functions of two or n variables [9-11].

Pachpatte [7] presented some new non-linear integro-differential inequalities of the Wendroff type for two-variable functions.

**Lemma 1.** (See Theorem 1 [7]) Let  $\Phi(x, y)$  and  $c(x, y)$  be non-negative continuous functions defined for  $x \geq 0, y \geq 0$ , and  $\Phi(0, y) = \Phi(x, 0) = 0$  for which the inequality

$$\Phi_{xy}(x, y) \leq a(x) + b(y) + \int_0^x \int_0^y c(s, t) (\Phi(s, t) + \Phi_{xy}(s, t)) dsdt,$$

holds for  $x \geq 0, y \geq 0$ , where  $a(x), b(y) \geq 0$ ;  $a'(x), b'(y) \geq 0$  are continuous functions defined for  $x \geq 0, y \geq 0$ . Then

$$\Phi_{xy}(x, y) \leq a(x) + b(y) + \int_0^x \int_0^y c(s, t) \left[ \frac{[a(0)+b(t)][a(s)+b(0)]}{[a(0)+b(0)]} \right] \exp \left( \int_0^s \int_0^t [1 + c(\tau, \sigma)] d\tau d\sigma \right) dsdt$$

Our main aim here, motivated by the works of Pachppate [7], Zhang, H. and Meng [12], is to establish some new non-linear retarded integro-differential inequalities for functions with tow and n independent variables which are

useful in the analysis of certain classes of partial differential equations and integro-differential inequalities. Some applications of our results are also given

Throughout this paper, we denote  $\mathbb{R}_+^n = [0, \infty[$  which is a subset of  $\mathbb{R}_+^n, (n \geq 1)$ . All the functions which appear in the inequalities are assumed to be real valued of  $n$ -variables ( $n \geq 1$ ) which are non-negative and continuous. All integrals are assumed to exist on their domains of definitions.

We note  $D = D_1 D_2 \dots D_n$ , where  $D_i$ , for  $i = 1, 2, \dots, n$ .

## II. MAIN RESULTS

In this section, we present some results of non-linear retarded integro-differential inequalities in two independent variables.

**Theorem 2.** Let  $u(x, y), c(x, y)$  and  $a(x, y), D_i u(x, y)$  and  $Du(x, y)$  be non-negative continuous functions for all  $i = 1, 2$  defined for  $x, y \in \mathbb{R}_+$  and  $\alpha, \beta \in C^1(\mathbb{R}_+, \mathbb{R}_+)$  be non-decreasing functions in each variable, with  $\alpha(x) \geq x$  on  $\mathbb{R}_+$ , and  $\beta(y) \geq y$  on  $\mathbb{R}_+$ . Let  $c(x, y)$  be non-decreasing in each variable  $x, y \in \mathbb{R}_+$ , and

$$\lim_{x \rightarrow \infty} u(x, y) = \lim_{x \rightarrow \infty} u(x, y) = 0.$$

If

$$Du(x, y) \leq c(x, y) + \int_{\alpha(x)}^{\infty} \int_{\beta(y)}^{\infty} a(s, t) [u(s, t) + Du(s, t)] dsdt, \tag{2.1}$$

for all  $x, y \in \mathbb{R}_+$ , then

$$Du(x, y) \leq c(x, y) \int_{\alpha(x)}^{\infty} \int_{\beta(y)}^{\infty} a(s, t) \exp \left[ \int_s^{\infty} \int_t^{\infty} [a(\tau, \sigma)] d\tau d\sigma \right] dsdt \tag{2.2}$$

For all  $x, y \in \mathbb{R}_+$ .

Proof: Fix any  $X, Y \in \mathbb{R}_+$ . Then, for  $x \leq X$  and  $y \leq Y$ , we have

$$Du(x, y) \leq c(X, Y) + \int_{\alpha(x)}^{\infty} \int_{\beta(y)}^{\infty} a(s, t)[u(s, t) + Du(s, t)]dsdt,$$

Define a function  $z(x, y)$  by

$$z(x, y) = c(X, Y) + \int_{\alpha(x)}^{\infty} \int_{\beta(y)}^{\infty} a(s, t)[u(s, t) + Du(s, t)]dsdt, \quad (2.3)$$

Then

$$\lim_{x \rightarrow \infty} z(x, y) = \lim_{y \rightarrow \infty} z(x, y) = c(X, Y),$$

And

$$Du(x, y) \leq z(x, y). \quad (2.4)$$

By differentiating (2.3)

$$Dz(x, y) \leq a(\alpha(x), \beta(y))[u(\alpha(x), \beta(y)) + Du(\alpha(x), \beta(y))] \alpha'(x) \beta'(y) \quad (2.5)$$

By integrating both sides of (2.4)

$$Du(x, y) \leq \int_{\alpha(x)}^{\infty} \int_{\beta(y)}^{\infty} z(s, t)dsdt, \quad (2.6)$$

Now, using (2.4) and (2.6) in (2.5), we get

$$Dz(x, y) \leq a(\alpha(x), \beta(y)) \left[ z(x, y) + \int_{\alpha(x)}^{\infty} \int_{\beta(y)}^{\infty} z(s, t)dsdt \right] \alpha'(x) \beta'(y). \quad (2.7)$$

If we put

$$v(x, y) = z(x, y) + \int_{\alpha(x)}^{\infty} \int_{\beta(y)}^{\infty} z(s, t)dsdt, \quad (2.8)$$

then

$$\lim_{x \rightarrow \infty} z(x, y) = \lim_{y \rightarrow \infty} z(x, y) = c(X, Y),$$

and

$$Dv(x, y) \leq Dz(x, y) + z(x, y) \alpha'(x) \beta'(y).$$

using the fact that

$$Dz(x, y) \leq a(\alpha(x), \beta(y))v(x, y) \alpha'(x) \beta'(y)$$

from (2.7) form (2.8) we have

$$Dv(x, y) \leq [1 + a(x, y)]v(x, y) \alpha'(x) \beta'(y).$$

It is easy to estimate  $v(x, y)$  by

$$v(x, y) \leq c(X, Y) \int_{\alpha(x)}^{\infty} \int_{\beta(y)}^{\infty} [1 + a(s, t)]dsdt. \quad (2.9)$$

By substituting (2.9) in (2.7) and integrating both sides, we get

$$z(x, y) \leq c(X, Y) \int_{\alpha(x)}^{\infty} \int_{\beta(y)}^{\infty} a(s, t) \exp \left[ \int_s^{\infty} \int_t^{\infty} [a(\tau, \sigma)]d\tau d\sigma \right] dsdt.$$

Since  $X$  and  $Y$  are arbitrarities and by substituting the value of  $z(x, y)$  in (2.4), we obtain the inequality (2.2).

**Remark 1** If we put  $\infty = 0, \alpha(x) = x, \beta(y) = y,$  and  $c(x, y) = c_1(x) + c_2(y)$  in Theorem 2 we obtain Theorem 1 in [7].

**Corollary 3.** Let  $u(x, y), c(x, y)$  and  $a(x, y), D_i u(x, y)$  and  $Du(x, y)$  be non-negative continuous functions for all  $i = 1, 2$  defined for  $x, y \in \mathbb{R}_+$  and  $\alpha, \beta \in C^1(\mathbb{R}_+, \mathbb{R}_+)$  be non-decreasing functions in each variable, with  $\alpha(x) \geq x$  on  $\mathbb{R}_+$ , and  $\beta(y) \geq y$  on  $\mathbb{R}_+$ . Let  $c(x, y)$  be non-decreasing in each variable  $x, y \in \mathbb{R}_+$ , and

$$\lim_{x \rightarrow \infty} u(x, y) = \lim_{y \rightarrow \infty} u(x, y) = 0,$$

If

$$Du(x, y) \leq c(x, y) + M \left[ u(x, y) + \int_{\alpha(x)}^{\infty} \int_{\beta(y)}^{\infty} a(s, t)[u(s, t) + Du(s, t)]dsdt \right], \quad (2.10)$$

for all  $x, y \in \mathbb{R}_+$ , where  $M > 0$  is constant, then

$$Du(x, y) \leq c(x, y) \exp \int_{\alpha(x)}^{\infty} \int_{\beta(y)}^{\infty} [M + Ma(s, t) + a(s, t)]dsdt, \quad (2.11)$$

for all  $x, y \in \mathbb{R}_+$ .

**Proof :** Fix any  $X, Y \in \mathbb{R}_+$ . Then, for  $x \leq X$  and  $y \leq Y$ , then from (2.10)

$$Du(x, y) \leq c(X, Y) + M \left[ u(x, y) + \int_{\alpha(x)}^{\infty} \int_{\beta(y)}^{\infty} a(s, t)[u(s, t) + Du(s, t)]dsdt \right],$$

Define a function  $z(x, y)$  by

$$z(x, y) = c(X, Y) + M \left[ u(x, y) + \int_{\alpha(x)}^{\infty} \int_{\beta(y)}^{\infty} a(s, t)[u(s, t) + Du(s, t)]dsdt \right], \quad (2.12)$$

Then

$$\lim_{x \rightarrow \infty} z(x, y) = \lim_{y \rightarrow \infty} z(x, y) = c(X, Y)$$

And

$$Du(x, y) \leq z(x, y). \quad (2.13)$$

By differentiating (2.12) and using (2.13), we have

$$Dz(x, y) \leq z(x, y) [M + Ma(\alpha(x), \beta(y)) + a(\alpha(x), \beta(y))] \alpha'(x) \beta'(y),$$

Therefore

$$z(x, y) \leq c(X, Y) \exp \int_{\alpha(x)}^{\infty} \int_{\beta(y)}^{\infty} [M + Ma(s, t) + a(s, t)]dsdt,$$

Since  $X$  and  $Y$  are arbitrary and by substituting the value of  $z(x, y)$  in (2.13), we obtain the inequality (2.11).

**Remark 2.** If we put  $\infty = 0, \alpha(x) = x, \beta(y) = y$ , and  $c(x, y) = c_1(x) + c_2(y)$  in corollary 3 we obtain theorem 2 in [8].

**Corollary 4.** Let  $u(x, y), c(x, y)$  and  $a(x, y), D_i u(x, y)$  and  $Du(x, y)$  be non-negative continuous functions for all  $i = 1, 2$  defined for  $x, y \in \mathbb{R}_+$  and  $\alpha, \beta \in C^1(\mathbb{R}_+, \mathbb{R}_+)$  be non-decreasing functions in each variable, with  $\alpha(x) \geq x$  on  $\mathbb{R}_+$ , and  $\beta(y) \geq y$  on  $\mathbb{R}_+$ . Let  $c(x, y)$  be non-decreasing in each variable  $x, y \in \mathbb{R}_+$ , and

$$\lim_{x \rightarrow \infty} u(x, y) = \lim_{y \rightarrow \infty} u(x, y) = 0,$$

If

$$Du(x, y) \leq c(x, y) + M \left[ u(x, y) + \int_{\alpha(x)}^{\infty} \int_{\beta(y)}^{\infty} a(s, t) Du(s, t) ds dt \right],$$

for all  $x, y \in \mathbb{R}_+$ , where  $M > 0$  is constant, then

$$Du(x, y) \leq c(x, y) \exp \int_{\alpha(x)}^{\infty} \int_{\beta(y)}^{\infty} M[a(s, t) + 1] ds dt,$$

for all  $x, y \in \mathbb{R}_+$ .

Proof : The proof of this Corollary follows the same arguments as in Corollary 3.

**Remark 3.** If we put  $\infty = 0, \alpha(x) = x, \beta(y) = y$ , and  $c(x, y) = c_1(x) + c_2(y)$  in Corollary 4 we obtain the result in [12].

**Theorem 5.** Let  $u(x, y), c(x, y)$  and  $a(x, y), b(x, y)$  be non-negative continuous functions defined for  $x, y \in \mathbb{R}_+$  and  $\alpha, \beta \in C^1(\mathbb{R}_+, \mathbb{R}_+)$  be non-decreasing functions in each variable, with  $\alpha(x) \geq x$  on  $\mathbb{R}_+$ , and  $\beta(y) \geq y$  on  $\mathbb{R}_+$ . Let  $c(x, y)$  be non-decreasing in each variable  $x, y \in \mathbb{R}_+$ . If

$$u(x, y) \leq c(x, y) + \int_{\alpha(x)}^{\infty} \int_{\beta(y)}^{\infty} a(s, t) u(s, t) ds dt + \int_{\alpha(x)}^{\infty} \int_{\beta(y)}^{\infty} a(s, t) \left[ \int_s^{\infty} \int_t^{\infty} b(\tau, \sigma) u(\tau, \sigma) d\tau d\sigma \right] ds dt \quad (2.14)$$

For all  $x, y \in \mathbb{R}_+$ , then

$$u(x, y) \leq c(x, y) \exp \int_{\alpha(x)}^{\infty} \int_{\beta(y)}^{\infty} a(s, t) ds dt + \int_{\alpha(x)}^{\infty} \int_{\beta(y)}^{\infty} a(s, t) \left[ \int_s^{\infty} \int_t^{\infty} b(\tau, \sigma) d\tau d\sigma \right] ds dt, \quad (2.15)$$

For all  $x, y \in \mathbb{R}_+$ .

Proof: Since  $c(x, y)$  is non-negative and non-decreasing, from (2.14) we have

$$\frac{u(x, y)}{c(x, y)} \leq 1 + \int_{\alpha(x)}^{\infty} \int_{\beta(y)}^{\infty} a(s, t) \frac{u(s, t)}{c(s, t)} ds dt + \int_{\alpha(x)}^{\infty} \int_{\beta(y)}^{\infty} a(s, t) \left[ \int_s^{\infty} \int_t^{\infty} b(\tau, \sigma) \frac{u(\tau, \sigma)}{c(\tau, \sigma)} d\tau d\sigma \right] ds dt,$$

Define a function  $z(x, y)$  by the right side of the last inequality. Then  $z(x, y) \geq 0$ ,

$$\lim_{x \rightarrow \infty} z(x, y) = \lim_{y \rightarrow \infty} z(x, y) = 1, \frac{u(x, y)}{c(x, y)} \leq z(x, y),$$

and

$$Dz(x, y) \leq z(x, y) \left[ a(x, y) + a(x, y) \int_{\alpha(x)}^{\infty} \int_{\beta(y)}^{\infty} b(s, t) ds dt \right] \alpha'(x) \beta'(y).$$

i.e

$$\frac{Dz(x, y) \cdot z(x, y)}{z^2(x, y)} - \frac{D_1 z(x, y) D_2 z(x, y)}{z^2(x, y)} \leq \left[ a(x, y) + a(x, y) \int_{\alpha(x)}^{\infty} \int_{\beta(y)}^{\infty} b(s, t) ds dt \right] \alpha'(x) \beta'(y).$$

Thus

$$D_2 \left[ \frac{D_1 z(x, y)}{z(x, y)} \right] \leq \left[ a(x, y) + a(x, y) \int_{\alpha(x)}^{\infty} \int_{\beta(y)}^{\infty} b(s, t) ds dt \right] \alpha'(x) \beta'(y) \quad (2.16)$$

By keeping  $y$  fixed, setting  $x = s$ , and integrating from  $\alpha(x)$  to  $\infty$  in (2.16), and again by keeping  $x$  fixed, setting  $y = t$ , and integrating from  $\beta(y)$  to  $\infty$  in the resulting inequality, we have

$$z(x, y) \leq c(x, y) \exp \int_{\alpha(x)}^{\infty} \int_{\beta(y)}^{\infty} a(s, t) ds dt + \int_{\alpha(x)}^{\infty} \int_{\beta(y)}^{\infty} a(s, t) \left[ \int_s^{\infty} \int_t^{\infty} b(\tau, \sigma) d\tau d\sigma \right] ds dt.$$

Finally, since

$$\frac{u(x, y)}{c(x, y)} \leq z(x, y)$$

We obtain the inequality (2.15).

**Remark 4.**

1. If we put  $\infty = 0, \alpha(x) = x, \beta(y) = y$ , and  $c(x, y) = c_1(x) + c_2(y)$  in theorem 5 we obtain theorem 3 [7].
2. In the particular case when  $b(x, y) = 0$ , then the bound obtained in [8] reduces to :

$$u(x, y) \leq c(x, y) \exp \int_{\alpha(x)}^{\infty} \int_{\beta(y)}^{\infty} a(s, t) ds dt. \quad (2.17)$$

**Theorem 6.** Let  $u(x, y), c(x, y)$  and  $a(x, y), b(x, y), f(x, y), D_i u(x, y)$  and  $Du(x, y)$  be non-negative continuous functions for all  $i = 1, 2$  defined for  $x, y \in \mathbb{R}_+$  and  $\alpha, \beta \in C^1(\mathbb{R}_+, \mathbb{R}_+)$  be non-decreasing functions in each variable, with  $\alpha(x) \geq x$  on  $\mathbb{R}_+$ , and  $\beta(y) \geq y$  on  $\mathbb{R}_+$ .

And

$$\lim_{x \rightarrow \infty} u(x, y) = \lim_{x \rightarrow \infty} u(x, y) = 0$$

Let  $K(u(x, y))$  be a real-valued, positive, continuous, strictly non-decreasing, sub-additive, and sub-multiplicative function for  $u(x, y) \geq 0$ , and  $H(u(x, y))$  be a real-valued, positive, continuous and non-decreasing function defined for  $x, y \in \mathbb{R}_+$ . Assume that  $c(x, y)$  and  $f(x, y)$  are non-decreasing in each of the variables  $x, y \in \mathbb{R}_+$ . If

$$Du(x, y) \leq c(x, y) + f(x, y)H\left(\int_{\alpha(x)}^{\infty} \int_{\beta(y)}^{\infty} a(s, t)K(u(s, t))dsdt\right) + \int_{\alpha(x)}^{\infty} \int_{\beta(y)}^{\infty} b(s, t)Du(s, t)dsdt, \quad (2.18)$$

for all  $x, y \in \mathbb{R}_+$ , then

$$u(x, y) \leq c(x, y) + f(x, y)H\left(G^{-1}\left[G(\xi) + \int_{\alpha(x)}^{\infty} \int_{\beta(y)}^{\infty} a(s, t)K(f(s, t)p(s, t))dsdt\right]\right)p(x, y) \quad (2.19)$$

for all  $x, y \in \mathbb{R}_+$ , where

$$p(x, y) = \int_{\alpha(x)}^{\infty} \int_{\beta(y)}^{\infty} \exp\left[\int_s^{\infty} \int_t^{\infty} b(\tau, \sigma)d\tau d\sigma\right] dsdt. \quad (2.20)$$

$$\xi = \int_0^{\infty} \int_0^{\infty} a(s, t)K(c(s, t)p(s, t))dsdt. \quad (2.21)$$

$$G(r) = \int_r^{\infty} \frac{ds}{K(H(s))}. \quad (2.22)$$

Where  $G^{-1}$  is the inverse function of  $G$ , and

$$G(\xi) + \int_{\alpha(x)}^{\infty} \int_{\beta(y)}^{\infty} a(s, t)K(f(s, t)p(s, t))dsdt \in \text{dom}(G^{-1})$$

for all  $x, y \in \mathbb{R}_+$ .

Proof : Define a function  $z(x, y)$  by

$$z(x, y) = c(x, y) + f(x, y)H\left(\int_{\alpha(x)}^{\infty} \int_{\beta(y)}^{\infty} a(s, t)K(u(s, t))dsdt\right), \quad (2.23)$$

then from (2.18), we have

$$Du(x, y) \leq z(x, y) + \int_{\alpha(x)}^{\infty} \int_{\beta(y)}^{\infty} b(s, t)Du(s, t)dsdt. \quad (2.24)$$

Clearly,  $z(x, y)$  is a positive, continuous, and decreasing function in each of the variables  $x, y \in \mathbb{R}_+$ . Using (2.17) from Theorem 5 in (2.24), we get

$$Du(x, y) \leq z(x, y)\exp\int_{\alpha(x)}^{\infty} \int_{\beta(y)}^{\infty} b(s, t)dsdt. \quad (2.25)$$

By integration, first with respect to  $x$  from  $x$  to  $\infty$ , and then with respect to  $y$  from  $y$  to  $\infty$  in the last inequality, we obtain

$$u(x, y) \leq z(x, y)p(x, y). \quad (2.26)$$

where  $p(x, y)$  is defined in (2.20). From (2.23) we have

$$z(x, y) = c(x, y) + f(x, y)H(v(x, y)), \quad (2.27)$$

where

$$v(x, y) = \int_{\alpha(x)}^{\infty} \int_{\beta(y)}^{\infty} a(s, t)K(u(s, t))dsdt. \quad (2.28)$$

Now, using (2.27) in (2.26) we get

$$u(x, y) \leq [c(x, y) + f(x, y)H(v(x, y))]p(x, y). \quad (2.29)$$

From (2.28) and (2.29) and since  $K$  is a sub-additive and sub-multiplicative function, we obtain

$$v(x, y) \leq \int_{\alpha(x)}^{\infty} \int_{\beta(y)}^{\infty} a(s, t)K\left([c(s, t) + f(s, t)H(v(s, t))]p(s, t)\right)dsdt \leq \int_{\alpha(x)}^{\infty} \int_{\beta(y)}^{\infty} a(s, t)K(c(s, t)p(s, t))dsdt + \int_{\alpha(x)}^{\infty} \int_{\beta(y)}^{\infty} a(s, t)K(f(s, t)H(v(s, t))p(s, t))dsdt.$$

Therefore

$$v(x, y) \leq \int_0^{\infty} \int_0^{\infty} a(s, t)K(c(s, t)p(s, t))dsdt + \int_{\alpha(x)}^{\infty} \int_{\beta(y)}^{\infty} a(s, t)K(f(s, t)p(s, t))K(H(v(s, t)))dsdt.$$

Define a function  $\Phi(x, y)$  by

$$\Phi(x, y) = \int_0^{\infty} \int_0^{\infty} a(s, t)K(c(s, t)p(s, t))dsdt + \int_{\alpha(x)}^{\infty} \int_{\beta(y)}^{\infty} a(s, t)K(f(s, t)p(s, t))K(H(v(s, t)))dsdt.$$

$$(2.30)$$

Then

$$\lim_{x \rightarrow \infty} \Phi(x, y) = \lim_{y \rightarrow \infty} \Phi(x, y) = \int_0^{\infty} \int_0^{\infty} a(s, t)K(c(s, t)p(s, t))dsdt = \xi. \quad (2.31)$$

and

$$v(x, y) \leq \Phi(x, y). \quad (2.32)$$

Clearly,  $\Phi(x, y)$  is a positive and decreasing function in  $y$ , then

$$D_1\Phi(x, y) = -\int_{\beta(y)}^{\infty} a(\alpha(x), t)K(f(\alpha(x), t)p(\alpha(x), t))K(H(v(\alpha(x), t)))dsdt \alpha'(x) \geq -K(H(\Phi(x, y)))\int_{\beta(y)}^{\infty} a(\alpha(x), t)K(f(\alpha(x), t)p(\alpha(x), t))dsdt \alpha'(x).$$

i.e

$$\begin{aligned} & \frac{D_1 \Phi(x, y)}{K(H(\Phi(x, y)))} \\ & \geq - \int_{\beta(y)}^{\infty} a(\alpha(x), t) K(f(\alpha(x), t) p(\alpha(x), t)) dsd. \end{aligned} \quad (2.33)$$

From (2.22) we have

$$\begin{aligned} & \frac{D_1 G(\Phi(x, y))}{K(H(\Phi(x, y)))} \\ & \geq - \int_{\beta(y)}^{\infty} a(\alpha(x), t) K(f(\alpha(x), t) p(\alpha(x), t)) dsdt \end{aligned} \quad (2.34)$$

Now, by setting  $x = s$  and integrating from  $x$  to  $\infty$  in (2.34), and using (2.31) we get

$$\begin{aligned} & \Phi(x, y) \leq G^{-1} \left[ G(\xi) + \int_{\alpha(x)}^{\infty} \int_{\beta(y)}^{\infty} a(s, t) K(f(s, t) p(s, t)) dsdt \right], \end{aligned} \quad (2.35)$$

Finally, by substituting (2.27), (2.32) and (2.25), (2.35) we obtain the inequality (2.19).

**Remark 5.**

1. From the inequalities (2.29), (2.32) and (2.35) in the proof of Theorem 6 we can find this inequality

$$u(x, y) \leq c(x, y) + f(x, y) H \left( G^{-1} \left[ G(\xi) + \int_{\alpha(x)}^{\infty} \int_{\beta(y)}^{\infty} a(s, t) K(f(s, t) p(s, t)) dsdt \right] \right) p(x, y).$$

2. If we put  $\infty = 0, \alpha(x) = x, \beta(y) = y$ , and  $c(x, y) = c_1(x) + c_2(y), f(x, y) = 1, H(x) = K(x) = x$  in theorem 6 we obtain Theorem 1 [12].

**Corollary 7.** Let  $u(x, y), c(x, y)$  and  $a(x, y), b(x, y), D_i u(x, y)$  and  $Du(x, y)$  be non-negative continuous functions for all  $i = 1, 2$  defined for  $x, y \in \mathbb{R}_+$  and  $\alpha, \beta \in C^1(\mathbb{R}_+, \mathbb{R}_+)$  be non-decreasing functions in each variable, with  $\alpha(x) \geq x$  on  $\mathbb{R}_+$ , and  $\beta(y) \geq y$  on  $\mathbb{R}_+$ .

And

$$\lim_{x \rightarrow \infty} u(x, y) = \lim_{x \rightarrow \infty} u(x, y) = 0$$

Let  $K(u(x, y))$  be a real-valued, positive, continuous, strictly non-decreasing, sub-additive, and sub-multiplicative function for  $u(x, y) \geq 0$ . Assume that  $c(x, y)$  is non-decreasing in each of the variables  $x, y \in \mathbb{R}_+$ . If

$$\begin{aligned} & Du(x, y) \\ & \leq c(x, y) + \int_{\alpha(x)}^{\infty} \int_{\beta(y)}^{\infty} a(s, t) K(u(s, t)) dsdt \\ & \quad + \int_{\alpha(x)}^{\infty} \int_{\beta(y)}^{\infty} b(s, t) Du(s, t) dsdt, \end{aligned} \quad (2.36)$$

for all  $x, y \in \mathbb{R}_+$ , then

$$u(x, y) \leq c(x, y) + H \left( T^{-1} \left[ T(\xi) + \int_{\alpha(x)}^{\infty} \int_{\beta(y)}^{\infty} a(s, t) K(p(s, t)) dsdt \right] \right) p(x, y), \quad (2.37)$$

for all  $x, y \in \mathbb{R}_+$ , where  $p(x, y)$  and  $\xi$  are defined in theorem 6.

$$T(r) = \int_r^{\infty} \frac{ds}{K(s)}.$$

Where  $T^{-1}$  is the inverse function of  $G$ , and

$$T(\xi) + \int_{\alpha(x)}^{\infty} \int_{\beta(y)}^{\infty} a(s, t) T(p(s, t)) dsdt \in \text{dom}(T^{-1})$$

for all  $x, y \in \mathbb{R}_+$ .

Proof : The proof of this Corollary follows the same arguments as in Theorem 6.

**Remark 6.**

1. If we put  $f(x, y) = 1, H(x) = x$  in theorem 6 then we obtain the result in Corollary 7.

2. If we put  $\infty = 0, \alpha(x) = x, \beta(y) = y$ , and  $c(x, y) = c_1(x) + c_2(y), a(x, y) = b(x, y), K(x) = x$  in corollary 7 we obtain theorem 1 in [7].

**Corollary 8.** Let  $u(x, y), a(x, y), b(x, y), D_i u(x, y)$  and  $Du(x, y)$  be non-negative continuous functions for all  $i = 1, 2$  defined for  $x, y \in \mathbb{R}_+$  and  $\alpha, \beta \in C^1(\mathbb{R}_+, \mathbb{R}_+)$  be non-decreasing functions in each variable, with  $\alpha(x) \geq x$  on  $\mathbb{R}_+$ , and  $\beta(y) \geq y$  on  $\mathbb{R}_+$ .

And

$$\lim_{x \rightarrow \infty} u(x, y) = \lim_{x \rightarrow \infty} u(x, y) = 0.$$

If

$$\begin{aligned} & Du(x, y) \leq M + \int_{\alpha(x)}^{\infty} \int_{\beta(y)}^{\infty} a(s, t) u(s, t) dsdt + \\ & \int_{\alpha(x)}^{\infty} \int_{\beta(y)}^{\infty} b(s, t) Du(s, t) dsdt, \end{aligned} \quad (2.38)$$

for all  $x, y \in \mathbb{R}_+$ , where  $M > 0$  is constant, then the following conclusions are true:

$$\begin{aligned} & Du(x, y) \leq M \left( 1 + \int_0^{\infty} \int_0^{\infty} a(s, t) p(s, t) dsdt \exp \int_{\alpha(x)}^{\infty} \int_{\beta(y)}^{\infty} a(s, t) p(s, t) dsdt \right) \\ & \quad \exp \int_{\alpha(x)}^{\infty} \int_{\beta(y)}^{\infty} b(s, t) dsdt, \end{aligned}$$

$$u(x, y) \leq M \left( 1 + \int_0^{\infty} \int_0^{\infty} a(s, t) p(s, t) dsdt \exp \int_{\alpha(x)}^{\infty} \int_{\beta(y)}^{\infty} a(s, t) p(s, t) dsdt \right) p(x, y)$$

For all  $x, y \in \mathbb{R}_+$ , where  $p(x, y)$  and  $\xi$  are defined in theorem 6.

Proof : By setting  $K(x) = x$  and  $c(x, y) = M$  in Corollary 7, we obtain the results of this Corollary.

**Corollary 9.** Let  $u(x, y), a(x, y), b(x, y), D_i u(x, y)$  and  $Du(x, y)$  be non-negative continuous functions for all  $i = 1, 2$  defined for  $x, y \in \mathbb{R}_+$  and  $\alpha, \beta \in C^1(\mathbb{R}_+, \mathbb{R}_+)$  be non-decreasing functions in each variable, with  $\alpha(x) \geq x$  on  $\mathbb{R}_+$ , and  $\beta(y) \geq y$  on  $\mathbb{R}_+$ .

And

$$\lim_{x \rightarrow \infty} u(x, y) = \lim_{x \rightarrow \infty} u(x, y) = 0$$

Let  $K(u(x, y))$  be a real-valued, positive, continuous, strictly non-decreasing, sub-additive, and sub-multiplicative function for  $u(x, y) \geq 0$ . If

$$\begin{aligned} Du(x, y) &\leq c_1(x) + c_2(y) \\ &+ \int_{\alpha(x)}^{\infty} \int_{\beta(y)}^{\infty} a(s, t) K(u(s, t)) ds dt \\ &+ \int_{\alpha(x)}^{\infty} \int_{\beta(y)}^{\infty} b(s, t) Du(s, t) ds dt, \end{aligned}$$

For all  $x, y \in \mathbb{R}_+$ , where  $c_1(x), c_2(y) > 0$ , and  $c'_1(x), c'_2(y) > 0$  are continuous functions defined for  $x \geq 0, y \geq 0$  then

$$\begin{aligned} Du(x, y) &\leq c_1(x) + c_2(y) \\ &+ \left( T^{-1} \left[ T(\xi) + \int_{\alpha(x)}^{\infty} \int_{\beta(y)}^{\infty} a(s, t) K(p(s, t)) ds dt \right] \right) \\ &exp \int_{\alpha(x)}^{\infty} \int_{\beta(y)}^{\infty} b(s, t) ds dt, \end{aligned}$$

For all  $x, y \in \mathbb{R}_+$ , where

$$\xi = \int_0^{\infty} \int_0^{\infty} a(s, t) K((c_1(s) + c_2(t))p(s, t)) ds dt$$

And  $p(x, y)$  and  $T$  are defined in corollary 7.

Proof : By setting  $c(x, y) = c_1(x) + c_2(y)$  in Corollary 7 and using the same arguments in theorem 6, we obtain the results of this Corollary.

### III. Retarded Non-Linear Integro-Differential Inequalities in n Independent Variables

In this section, we present some results of non-linear retarded integro-differential inequalities in  $n$  independent variables.

In what follows, for

$$x = (x_1, x_2, \dots, x_n), t = (t_1, t_2, \dots, t_n), \infty = (\infty, \infty, \dots, \infty),$$

We denote :

For  $x, t \in \mathbb{R}_+^n$ , we shall write  $t \leq x$  whenever  $t_i \leq x_i, i = 1, 2, \dots, n$ . For any  $X = (X_1, X_2, \dots, X_n) \in \mathbb{R}_+^n$ , we shall write  $x \leq X$  whenever  $x_i \leq X_i, i = 1, 2, \dots, n$ .

$$\tilde{\alpha}(x) = (\alpha_1(x_1), \alpha_2(x_2), \dots, \alpha_n(x_n)) \in C^1(\mathbb{R}_+^n, \mathbb{R}_+^n).$$

We denote  $\hat{\alpha}(x) \geq x$  whenever  $\alpha_i(x_i) \geq x_i$  for  $i = 1, 2, \dots, n$ .

$$\int_{\tilde{\alpha}}^{\infty} dt = \int_{\alpha_1(x_1)}^{\infty} \int_{\alpha_2(x_2)}^{\infty} \dots \int_{\alpha_n(x_n)}^{\infty} dt_n \dots dt_2 dt_1.$$

Our main results are given in the following theorems.

**Theorem 10.** Let  $u(x), a(x)$  and  $c(x)$  be non-negative continuous functions defined for  $x \in \mathbb{R}_+^n$  and  $\tilde{\alpha} \in C^1(\mathbb{R}_+^n, \mathbb{R}_+^n)$  be non-decreasing functions in each variable, with  $\tilde{\alpha}(x) \geq x$  on  $\mathbb{R}_+^n$ . Assume that  $c(x)$  is non-decreasing in each variable  $x \in \mathbb{R}_+^n$ , if

$$u(x) \leq c(x) + \int_{\tilde{\alpha}(x)}^{\infty} a(t) u(t) dt, \tag{3.1}$$

for  $x \in \mathbb{R}_+^n$ , then

$$u(x) \leq c(x) exp \int_{\tilde{\alpha}(x)}^{\infty} a(t) dt. \tag{3.2}$$

Proof : Since  $c(x)$  is non-negative and non-decreasing, from (3.1) we have

$$\frac{u(x)}{c(x)} \leq 1 + \int_{\tilde{\alpha}(x)}^{\infty} a(t) \frac{u(t)}{c(t)} dt$$

Define a function  $z(x)$  by

$$z(x) = 1 + \int_{\tilde{\alpha}(x)}^{\infty} a(t) \frac{u(t)}{c(t)} dt,$$

then

$$z(x) > 0, \lim_{x_i \rightarrow \infty} z(x_1, \dots, x_n) = 1, i = 1, 2, \dots, n, \frac{u(x)}{c(x)} \leq z(x)$$

$$\begin{cases} Dz(x) \leq a(x)z(x)\tilde{\alpha}'(x); \text{ if } n \text{ is even} \\ Dz(x) \geq -a(x)z(x)\tilde{\alpha}'(x); \text{ if } n \text{ is odd} \end{cases}$$

i.e

$$\frac{z(x)Dz(x)}{z^2(x)} - \frac{D_n z(x)(D_1 \dots D_{n-1} z(x))}{z^2(x)} \leq a(x)\tilde{\alpha}'(x).$$

Therefore

$$\begin{cases} D_n \left( \frac{D_1 \dots D_{n-1} z(x)}{z^2(x)} \right) \leq a(x)\tilde{\alpha}'(x); \text{ if } n \text{ is even} \\ D_n \left( \frac{D_1 \dots D_{n-1} z(x)}{z(x)} \right) \geq -a(x)\tilde{\alpha}'(x); \text{ if } n \text{ is odd} \end{cases} \tag{3.3}$$

By integrating (3.3) with respect to  $x_n$  from  $x_n$  to  $\infty$ , we have

$$\begin{cases} -\left(\frac{D_1 \dots D_{n-1} z(x)}{z^2(x)}\right) \leq \int_{\alpha_n(x_n)}^{\infty} a(x_1, \dots, x_{n-1}, t_n) dt_n \alpha_1'(x_1) \dots \alpha_{n-1}'(x_{n-1}); \text{ if } n \text{ is even} \\ -\left(\frac{D_1 \dots D_{n-1} z(x)}{z^2(x)}\right) \geq - \int_{\alpha_n(x_n)}^{\infty} a(x_1, \dots, x_{n-1}, t_n) dt_n \alpha_1'(x_1) \dots \alpha_{n-1}'(x_{n-1}); \text{ if } n \text{ is odd} \end{cases},$$

thus

$$\begin{cases} \frac{D_1 \dots D_{n-1} z(x)}{z(x)} \geq D_{n-1} \left(\frac{D_1 \dots D_{n-2} z(x)}{z(x)}\right); \text{ if } n \text{ is even} \\ \frac{D_1 \dots D_{n-1} z(x)}{z(x)} \leq D_{n-1} \left(\frac{D_1 \dots D_{n-2} z(x)}{z(x)}\right); \text{ if } n \text{ is odd} \end{cases},$$

hence

$$\begin{cases} -D_{n-1} \left(\frac{D_1 \dots D_{n-2} z(x)}{z(x)}\right) \leq \int_{\alpha_n(x_n)}^{\infty} a(x_1, \dots, x_{n-1}, t_n) dt_n \alpha_1'(x_1) \dots \alpha_{n-1}'(x_{n-1}); \text{ if } n \text{ is even} \\ -D_{n-1} \left(\frac{D_1 \dots D_{n-2} z(x)}{z(x)}\right) \geq - \int_{\alpha_n(x_n)}^{\infty} a(x_1, \dots, x_{n-1}, t_n) dt_n \alpha_1'(x_1) \dots \alpha_{n-1}'(x_{n-1}); \text{ if } n \text{ is odd} \end{cases},$$

By integrating the last inequality with respect to  $x_{n-1}$  from  $x_{n-1}$  to  $\infty$ , we have

$$\begin{cases} \frac{D_1 \dots D_{n-2} z(x)}{z(x)} \leq \int_{\alpha_{n-1}(x_{n-1})}^{\infty} \int_{\alpha_n(x_n)}^{\infty} a(x_1, \dots, x_{n-2}, t_{n-1}, t_n) dt_n dt_{n-1} \alpha_1'(x_1) \dots \alpha_{n-2}'(x_{n-2}); \text{ if } n \text{ is even} \\ \frac{D_1 \dots D_{n-2} z(x)}{z(x)} \geq - \int_{\alpha_{n-1}(x_{n-1})}^{\infty} \int_{\alpha_n(x_n)}^{\infty} a(x_1, \dots, x_{n-2}, t_{n-1}, t_n) dt_n dt_{n-1} \alpha_1'(x_1) \dots \alpha_{n-2}'(x_{n-2}); \text{ if } n \text{ is odd} \end{cases},$$

By continuing this process, we get

$$\begin{cases} -\frac{D_1 z(x)}{z(x)} \leq \int_{\alpha_2(x_2)}^{\infty} \dots \int_{\alpha_n(x_n)}^{\infty} a(x_1, t_2, \dots, t_n) dt_n \dots dt_2 \alpha_1'(x_1); \text{ if } n \text{ is even} \\ \frac{D_1 z(x)}{z(x)} \geq - \int_{\alpha_2(x_2)}^{\infty} \dots \int_{\alpha_n(x_n)}^{\infty} a(x_1, t_2, \dots, t_n) dt_n \dots dt_2 \alpha_1'(x_1); \text{ if } n \text{ is odd} \end{cases}, \quad (3.4)$$

By integrating (3.4) with respect to  $x_1$  from  $x_1$  to  $\infty$ , we have

$$z(x) \leq \exp \int_{\tilde{\alpha}(x)}^{\infty} a(t) dt.$$

Finally, since  $\frac{u(x)}{c(x)} \leq z(x)$  we obtain the inequality (3.2).

**Remark 7.** In the particular case when  $n = 2$ ,  $x \in \mathbb{R}_+^2$ ,  $(\infty, \infty) = (0, 0)$ ,  $\alpha_1(x_1) = x_1$ ,  $\alpha_2(x_2) = x_2$ , and  $c(x) = c_1(x_1) + c_2(x_2)$  then theorem 10 reduces to lemma 1 in [12].

**Theorem 11.** Let  $u(x)$ ,  $c(x)$ ,  $a(x)$ ,  $D_i u(x)$  and  $Du(x)$  be non-negative continuous functions for all  $i = 1, 2, \dots, n$  defined for  $x \in \mathbb{R}_+^n$ ,

$$\lim_{x_i \rightarrow \infty} u(x_1, x_2, \dots, x_n) = 0, \forall i = 1, 2, \dots, n.$$

Let  $\tilde{\alpha} \in C^1(\mathbb{R}_+^n, \mathbb{R}_+^n)$  be non-decreasing functions in each variable, with  $\tilde{\alpha}(x) \geq x$  on  $\mathbb{R}_+^n$ . Assume that  $c(x)$  is non-decreasing in each variable  $x \in \mathbb{R}_+^n$ . if

$$Du(x) \leq c(x) + \int_{\tilde{\alpha}(x)}^{\infty} a(t)[u(t) + Du(t)] dt, \quad (3.5)$$

for  $x \in \mathbb{R}_+^n$ , then

$$u(x) \leq c(x) \left[ 1 + \int_{\tilde{\alpha}(x)}^{\infty} \left( a(t) \exp \int_t^{\infty} (1 + a(\tau)) d\tau \right) dt \right]. \quad (3.6)$$

Proof: Fixe any  $X \in \mathbb{R}_+^n$ . Then, for  $x \leq X$  and from (3.5), we have

$$Du(x) \leq c(X) + \int_{\tilde{\alpha}(x)}^{\infty} a(t)[u(t) + Du(t)]dt,$$

Define a function  $z(x)$  by

$$z(x) = c(X) + \int_{\tilde{\alpha}(x)}^{\infty} a(t)[u(t) + Du(t)]dt, \quad (3.7)$$

Then

$$\lim_{x_i \rightarrow \infty} z(x_1, \dots, x_n) = c(X), i = 1, 2, \dots, n,$$

$$Du(x) \leq z(x), \quad (3.8)$$

By differentiating (3.8)

$$\begin{cases} Dz(x) \leq a(x)[u(x) + Du(x)]\tilde{\alpha}'(x); \text{ if } n \text{ is even} \\ Dz(x) \geq -a(x)[u(x) + Du(x)]\tilde{\alpha}'(x); \text{ if } n \text{ is odd} \end{cases} \quad (3.9)$$

By integrating both sides of (3.8)

$$u(x) \leq \int_{\tilde{\alpha}(x)}^{\infty} z(t)dt, \quad (3.10)$$

Now, using (3.8) and (3.10) in (3.9) we get

$$\begin{cases} Dz(x) \leq a(x) \left[ z(x) + \int_{\tilde{\alpha}(x)}^{\infty} z(t)dt \right] \tilde{\alpha}'(x); \text{ if } n \\ Dz(x) \geq -a(x) \left[ z(x) + \int_{\tilde{\alpha}(x)}^{\infty} z(t)dt \right] \tilde{\alpha}'(x); \text{ if } n \end{cases} \quad (3.11)$$

If we put

$$v(x) = z(x) + \int_{\tilde{\alpha}(x)}^{\infty} z(t)dt, \quad (3.12)$$

Then

$$\lim_{x_i \rightarrow \infty} v(x_1, \dots, x_n) = c(X), i = 1, 2, \dots, n,$$

And

$$\begin{cases} Dv(x) = Dz(x) + z(x)\tilde{\alpha}'(x); \text{ if } n \text{ is even} \\ Dv(x) = Dz(x) - z(x)\tilde{\alpha}'(x); \text{ if } n \text{ is odd} \end{cases}$$

Using the fact that

$$\begin{cases} Dz(x) \leq a(x)v(x)\tilde{\alpha}'(x); \text{ if } n \text{ is even} \\ Dz(x) \geq -a(x)v(x)\tilde{\alpha}'(x); \text{ if } n \text{ is odd} \end{cases}$$

From (3.11) and  $z(x) \leq v(x)$  from (3.12), we have

$$\begin{cases} Dv(x) \leq [1 + a(x)]v(x)\tilde{\alpha}'(x); \text{ if } n \text{ is even} \\ Dv(x) \geq -[1 + a(x)]v(x)\tilde{\alpha}'(x); \text{ if } n \text{ is odd} \end{cases}$$

It is easy to estimate  $v(x)$  by following the same arguments as in the proof of Theorem 10 as follows

$$v(x) \leq c(X) \exp \left[ \int_{\tilde{\alpha}(x)}^{\infty} (1 + a(t))dt \right]. \quad (3.13)$$

By substituting (3.13) in, (3.11) we get

$$\begin{cases} Dz(x) \leq a(x)c(X) \exp \left[ \int_{\tilde{\alpha}(x)}^{\infty} (1 + a(t))dt \right] \tilde{\alpha}'(x); \text{ if } n \text{ is even} \\ Dz(x) \geq -a(x)c(X) \exp \left[ \int_{\tilde{\alpha}(x)}^{\infty} (1 + a(t))dt \right] \tilde{\alpha}'(x); \text{ if } n \text{ is odd} \end{cases} \quad (3.14)$$

$$\lim_{x_n \rightarrow \infty} D_1 \dots D_{n-1} z(x_1, \dots, x_{n-1}, x_n) = 0.$$

By integrating (3.14) to  $x_n$  from  $x_n$  to  $\infty$ , we have

$$\left\{ \begin{array}{l} -D_1 \dots D_{n-1} z(x) \leq c(X) \int_{\alpha_n(x_n)}^{\infty} a(x_1, \dots, x_{n-1}, t_n) \exp \left[ \int_{\tau}^{\infty} (1 + a(\tau)) d\tau \right] \\ \quad dt_n \alpha_1'(x_1) \dots \alpha_{n-1}'(x_{n-1}); \text{ if } n \text{ is even} \\ -D_1 \dots D_{n-1} z(x) \geq -c(X) \int_{\alpha_n(x_n)}^{\infty} a(x_1, \dots, x_{n-1}, t_n) \exp \left[ \int_{\tau}^{\infty} (1 + a(\tau)) d\tau \right] \\ \quad dt_n \alpha_1'(x_1) \dots \alpha_{n-1}'(x_{n-1}); \text{ if } n \text{ is odd} \end{array} \right.$$

By continuing this process, we obtain

$$\left\{ \begin{array}{l} -D_1 z(x) \leq c(X) \int_{\alpha_2(x_2)}^{\infty} \dots \int_{\alpha_n(x_n)}^{\infty} a(x_1, t_2, \dots, t_n) \exp \left[ \int_{\tau}^{\infty} (1 + a(\tau)) d\tau \right] dt_n \dots dt_2 \alpha_1'(x_1); \text{ if } n \text{ is even} \\ D_1 z(x) \geq -c(X) \int_{\alpha_2(x_2)}^{\infty} \dots \int_{\alpha_n(x_n)}^{\infty} a(x_1, t_2, \dots, t_n) \exp \left[ \int_{\tau}^{\infty} (1 + a(\tau)) d\tau \right] dt_n \dots dt_2 \alpha_1'(x_1); \text{ if } n \text{ is odd} \end{array} \right. ,$$

By integrating the last inequality with respect to  $x_1$  from  $x_1$  to  $\infty$ , we have

$$z(x) \leq c(X) \exp \int_{\tilde{\alpha}(x)}^{\infty} a(t) \exp \left[ \int_{\tau}^{\infty} (1 + a(\tau)) d\tau \right] dt.$$

Since  $X$  is arbitrary, by substituting the value of  $z(x)$  in (3.8), we obtain the inequality (3.6).

**Remark 8.** In the particular case when  $n = 2$ ,  $x \in \mathbb{R}_+^2$ ,  $(\infty, \infty) = (0, 0)$ ,  $\alpha_1(x_1) = x_1$ ,  $\alpha_2(x_2) = x_2$ , and  $c(x) = c_1(x_1) + c_2(x_2)$  then theorem 11 reduces to Theorem 1 in [8]

**Corollary 12.** Let  $u(x)$ ,  $c(x)$ ,  $a(x)$ ,  $D_i u(x)$  and  $Du(x)$  be non-negative continuous functions for all  $i = 1, 2, \dots, n$  defined for  $x \in \mathbb{R}_+^n$ ,

$$\lim_{x_i \rightarrow \infty} u(x_1, x_2, \dots, x_n) = 0, \forall i = 1, 2, \dots, n.$$

Let  $\tilde{\alpha} \in C^1(\mathbb{R}_+^n, \mathbb{R}_+^n)$  be non-decreasing functions in each variable, with  $\tilde{\alpha}(x) \geq x$  on  $\mathbb{R}_+^n$ . Assume that  $c(x)$  is non-decreasing in each variable  $x \in \mathbb{R}_+^n$ . if

$$\left. \begin{array}{l} Du(x) \leq c(x) + M \left[ u(t) + \int_{\tilde{\alpha}(x)}^{\infty} a(t) [u(t) + Du(t)] dt \right] \end{array} \right\} \quad (3.15),$$

for  $x \in \mathbb{R}_+^n$ , then

$$Du(x) \leq c(x) \exp \int_{\tilde{\alpha}(x)}^{\infty} [M + a(t) + Ma(t)] dt. \quad (3.16)$$

Proof : Fixe any  $X \in \mathbb{R}_+^n$ . Then, for  $x \leq X$  and from (3.15), we have

$$Du(x) \leq c(X) + M \left[ u(t) + \int_{\tilde{\alpha}(x)}^{\infty} a(t) [u(t) + Du(t)] dt \right],$$

Define a function  $z(x)$  by

$$z(x) = c(X) + M \left[ u(t) + \int_{\tilde{\alpha}(x)}^{\infty} a(t) [u(t) + Du(t)] dt \right], \quad (3.17)$$

then

$$\lim_{x_i \rightarrow \infty} z(x_1, \dots, x_n) = c(X), i = 1, 2, \dots, n, \quad Du(x) \leq z(x), \quad (3.18)$$

By differentiating (3.8)

$$\left\{ \begin{array}{l} Dz(x) \leq M[a(x) + Du(x)][u(x) + Du(x)]\tilde{\alpha}'(x); \text{ if } n \text{ is even} \\ Dz(x) \geq -M[a(x) + Du(x)][u(x) + Du(x)]\tilde{\alpha}'(x); \text{ if } n \text{ is odd} \end{array} \right.$$

Using (3.18) and the fact that  $Ma(x) \leq z(x)$ , we have

$$\left\{ \begin{array}{l} Dz(x) \leq [Ma(x) + a(x) + M]z(x)\tilde{\alpha}'(x); \text{ if } n \text{ is even} \\ Dz(x) \geq -[Ma(x) + a(x) + M]z(x)\tilde{\alpha}'(x); \text{ if } n \text{ is odd} \end{array} \right.$$

Therefore

$$z(x) \leq c(X) \exp \int_{\tilde{\alpha}(x)}^{\infty} [M + a(t) + Ma(t)] dt.$$

Since  $X$  is arbitrary, by substituting the value of  $z(x)$  in (3.18) we obtain the inequality (3.16).

**Remark 9.** In the particular case when  $n = 2$ ,  $x \in \mathbb{R}_+^2$ ,  $(\infty, \infty) = (0, 0)$ ,  $\alpha_1(x_1) = x_1$ ,  $\alpha_2(x_2) = x_2$ , and  $c(x) = c_1(x_1) + c_2(x_2)$  then corollary 12 reduces to theorem 2 in [7].

**Theorem 13.** Let  $u(x)$ ,  $c(x)$ ,  $a(x)$ ,  $b(x)$ ,  $f(x)$ ,  $D_i u(x)$  and  $Du(x)$  be non-negative continuous functions for all  $i =$

$1, 2, \dots, n$  defined for  $x \in \mathbb{R}_+^n$ , and  $\tilde{\alpha} \in C^1(\mathbb{R}_+^n, \mathbb{R}_+^n)$  be non-decreasing functions in each variable, with  $\tilde{\alpha}(x) \geq x$  on  $\mathbb{R}_+^n$ .

$$\lim_{x_i \rightarrow \infty} u(x_1, x_2, \dots, x_n) = 0, \forall i = 1, 2, \dots, n.$$

Let  $K(u(x))$  be a real-valued, positive, continuous, strictly non-decreasing, sub-additive, and sub-multiplicative function for  $u(x) \geq 0$ , and  $H(u(x))$  be a real-valued, positive, continuous and non-decreasing function defined for  $x \in \mathbb{R}_+^n$ . Assume that  $c(x)$  and  $f(x)$  are non-decreasing functions in each of the variables  $x \in \mathbb{R}_+^n$ . If

$$Du(x) \leq c(x) + f(x)H\left(\int_{\tilde{\alpha}(x)}^{\infty} a(t)K(u(t))dt\right) + \int_{\tilde{\alpha}(x)}^{\infty} b(t)Du(t)dt, \quad (3.19)$$

for all  $x \in \mathbb{R}_+^n$ , then

$$Du(x) \leq c(x) + f(x)H\left(G^{-1}\left[G(\xi) + \int_{\tilde{\alpha}(x)}^{\infty} a(t)K(f(t)p(t))dt\right]\right) \exp \int_{\tilde{\alpha}(x)}^{\infty} b(t)dt, \quad (3.20)$$

for all  $x \in \mathbb{R}_+^n$ , where

$$p(x) = \int_{\tilde{\alpha}(x)}^{\infty} \left( \exp \int_t^{\infty} b(\tau)d\tau \right) dt. \quad (3.21)$$

$$\xi = \int_0^{\infty} a(t)K(c(t)p(t))dt. \quad (3.22)$$

$$G(r) = \int_r^{\infty} \frac{ds}{K(H(s))}. \quad (3.23)$$

Where  $G^{-1}$  is the inverse function of  $G$ , and

$$G(\xi) + \int_{\tilde{\alpha}(x)}^{\infty} a(t)K(f(t)p(t))dt \in \text{dom}(G^{-1})$$

for all  $x \in \mathbb{R}_+^n$ .

Proof : Define a function  $z(x)$  by

$$z(x) = c(x) + f(x)H\left(\int_{\tilde{\alpha}(x)}^{\infty} a(t)K(u(t))dt\right), \quad (3.24)$$

then from (3.19), we have

$$Du(x) \leq z(x) + \int_{\tilde{\alpha}(x)}^{\infty} b(t)Du(t)dt, \quad (3.25)$$

Clearly,  $\Phi(x)$  is a positive and non-decreasing function in each variable  $x_2, x_3, \dots, x_n$ , then

$$D_1 \Phi(x) = - \int_{\alpha_2(x_2)}^{\infty} \dots \int_{\alpha_n(x_n)}^{\infty} \alpha(\alpha_1(x_1), t_2, \dots, t_n) K(f(\alpha_1(x_1), t_2, \dots, t_n)p(\alpha_1(x_1), t_2, \dots, t_n)) K(H(v(\alpha_1(x_1), t_2, \dots, t_n))) dt_2 \dots dt_n \alpha'_1(x_1),$$

hence

Clearly,  $z(x)$  is a positive, continuous, and non-decreasing function in each of the variables  $x \in \mathbb{R}_+^n$ . Using Theorem 10 in (3.25), we get

$$Du(x) \leq z(x) \exp\left(\int_{\tilde{\alpha}(x)}^{\infty} b(t)dt\right). \quad (3.26)$$

By integrating (3.26) with respect to  $x$  from  $x$  to  $\infty$ , we obtain

$$u(x) \leq z(x)p(x), \quad (3.27)$$

where  $p(x)$  is defined in (3.21). From (3.24) we have

$$z(x) = c(x) + f(x)H(v(x)), \quad (3.28)$$

$$v(x) = \int_{\tilde{\alpha}(x)}^{\infty} a(t)K(u(t))dt, \quad (3.29)$$

Now, using (3.28) in (3.27) we get

$$u(x) \leq [c(x) + f(x)H(v(x))]p(x), \quad (3.30)$$

From (3.29) and (3.30) and since  $K$  is a sub-additive and sub-multiplicative function, we obtain

$$v(x, y) \leq \int_{\tilde{\alpha}(x)}^{\infty} a(t)K([c(t) + f(t)H(v(t))]p(t))dt \leq \int_{\tilde{\alpha}(x)}^{\infty} a(t)K(c(t)p(t))dt + \int_{\tilde{\alpha}(x)}^{\infty} a(t)K(f(t)H(v(t))p(t))dt.$$

Therefore

$$v(x, y) \leq \int_0^{\infty} a(t)K(c(t)p(t))dt + \int_{\tilde{\alpha}(x)}^{\infty} a(t)K(f(t)H(v(t))p(t))dt.$$

Define a function  $\Phi(x)$  by

$$\Phi(x, y) = \int_0^{\infty} a(t)K(c(t)p(t))dt + \int_{\tilde{\alpha}(x)}^{\infty} a(t)K(f(t)p(t))K(H(v(t)))dt. \quad (3.31)$$

Then

$$\lim_{x_i \rightarrow \infty} \Phi(x) = \int_0^{\infty} a(t)K(c(t)p(t))dt = \xi. \quad (3.32)$$

And

$$v(x) \leq \Phi(x).$$

$$D_1 \Phi(x) \geq - \int_{\alpha_2(x_2)}^{\infty} \dots \int_{\alpha_n(x_n)}^{\infty} a(\alpha_1(x_1), t_2, \dots, t_n) K(f(\alpha_1(x_1), t_2, \dots, t_n) p(\alpha_1(x_1), t_2, \dots, t_n)) K(H(\Phi(x_1, t_2, \dots, t_n))) dt_2 \dots dt_n \alpha'_1(x_1)$$

$$D_1 \Phi(x) \geq -K(H(\Phi(x))) \int_{\alpha_2(x_2)}^{\infty} \dots \int_{\alpha_n(x_n)}^{\infty} a(\alpha_1(x_1), t_2, \dots, t_n) K(f(\alpha_1(x_1), t_2, \dots, t_n) p(\alpha_1(x_1), t_2, \dots, t_n)) dt_2 \dots dt_n \alpha'_1(x_1)$$

i.e

$$\frac{D_1 \Phi(x)}{K(H(\Phi(x)))} \geq - \int_{\alpha_2(x_2)}^{\infty} \dots \int_{\alpha_n(x_n)}^{\infty} a(\alpha_1(x_1), t_2, \dots, t_n) K(f(\alpha_1(x_1), t_2, \dots, t_n) p(\alpha_1(x_1), t_2, \dots, t_n)) dt_2 \dots dt_n \alpha'_1(x_1). \quad (3.33)$$

From (3.23) we have

$$D_1 G(\Phi(x)) = \frac{D_1 \Phi(x)}{K(H(\Phi(x)))}. \quad (3.34)$$

$$D_1 G(\Phi(x)) \geq - \int_{\alpha_2(x_2)}^{\infty} \dots \int_{\alpha_n(x_n)}^{\infty} a(\alpha_1(x_1), t_2, \dots, t_n) K(f(\alpha_1(x_1), t_2, \dots, t_n) p(\alpha_1(x_1), t_2, \dots, t_n)) dt_2 \dots dt_n \alpha'_1(x_1). \quad (3.35)$$

Now, by setting  $x_1 = t$  and integrating from  $x_1$  to  $\infty$  in (3.35), and using (3.31) we get

$$\Phi(x) \leq G^{-1} \left[ G(\xi) + \int_{\tilde{\alpha}(x)}^{\infty} a(t) K(f(t) p(t)) dt \right] \quad (3.36)$$

Finally, by substituting (3.28), (3.32) and (3.36), (3.34) we obtain the inequality (3.20).

**Remark 10.**

From the inequalities (3.30) and (3.36) in the proof of theorem 13, we can find this inequality

$$u(x) \leq c(x) + f(x) H \left( G^{-1} \left[ G(\xi) + \int_{\tilde{\alpha}(x)}^{\infty} a(t) K(f(t) p(t)) dt \right] \right) p(x). \quad (3.37)$$

If we put  $n = 2$ ,  $x \in \mathbb{R}_+^2$ ,  $(\infty, \infty) = (0, 0)$ ,  $\alpha_1(x_1) = x_1$ ,  $\alpha_2(x_2) = x_2$ , and  $c(x) = c_1(x_1) + c_2(x_2)$ ,  $f(x) = 1$ ,  $H(x) = K(x) = x$ , and  $a(x) = b(x)$  then Theorem 13 reduces to Theorem 1 in [7]

**Corollary 14.** Let  $u(x), c(x), a(x), b(x), D_i u(x)$  and  $Du(x)$  be non-negative continuous functions for all  $i = 1, 2, \dots, n$  defined for  $x \in \mathbb{R}_+^n$ , and  $\tilde{\alpha} \in C^1(\mathbb{R}_+^n, \mathbb{R}_+^n)$  be non-decreasing functions in each variable, with  $\tilde{\alpha}(x) \geq x$  on  $\mathbb{R}_+^n$ .

$$\lim_{x_i \rightarrow \infty} u(x_1, x_2, \dots, x_n) = 0, \forall i = 1, 2, \dots, n.$$

Let  $K(u(x))$  be a real-valued, positive, continuous, strictly non-decreasing, sub-additive, and sub-multiplicative function for  $u(x) \geq 0$ , and  $H(u(x))$  be a real-valued, positive, continuous and non-decreasing function defined for  $x \in \mathbb{R}_+^n$ . Assume that  $c(x)$  is non-decreasing function in each of the variables  $x \in \mathbb{R}_+^n$ . If

$$Du(x) \leq c(x) + \int_{\tilde{\alpha}(x)}^{\infty} a(t) K(u(t)) dt + \int_{\tilde{\alpha}(x)}^{\infty} b(t) Du(t) dt, \quad (3.38)$$

for all  $x \in \mathbb{R}_+^n$ , then

$$Du(x) \leq c(x) + \left( T^{-1} \left[ T(\xi) + \int_{\tilde{\alpha}(x)}^{\infty} a(t) K(p(t)) dt \right] \right) \exp \int_{\tilde{\alpha}(x)}^{\infty} b(t) dt,$$

for  $x \in \mathbb{R}_+^n$ , where where  $p(t)$  and  $\xi$  are defined in theorem 13, and

$$T(r) = \int_r^{\infty} \frac{ds}{K(s)}.$$

Where  $T^{-1}$  is the inverse function of  $G$ , and

$$T(\xi) + \int_{\tilde{\alpha}(x)}^{\infty} a(t) K(p(t)) dt \in \text{dom}(T^{-1})$$

for  $x \in \mathbb{R}_+^n$ .

Proof: The proof of this Corollary follows the same arguments as in Theorem 13.

**Remark 11.** If we put  $H(x) = x$  and  $f(x) = 1$  in Theorem 13, then we obtain the result in corollary 14.

**Corollary 15.** Let  $u(x), a(x), b(x), D_i u(x)$  and  $Du(x)$  be non-negative continuous functions for all  $i = 1, 2, \dots, n$  defined for  $x \in \mathbb{R}_+^n$ , and  $\tilde{\alpha} \in C^1(\mathbb{R}_+^n, \mathbb{R}_+^n)$  be non-decreasing functions in each variable, with  $\tilde{\alpha}(x) \geq x$  on  $\mathbb{R}_+^n$ .

$$\lim_{x_i \rightarrow \infty} u(x_1, x_2, \dots, x_n) = 0, \forall i = 1, 2, \dots, n.$$

If

$$Du(x) \leq M + \int_{\tilde{\alpha}(x)}^{\infty} a(t)u(t)dt + \int_{\tilde{\alpha}(x)}^{\infty} b(t)Du(t)dt,$$

for all  $x \in \mathbb{R}_+^n$ , where  $M > 0$  is constant, then the following conclusion are true:

$$Du(x) \leq M \left( 1 + \int_0^{\infty} a(t)p(t)dt \exp \int_{\tilde{\alpha}(x)}^{\infty} a(t)p(t)dt \right) \exp \int_{\tilde{\alpha}(x)}^{\infty} b(t)dt,$$

$$u(x) \leq M \left( 1 + \int_0^{\infty} a(t)p(t)dt \exp \int_{\tilde{\alpha}(x)}^{\infty} a(t)p(t)dt \right) p(x)$$

for  $x \in \mathbb{R}_+^n$ , where

$$p(x) = \int_{\tilde{\alpha}(x)}^{\infty} \left( \exp \int_t^{\infty} b(\tau)d\tau \right) dt.$$

Proof: By setting  $K(x) = x$  and  $c(x) = M$  in Corollary 14, we obtain the results of this Corollary.

**Corollary 16.** Let  $u(x), a(x), b(x), D_i u(x)$  and  $Du(x)$  be non-negative continuous functions for all  $i = 1, 2, \dots, n$  defined for  $x \in \mathbb{R}_+^n$ , and  $\tilde{\alpha} \in C^1(\mathbb{R}_+^n, \mathbb{R}_+^n)$  be non-decreasing functions in each variable, with  $\tilde{\alpha}(x) \geq x$  on  $\mathbb{R}_+^n$ .

$$\lim_{x_i \rightarrow \infty} u(x_1, x_2, \dots, x_n) = 0, \forall i = 1, 2, \dots, n.$$

Let  $K(u(x))$  be a real-valued, positive, continuous, strictly non-decreasing, sub-additive, and sub-multiplicative function for  $u(x) \geq 0$ . If

$$Du(x) \leq \sum_{i=1}^n c_i(x_i) + \int_{\tilde{\alpha}(x)}^{\infty} a(t)K(u(t))dt + \int_{\tilde{\alpha}(x)}^{\infty} b(t)Du(t)dt,$$

for all  $x \in \mathbb{R}_+^n$ , where  $c_i(x_i) > 0$  and  $c'_i(x_i) \geq 0$  are continuous functions for  $x_i \geq 0$  for all  $i = 1, \dots, n$  then

$$Du(x) \leq \sum_{i=1}^n c_i(x_i) + \left( T^{-1} \left[ T(\xi) + \int_0^{\infty} a(t)K(p(t))dt \exp \int_{\tilde{\alpha}(x)}^{\infty} a(t)K(p(t))dt \right] \right) \exp \int_{\tilde{\alpha}(x)}^{\infty} b(t)dt,$$

for  $x \in \mathbb{R}_+^n$ , where where  $p(t)$  and  $T$  are defined in corollary 14, and

$$\xi = \int_{\tilde{\alpha}(x)}^{\infty} a(t)K \left( p(t) \sum_{i=1}^n c_i(t_i) \right) dt.$$

Proof: By setting  $c(x) = \sum_{i=1}^n c_i(x_i)$  in Corollary 14 and using the same arguments in [ ] and Theorem 13, we obtain the result of this Corollary.

**REFERENCES**

[1] Bainov, D., and P. Simeonov. Integral inequalities and applications. Kluwer Academic Publishers (1992).

[2] Denche, M. and Khellaf, H. Integral inequalities similar to Gronwall inequality. Electronic Journal of Differential Equations,176 (2007), 1-14.

[3] Khellaf, H. On integral inequalities for functions of several independent variables. Electronic Journal of Differential Equations,123 (2003), 1-12.

[4] Khellaf,H. Nonlinear delay integral inequalities for multi-variable functions. Electronic Journal of Differential Equations,169 (2011), 1-14.

[5] Oguntuase, J. A. On an inequality of Gronwall. Journal of Inequalities in Pure and Applied Mathematics,2(2001).

[6] Pachpatte, B. G. On some fundamental integrodifferential and integral inequalities. An. Sci. Univ. Al. I. Cuza, Iasi,29(1977), 77–86.

[7] Pachpatte, B. G. On some new integrodifferential inequalities of the Wendroff type. Journal of Mathematical Analysis and Applications,73(1980), 491–500.

[8] Pachpatte, B. G. Inequalities for differential and integral equations. Academic Press (1998).

[9] Pachpatte, B. G. On a certain retarded integral inequality and its applications. Journal of Inequalities in Pure and Applied Mathematics,5(2004).

[10] Snow, D. R. Gronwall’s inequality for systems of partial differential equations in two independent variables. Proceedings of the American Mathematical Society,33(1972), 46-54.

[11] Yeh, C. C. and Shih, M. H. The Gronwall-Bellman inequality in several variables. Journal of Mathematical Analysis and Applications,86(1982), 157-167.

[12] Zhang, H. and Meng, F. Integral inequalities in two independent variables for retarded Volterra equations. Applied Mathematics and Computation,199(2008), 90–98.

# STUDY OF PLASMA-DEPOSITED LAYERS OF W-TIN ON CUTTING TOOLS.

Submitted on 21/06/2018 – Accepted on 05/11/2019

## Abstract

In the mechanical industry, the success and the results obtained by the heat treatments in the improvement of the properties of mechanical parts and mechanisms, with the introduction of new alloy and composite materials, found that the introduction of other techniques is essential. The metal parts subject to wear must be hard, but the hard metals can be brittle, fragile and difficult to work.

A solution to this dilemma may consist in manufacturing the parts in a relatively soft and resistant alloy and then modifying its surface by the action of an appropriate treatment.

The application of surface treatments by the various spray coating techniques allow a considerable contribution to be made in order to improve the properties of resistance to wear, the friction and to increase the life time in the mechanical parts.

**Keywords:** *Hardening, Wear, Spraying, Plasma, Coating. Titanium nitrides, cutting tools, machining.*

**A. DJERIBAA**<sup>1</sup>  
**E. FERKOUS**<sup>1</sup>  
**N. SAOULA**<sup>2</sup>  
**I. AMARA**<sup>3</sup>

<sup>1</sup> Department of Mechanical Engineering, Frères Mentouri University Constantine, Algeria.

<sup>2</sup> Advanced Technologies Development Center, Algiers, Algeria.

<sup>3</sup> Department of Transport Engineering, Frères Mentouri University Constantine, Algeria.

## INTRODUCTION

In spite of the progress made in materials science, the use of traditional treatments, the introduction of new carbide materials and nitrides, the performances of mechanical parts and cutting tools are still in a state of improvement. This is why the search for new substitute materials and coatings remains a covers area, in view of the fact that it is part of a very competitive industrial challenge, particularly in the field of mechanics and modern machining centers.

In this work, and on the basis of a comparative idea, we have introduced for the first time the plasma as a technique of deposition of layers of coatings of titanium nitrides on the active part of the cutting tools [1]

### 2. Preparation of coatings and their testing:

Despite the success achieved by the deposition of carbides and the development of cutting tools with high hardness and better endurance, it is noted that great interest is being paid to coatings by depositing thin layers of tungsten W-TIN (W 80% Ti 20%),

The applications of thin layers are multiple. They are generally based on the principle of modifying the surface of a material to make it a composite whose surface properties are different from that of the solid material. The so-called hard layers find uses in the protection of mechanical parts against wear, oxidation and corrosion and can considerably improve the mechanical properties of cutting tools and in particular their hardness, resistance to Wear, and therefore their lifetime, titanium nitride and is the most answered material for this type of application,

the last years the deposition of a harder material such as tungsten became possible. W-TIN thin films produced by physical vapor deposition (PVD) are used for wear protection as a diffusion barrier. The development of protective coatings for cutting tools dates back to the early 1970s.

Coated cutting tools have invaded machining centers because they allow high production rates to be maintained by reducing the frequency of machine shutdown to replace worn tools. W-TiN coatings with a thickness of the order of 5  $\mu\text{m}$  and a micro-hardness of more than 4000 HV make it possible to increase the lifetime of the cutting tools by a factor of 4 to 20 depending on the conditions of use [2][3]

For the deposition of coatings on cutting tools we used the RF sprayer, designed and made locally in the laboratory of ionized media on the CDTA center for advanced technology development, during this study the W-TIN coatings were developed in the sprayer after different preparation of the cutting tools.

### 3. Preparation of substrates:

In this stage of the work, the titanium layer coatings will be produced on cutting plates of high-speed steels TNMM 160 408 K10. Before being placed in the enclosure, the latter and in particular the active part of them have undergone, first a trichloroethylene degreasing treatment by ultrasound, then they are rinsed with deionized water and then with alcohol.

### 3.1 Deposition and Procedure:

After the preparation of the cutting tools and the pickling of the target by a bombardment flow which lasts a few minutes, the protective shield is activated and the coating operation is initiated under favorable conditions and deposition parameters.

These parameters were set as follows:

- ❖ Partial pressure of the first gas:  $4 \cdot 10^{-5}$  mbar;
- ❖ Partial pressure of the second gas:  $8.7 \cdot 10^{-4}$  mbar;
- ❖ Working pressure = 30 mtor
- ❖ Inter-target distance - substrate: 3 cm;
- ❖ Power: 200 watt
- ❖ Intensity applied = 0.3 - 0.5 amperes;
- ❖ Time of deposit = 50 minutes.

In order to carry out this coating operation of the cutting tools, which will subsequently be subjected to the various mechanical tests (hardness and life tests) by the operation of turning at different cutting speeds, We have made a deposit for which we have placed a cutting tool and performed a coating deposit of W-TIN and by following we will compare the mechanical characteristics without and with deposition, the operation of this study involves two steps:

In the first step, the control tools kept as reference samples were selected for the subsequent comparison of the initial mechanical properties.

In the second step: in this step the cutting tools on their active part have undergone a W-TIN coating layer.

### 4. Tests carried out:

After completing the coating operation and obtaining the layers, we have determined certain properties by subjecting these cutting tools to the various tests, which are preconditioned by the properties and quality of the coatings

#### 4.1 Properties of coatings obtained:

Before the coated cutting tools are subjected to the machining operations by turning, we present the methods used for the characterization of the coatings obtained on the cutting tools.

Among the main mechanical characteristics favoring the performance of the cutting tools and their lifetime, attention is paid to the value of the thickness of the deposited layer, its adhesion and its hardness.

##### 4.1.1 Thickness of the deposited layer:

#### Methods of measuring the thickness of the layer:

Two methods of measurement can be distinguished:

Direct measurement of thickness: it has two methods:

- Mechanical methods use a stylus that moves over the surface of the layer.

- Profile-meter (with laser emission) (ALTISURF 500) This method requires the creation of a step which is carried out either by hiding part of the substrate during the deposition or by eliminating a part of the deposit (HNO 3 solution at 10 %). This measurement can be obtained by a mechanical Diamond tip that moves at constant speed along a defined line on the work piece or with profilometer.

The tip, all remaining in permanent contact, whose amplitude is recorded electronically. [4]

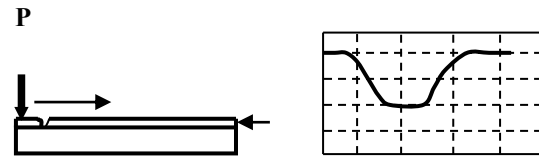


Figure 1: System for measuring the deposited layer (Perthometre-S10 D) mahr.

### 4.2 Adherence of the deposit:

These tests can be carried out using a scratch test or a stylus whose diamond tip is normally applied to the surface of the sample while progressively increasing the load and ending with a feeler Mechanical (Perthometre-S10 D) mahr, with scale  $5 \mu\text{m}$  and a stroke of 5 mm in plotted the graphs (spectrum) of the surface and the depth of the step. The results can be given in the form of a curve or an adhesion diagram.

### 4.3 Hardness:

In the case of measuring the micro-hardness of the coatings, the most commonly used methods are Knoop hardness or Vickers hardness. In this case, the measurement of the Vickers hardness was carried out on a micro durometer (mechanical laboratory). W-TIN coatings were subjected to these tests under loads ranging generally from (200 to 1000) gf, expressed as the ratio of the maximum load applied to the surface of the contact impression.

$$H_v = \frac{1,854 \cdot P}{9,81 \cdot d^2} \quad P: \text{applied load (N)}$$

d : The diagonal of the impression in mm [5]

### 4.4 Wear:

After the hardness tests, the coated cutting tools were subjected to wear and endurance tests by the direct application of the machining processes by removal of chips. We selected the Taylor model for studying and evaluating wear and for establishing the relationship between the cutting time of a tool and the cutting speed under well-defined working conditions. We performed turning tests at different cutting speeds in accordance with

the ISO3685 standard for life testing which is presented in table. [6]

Table 1: Machining Parameters

| Parametres              |     |     |     |     |     |
|-------------------------|-----|-----|-----|-----|-----|
| Cutting speed (m / min) | 400 | 300 | 150 | 100 | 70  |
| Feedrate (mm)           | 0,1 | 0,1 | 0,1 | 0,1 | 0,1 |
| Depth of cut (mm)       | 1   | 1   | 1   | 1   | 1   |
| Wear Criteria (mm)      | VB  | VB  | VB  | VB  | VB  |

5. The results of the various tests:

5.1 Layer thickness:

In this work and to be sure to get exact results we measured the thickness of the deposited layer by two methods, with an electronic probe (Sth-perthometer-S10) mahr, with a scale of 5 μm and a stroke of 5 mm. we obtained the thickness around 2,50 μm, then to confirm that we use a profilometre with laser, the specter below show the final thickness value around 2,25 μm. figure 2.

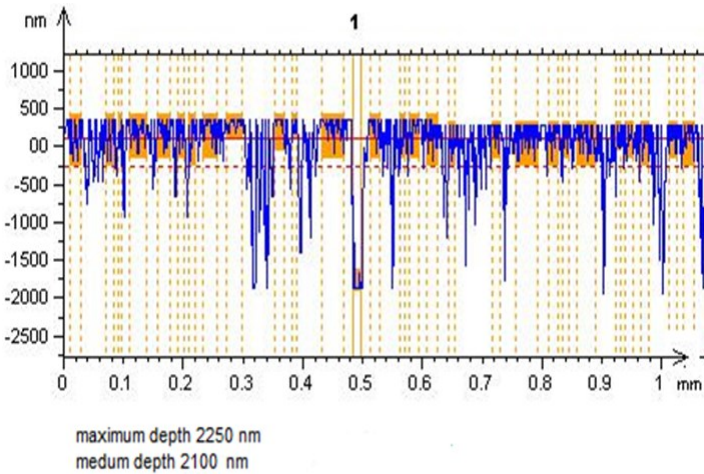


Figure 2: Measurement of the thickness of the deposited layer.

This figure shows that the value of the thickness of the deposited layer is 2.25 μm.

6.2 Adhesion of the layer

Among the techniques for determining the adhesion of the materials and the layers of deposited coatings are the scratch test method and the polishing method of the layer. For this study, the second method was carried out on a polisher (KNUTH-ROTOR.2 strueers). Thus, starting from an initial thickness of 2.5 μm, the polishing carried out at a speed of 3000 rpm with an abrasive paper of 1000, gave a reduction in the thickness of 1.45 μm during a severe exposure of 55 minutes.

This consumption of material expressed by the variation of the thickness is represented by the following spectrum. Measurement of the depth of the layer deposited after 55 minutes of polishing is around 0.80 μm. Figure 3.

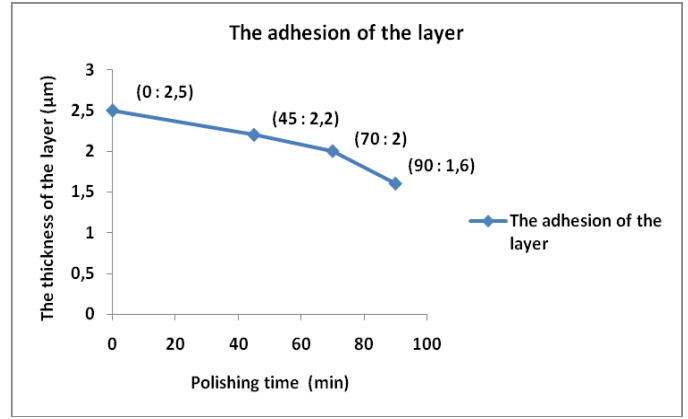


Figure 3: Measurement of the depth of the deposited layer after 55 minutes, 0.80 μm

6.3 Hardness:

Compared to the hardness value of an uncoated cutting tool, the comparative curves obtained show a marked increase in hardness. The evolution of this hardness is due to the W-TIN coating layer there is a marked significant difference in hardness. This hardness improves progressively from the initial state of a tool with a traditional surface treatment (toughening, tempering, annealing, etc.) to the W-TIN coating state.

The presentation of the hardness variation of these high-speed steel cutting tools is given in the following graphs:

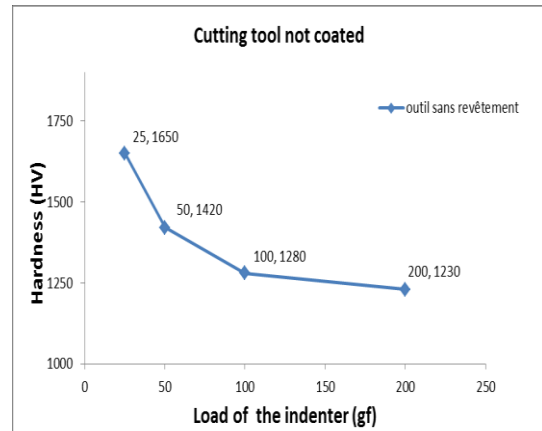


Figure 4: Hardness of the uncoated cutting tool

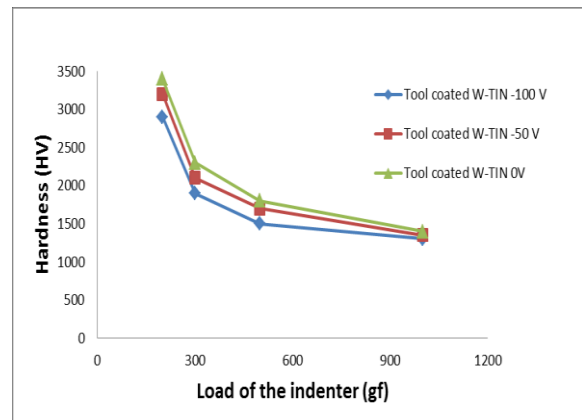


Figure 5: Hardness of cutting tools coated by W-TIN

We noticed an improvement over the hardness compared with uncoated cutting tools, on the other hand, the hardness of the W-TIN layers also corresponds to the polarization, higher polarization gives a high hardness, [7].

lower volt gives a hardness better than -50 volt and -100 volt.

In this case, we found that the hardness tends to increase with polarization. This result is directly related to a high dense structure, and reduced grain size at a small amount of structural defaults.

**6.4 Evaluation of wear (VB):**

Because of the W-TIN coating surface treatment operation and after an improvement in the hardness, we have recorded the influence of this improvement on the tribological side of the wear of the cutting tools. For this purpose, we have subjected the cutting tools to turning tests with different cutting speeds and without lubrication (dry turning). After machining by turning, we have seen a considerable improvement in the wear resistance, resulting in an increase in the service life of the cutting tools submitted.

To demonstrate these mechanical properties and to make an effective comparison of these tools, we have performed a series of operations at different speeds. The results for the two types of tools are presented in the following figures:

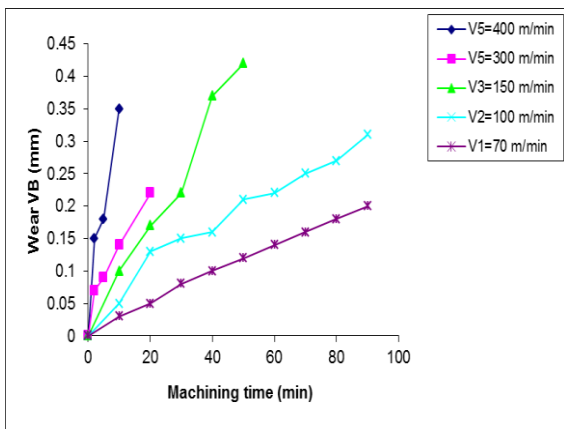


**Figure 6:** Combinations of the different wear curves for uncoated cutting tools.

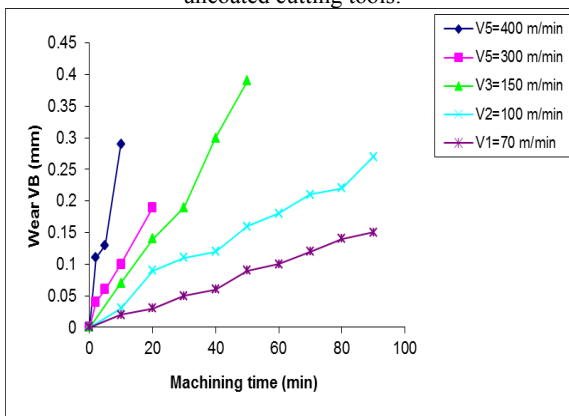


**Figure 7:** Combinations of different wear curves for W-TIN coated cutting tools

During the turning tests carried out according to the Taylor law, and in accordance with the conditions of ISO 3685 the graphs obtained in this work with different speeds show a rightward displacement

$VB = f(T)$ , which Explains a significant reduction in the wear of these coated plates.

This grouping graph, compared to the graph of **Figure 6**, makes it possible to say and in a significant way that there is indeed an improvement in the lifetime of these cutting tools, resulting in a collective displacement of these curves towards the right-hand side, thus reducing wear and thus increasing the service life.

**7. Conclusion**

This study allowed us to compare the evolution of the mechanical properties between the cutting tools covered by W-TIN and not covered one which is the main objective.

The results obtained in limit of the improvement of the mechanical characteristics are presented and commented, Result of the exposure of hardness has a very clear improvement of this in the direction of the evolution of the coating structure.

As for the second significant characteristic for the wear resistance, within the limit of the strength and lifetime of the cutting tools, and after the comparison of the tools covered by the uncovered tools subject to the Machining work by dry rotation, we have recorded a clear improvement of the wear resistance.

The rotation operations performed at different cutting speeds proved that the criterion of the use of VB (mm) cannot be reached which has periods of machining T (minute), largely considerable compared to the periods of the use of coating feel of cutting tools.

**REFERENCES**

[1] : W.Herr, B.Mathes, E.Broszeit and S.Kloos. Surface and coating Technology 57 (1993).

[2] : José Miguel Fernandes Figueiredo. Analysis of the tribological behaviour of W-Ti-N coatings. Mmoire de master. Université de Prague 2013.

[3] : V. Severo. Tribological behaviour of W-Ti-N coatings in semi-industrial strip-drawing tests. Journal of Materials Processing Technology 209 (2009) 4662–4667. Page 1.

[4] : C. Perm. Jindal and Dennis T. quinto. Surface and coating Technology 36 (1988) 683.

[5] : W. D. Sproul, Thin solid Films, 107 (1983) 141.

[6] : Elaboration des normes, organisation internationale de normalisation ISO 3685 (1993), Essais de durée de vie des outils de tournage a partie active.

[7]: Yu Xi Wang, Sam Zhang, Jyh-Wei Lee, Wen Siang Lew, Bo Li. Surface & Coatings Technology 206 (2012) 5103–5107.

[8]: S.V. Subramanian, S.S. Ingle, D.A.R. Kay. Design of coatings to minimize tool crater wear, *Surf Coat. Tech.* 61, 293-299 (1993).

[9]: M. Yalles, L. Boulanouar, S. Belhadi. Etude de l'endommagement des outils de coupe en céramique noire et en CBN lors du tournage d'un acier durci, *Revue de Mécanique*

[10]: R.F. Ávila, C. Godoy, A.M. Abrão and M.M. Lima. Topographic analysis of the crater wear on TiN, Ti(C, N) and (Ti,Al)N coated carbide tools. *Wear*, 265(1-2):49-56 (2008).